Mihăiţă HORODINCĂ

LABORATORY EXPERIMENTS ON DYNAMICS OF CANTILEVER BEAMS.

Performantica

Preface

This book is intended especially for the laboratory work of Romanian students and fellowship students from abroad, attending the course of Dynamics of Structures and Machines Systems at Gheorghe Asachi Technical University of Iasi.

This book is based on three scientific papers already published in scientific journals, as it follows:

1. Horodinca, M., Seghedin, N., Carata, E., Filipoaia, C., Boca, M. Chitariu, D. (2013), *Experimental Investigations of the Power Absorbed at Mechanical Resonance*, Experimental Techniques, vol. 30, Issue 7, pp. 21-31, 2013.
2. Horodinca, M., Seghedin, N., Carata, E., Boca, M., Filipoaia, C., Chitariu, D., (2014), *Dynamic Characterization of a Piezoelectric Actuated Cantilever Beam Using Energetic Parameters*, Mechanics of Advanced Materials and Structures, vol. 21, issue 2, pp. 154-164, 2014.
3. Horodinca, M., (2013) *A study on actuation power produced in an active damping system*, Mechanical Systems and Signal processing, vol. 39, Issue 1-2, pp. 297-315, 2013.

These aforementioned papers are reproduced here, though in a slightly revised form, each one representing the main part of a particular chapter in this book.

The primary reason that led to the writing of this book was that many unrevealed aspects of research behind every scientific paper published can be identified, aspects that prove useful for students undertaking learning and training. Therefore, an original and inovative aspect of this book can be observed. At the end of each chapter all the necessary information and indications (about computer programs and data files acquired in experiments) are provided allowing students to fully understand the main theoretical and experimental elements of each paper. As a result, students can achieve the reconstruction of the key graphical representations (figures) related to each experiment from

the papers, with added focus on computer-aided data processing in Matlab. The computer programs and data files are available on the computers used by students in the laboratory or may be obtained upon request to the email address of the author (horodinca@tuiasi.ro or hmihaita@yahoo.com). At the end of each chapter a number of items for individual study and practical work on some experiments are proposed mainly based on computer assisted monitoring of actuation power flows in dynamics of structures. All the experimental features are fully available in the laboratory.

Last but not least, there is also another reason for writing this book. This is an opportunity for Romanian students to become familiar with English scientific terminology used in dynamics of structures, to be in touch with new trends and challenges of their future profession.

To conclude, I truly hope that upon reading this book students will be given the chance to improve their skills in experimental research as an added bonus to their theoretical training.

Mihăiţă HORODINCĂ Iasi, June 2014

Contents

Paper 1

EXPERIMENTAL INVESTIGATIONS OF THE POWER ABSORBED AT MECHANICAL RESONANCE

ABSTRACT

This paper describes the results of an investigation concerning the power absorbed at mechanical resonance for a single degree of freedom vibration system. Regarding the experimental purposes, the paper proposes a cantilever beam set-up actuated by a voice coil actuator and a computer aided power monitoring technique.
The absorbed power is evaluated in a steady-state regime for different values of excitation frequency around the resonance (the first mode of vibration). The experimental results are afterwards compared to the theoretical predictions. In addition, some transient regimes generated by beat vibrations are explored. The negative absorbed power has been observed. The paper proposes an active vibration damping technique, based on actuation with a negative modal power supply.

Keywords: Active vibration damping, mechanical power, measurement, negative power.

1.1 INTRODUCTION

In vibration engineering and experimental research, the usage of measurement and the study of the mechanical power transmitted by

electrodynamic excitation in mechanical structures, is an interesting option. The measurement and monitoring of the mechanical power flows can be useful in various research domains such as: dynamic behaviour identification and optimisation, active damping and vibration isolation, power harvesting, etc.

Benassi [1] performs an investigation in dynamic behaviour identification and optimisation. He focuses on the suppression of the vibrations of plates by considering the equivalent impedance of power-minimising vibration controllers. Mak [2] proposes an analytical study of the effects of the interaction between two coherent vibratory sources on the power transmitted to the floor. Mandal [3] presents a study on vibration power transmission in technically orthotropic plates. Reinji [4] obtains results researching the vibration energy transfer in a system of three plates separated by a small distance and connected at a few discrete points.

In the active damping and vibration isolation domain, Howard [5] proposes a vibratory power transducer. He does so in order to reduce the vibration energy transmitted into a beam. Xie [6] presents a study on the vibration power transmission behaviour for a vibration isolation system.

In the power harvesting domain, research is focused on alternative power sources for MEMS devices. According to Glynne-Jones [7], Sari [8] and Stephen [9], micro generators (consisting of mass-spring system and magnet-coil generators) should be used to extract energy from a vibrating environment. The research is focused on the maximisation of the power delivered.

In scientific literature the measurement of the mechanical power is generally done by using transducers. Howard [5] uses a six axis transducer to measure the translation and rotational vibratory power. The time averaged vibratory mechanical power is calculated as half the real part of the force multiplied by the complex conjugate of the velocity. Renji [4] proposes a power measurement technique in a few discrete points of actuation using the excitation force and the real part of the driving point admittance. Mandal [3] proposes the measurement of power flow in orthotropic plates using the cross-spectrum of force and acceleration signal divided by angular frequency, or the cross-spectrum of velocity and shear force signal.

The main objective of this paper is to measure the absorbed average mechanical power of a vibratory system using the active power absorbed by the actuating system (a voice-coil actuator or electrodynamic actuator as well). The actuator is used as mechanical power source and loading sensor. A method for evaluating the electrical and mechanical characteristics of a voice coil actuator has already been developed by Fujii [10].

This paper proposes a computer aided measurement technique of the average mechanical power delivered by a voice coil actuator and absorbed by a vibratory system. To prove the reliability of the measurement technique, a single degree of freedom mass-spring-damper system is used as vibratory system excited at resonance. From a dynamic point of view, the resonant behaviour of the motion of a low damped mass-spring-damper mechanical system, excited by a harmonic force, is well known. At resonance, when the frequency of the exciting

force is close to the natural damped frequency, the amplitude of the motion of the mass increases significantly (tens or even hundreds of times) compared to the motion amplitude level when the system is excited by a very low frequency force.

The vibration theory [11] indicates that at resonance the mechanical power absorbed by a mass-spring-damper system from the excitation source (actuator) increases, while a big amount of modal energy is stored inside.

The proposed measurement technique is used on a cantilever beam experimental set-up, basically to validate the theoretical prediction on the absorbed average mechanical power at resonance. The paper also proposes an experimental research on transient regimes during the excitation (beat vibration). Based on a transient regime with negative mechanical power absorbed from the actuator, the authors propose a damping technique with actuator and active negative modal power supply.

1.2 THEORETICAL PREDICTION OF THE MECHANICAL POWER EVOLUTION

Let us consider a mass-spring-damper system, with a single degree of freedom, as described in Fig. 1.1. Here *m[Kg]* is the mass, *k[N/m]* is the spring constant, and *c[N·s/m]* is the viscous damping coefficient. *MS* is a mechanical on-off switch used to cancel the elastic suspension of the system when necessary. The easiest way to excite the system

with a harmonic force F_e is to use an electrodynamic actuator (voice-coil actuator) placed between the mass and the reference point *RP*. This actuator uses a coil (connected to the mass *m*) and a magnet near the coil. The magnet is attached to the reference point *RP*. Paulitsch [12] already performed a study on the electrodynamic parameters which are involved in the voice coil actuators design. Suppose we have a harmonic signal generator with adjustable frequency, that supplies the coil with a harmonic voltage *u(t)* and a current *i(t)*, if the electrical on-off switch *ES* is switched-on.

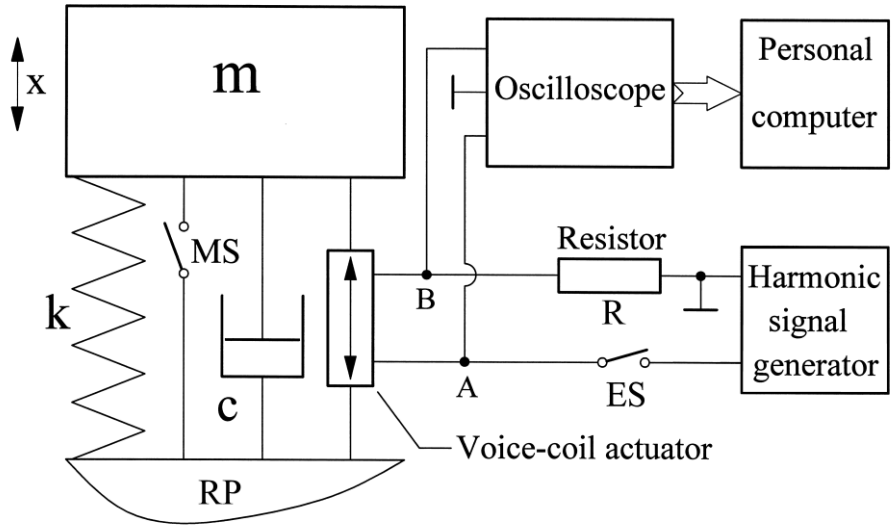

Fig. 1.1: *Description of the experimental set-up.*

There is an interaction between the current *i(t)* in the coil and the magnetic field, so that a harmonic Lorentz force occurs and works as an exciting force F_e in this vibratory system:

$$F_e = F \cdot sin(\omega \cdot t) \tag{1.1}$$

Here $\omega[rad/s]=2\cdot\pi\cdot f_e$ is the angular frequency, which is the same for force, voltage and current, while $f_e[Hz]$ is the frequency of exciting force.

As a result, in stationary regime, the mass m has a harmonic motion $x(t)$ given by:

$$x(t)=A\cdot sin(\omega\cdot t-\alpha) \tag{1.2}$$

Here $A[m]$ is the motion amplitude given by [13]:

$$A=\frac{F}{k}\cdot\frac{1}{\sqrt{(1-\eta^2)^2+(2\cdot\eta\cdot\xi)^2}}=\frac{F}{k}\cdot A_0 \tag{1.3}$$

and $\alpha[rad]$ is the phase angle between the exciting force F_e and the motion $x(t)$ given by [13]:

$$tan(\alpha)=\frac{2\cdot\xi\cdot\eta}{1-\eta^2} \tag{1.4}$$

In Eqs. 1.3 and 4 η is the relative angular frequency $\eta=\omega/p$, $p[rad/s]$ is the undamped angular frequency, $p=\sqrt{k/m}$ and $\xi[1/rad]$ is the damping ratio, $\xi=c/(2\cdot m\cdot p)$, with $c[N\cdot s/m]$ the viscous damping coefficient .

If the damping ratio ξ is very small, the resonance of the mass-spring-damper system is produced when $\omega\rightarrow p$ thus $\eta\rightarrow 1$, the factor A_0 and the amplitude A of the motion $x(t)$ from Eq. 1.3 has the highest value possible.

There is, of course, a mechanical work produced by the exciting force, thus a mechanical power *N(t)* produced by the actuator and absorbed by the mechanical system, given by:

$$N(t) = F_e(t) \cdot \frac{dx}{dt} \tag{1.5}$$

Using Eqs. 1.1, 1.2 and 1.3 the mechanical power *N(t)* becomes:

$$N(t) = F \cdot sin(\omega \cdot t) \cdot \frac{F}{k} \cdot A_0 \cdot \omega \cdot cos(\omega \cdot t - \alpha) \tag{1.6}$$

If $T=2 \cdot \pi / \omega [s]$ is the period of the harmonic evolution of the exciting force, then:

$$\overline{N} = \frac{1}{T} \cdot \int_0^T N(t) \cdot dt = \frac{F^2 \cdot \omega \cdot A_0}{2 \cdot k} \cdot sin(\alpha) \tag{1.7}$$

is the average mechanical power absorbed by the system in the period *T*.

Based on the last result, it is possible to describe the average mechanical power as:

$$\overline{N} = F_{rms} \cdot V_{rms} \cdot cos(\theta) \tag{1.8}$$

Here $F_{rms} = F / \sqrt{2}$ is the root mean square exciting force, $V_{rms} = \omega \cdot A_0 / (k \cdot \sqrt{2})$ is the root mean square velocity and $\theta = \pi/2 - \alpha$ is the phase angle between exciting force F_e and vibration velocity *dx/dt*.

Using A_0 given in Eq. 1.3 and the definition of *sin(α)* deduced [11] from Eq. 1.4, the average mechanical power from Eq. 1.7 becomes:

$$\overline{N} = \overline{N}(\omega, p, \xi) = \frac{F^2}{k} \cdot \frac{\omega \cdot \xi \cdot \eta}{(1-\eta^2)^2 + (2 \cdot \eta \cdot \xi)^2} \tag{1.9}$$

In stationary regime of excitation the average mechanical power is absorbed from the actuator and is dissipated as heat in the damper. It has the highest possible value on the resonance frequency and it is asymptotic to zero at lower and higher frequencies as proved below in the experimental results shown in Fig. 1.5(a).

The average mechanical power can be evaluated using a force sensor (placed between the actuator and the mass *m*) and an absolute velocity sensor (placed on the mass).

The power can be calculated using Eq. 1.5 and the first part of Eq. 1.7.

1.3 NUMERICAL MEASUREMENT TECHNIQUE OF THE MECHANICAL POWER

There is an easier way to measure the average mechanical power, without any additional sensor on the Fig. 1.1 set-up. It can be used the electrical power *P(t)* absorbed by the coil:

$$P(t) = u(t) \cdot i(t) \tag{1.10}$$

Here $u(t)=U\cdot sin(\omega\cdot t)$ is the input voltage applied on the actuation coil, $i(t)=I\cdot sin(\omega\cdot t-\varphi)$ is the current inside the coil, U is the voltage amplitude, I is the current amplitude, φ is the phase angle between voltage and current.

The absorbed average electrical power (also called active electrical power) in the period $T=1/f_e$ is given by:

$$\overline{P}=\frac{1}{T}\cdot\int_0^T P(t)\cdot dt=\frac{1}{T}\cdot\int_0^T u(t)\cdot i(t)\cdot dt \qquad (1.11)$$

The mathematical calculus in Eq. 1.11 gives the result:

$$\overline{P}=U_{rms}\cdot I_{rms}\cdot cos(\varphi) \qquad (1.12)$$

Here $U_{rms}=U/\sqrt{2}$ is the root mean square voltage (also called effective voltage), $I_{rms}=I/\sqrt{2}$ is the root mean square current.

It is very interesting to remark the analogy between Eq. 1.12 (description of electrical power) and Eq. 1.8 (description of mechanical power).

The measurement and calculus of the average electrical power according with Eq. 1.12 is relatively difficult. This is why a numerical technique has been developed, as it is described below.

Let us assume that $u_A(t)=u(t)$ and $u_B(t)$ are the voltages measured in the points A and B, (on Fig. 1.1). The electrical ground is used as voltage reference.

The current $i(t)$ inside the coil can be calculated using the voltage $u_B(t)$ with the formula $i(t)=u_B(t)/R$, according to Ohm's law

(measuring a current using a shunt resistor $R=1.9\ \Omega$). Both voltages $u_B(t)$ and $u_A(t)$ can be acquired and converted (from analogue signals to discrete time signals) using a numerical oscilloscope with two input channels and can be transferred to a personal computer for calculus (Fig.1.1).

Let us consider that Δt is the sampling period of data acquisition, $t_j=j\cdot\Delta t$ is the time of the current sample and n is the number of samples in each period T (calculated as the nearest integer of the ratio $T/\Delta t$). The numerical evaluation of the average electrical power given in Eq. 1.11 becomes:

$$\overline{P} \approx \frac{1}{R\cdot n}\cdot \sum_{j=1}^{n} u_A(t_j)\cdot\ u_B(t_j) \qquad \text{with} \quad t_j = j\cdot\Delta t \tag{1.13}$$

If $\Delta t \rightarrow 0$ then in Eq. 13 the symbol ≈ becomes =. Suppose that the frequency f_e of the exciting force is constant and that it is necessary to evaluate the average electrical power for a long time t_m. Suppose that the time t_m is marked as $t_m = m\cdot T = m\cdot n\cdot\Delta t$. Assume that $t_s = l\cdot T = l\cdot n\cdot\Delta t$ is the time of the average electrical power sample (one sample in each period T), with $l=1, 2, 3\ldots m$. The average electrical power sample can be marked (and calculated) as it follows:

$$\overline{P}(t_s) \approx \frac{1}{R\cdot n}\cdot \sum_{j=n\cdot l+1}^{n\cdot(l+1)} u_A(t_j)\cdot\ u_B(t_j) \quad \text{with } l = 0,1,2,\ldots..,m \tag{1.14}$$

If *MS* is switched-off, then a part of the average electrical power $\overline{P}(t_s)$ absorbed by the coil is used to produce the average mechanical

power $\overline{N}(t_s)$ absorbed by the mass-spring-damper system, as it is described below:

$$\overline{P}(t_s) \approx \overline{P}_h + \frac{\overline{N}(t_s)}{\mu} \tag{1.15}$$

Here $\overline{P}_h$ is the average electrical power dissipated as heat in the coil and in the resistor *R[Ω]* (according with Fig. 1.1), *μ[]* is the power conversion efficiency (from electrical into mechanical, $\mu<1$). If we suppose that $\overline{P}_h$ is constant, its value can be estimated using Eq. 1.15. If the coil is supplied and the mechanical switch *MS* is switched-on, then *x(t)=0* (no vibratory motion) and $\overline{N}(t_s)$ is null. This means that $\overline{P}(t_s) \approx \overline{P}_h$.

Based on Eq. 1.15 the average mechanical power sample can be calculated as follows:

$$\overline{N}(t_s) \approx \mu \cdot [\overline{P}(t_s) - \overline{P}_h] \tag{1.16}$$

A power conversion efficiency $\mu=1$ will be considered in experimental research. The time evolution of the average mechanical power given in Eq. 1.16 is used for data analysis or monitoring purposes of this paper.

1.4 EXPERIMENTAL SET-UP AND EQUIPMENT

Fig. 1.2 shows an overview of the experimental set-up and equipment. The mass-spring-damper system consists of an Aluminium

cantilever beam (200×40×2 mm) with an excitation coil and a Bruel & Kjær 4302 accelerometer placed at the free end of the beam. The system has a low viscous damping ratio (ξ *=0.44%*). The linear vibrating motion *x(t)* used in Fig. 1.1 is replaced here by the bending motion (first flexural mode of the free end of the cantilever beam).

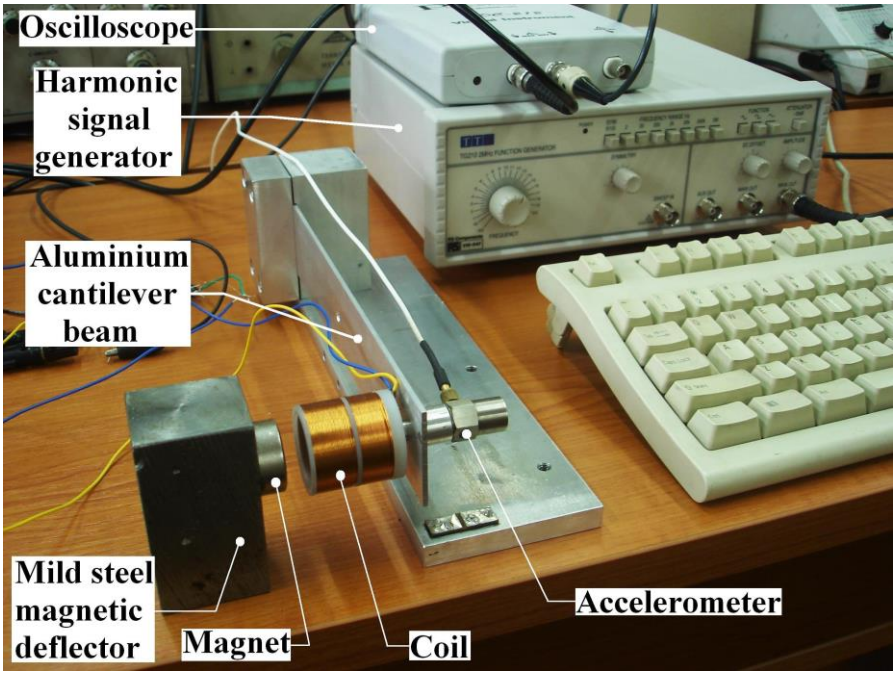

Fig. 1.2: *A view on the experimental set-up and equipment.*

The voice-coil actuator consists of the excitation coil and a rare-earth neodymium-iron-boron permanent magnet (NdFeB) placed on a mild steel magnetic deflector. The magnet generates a strong radial magnetic field inside the coil. The coil is supplied by a harmonic signal generator (TTi, TG 210) with adjustable frequency. The interaction between the magnetic field and the current in the coil generates a Lorentz force which actuates the beam. The electrical and mechanical

switches *ES* and *MS* (see Fig. 1.1) are hand operated. The voltages $u_A(t)$ and $u_B(t)$ are acquired using a computer assisted numerical oscilloscope (ADC 212-50, PicoScope Technology, UK). Several computer assisted calculation procedures and programms were created in Matlab, for experimental research, data processing, signal filtering and data fitting.

1.5 THE MEASUREMENT OF THE ABSORBED MECHANICAL POWER IN EXPERIMENTAL TERMS

The reliability of the proposed measurement technique of the mechanical power can be established using some experimental procedures described below.

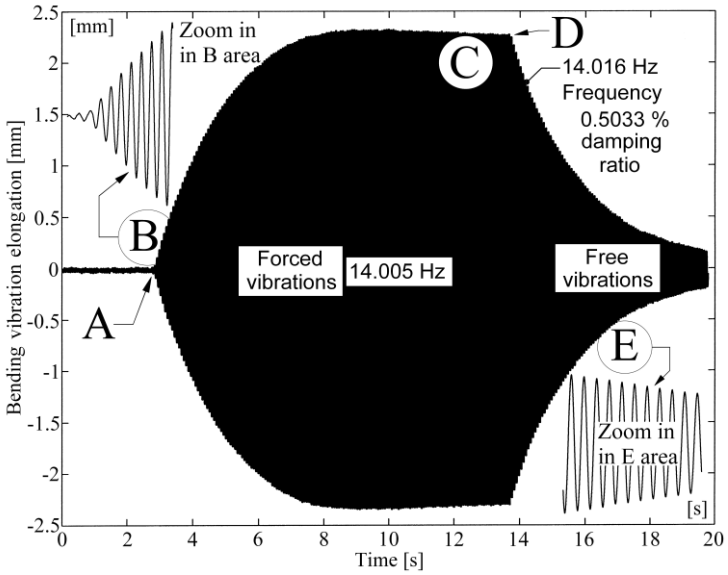

Fig. 1.3: *The evolution of forced bending vibration (close to resonance frequency of first mode) and free bending vibration* (***see the chapter 1.12***).

A first experiment describes the behaviour of the cantilever beam if the coil is temporary supplied with a voltage $U_{rms}=418\ mV$ and an exciting frequency $f_e = 14.005\ Hz$ (very close to first bending mode resonance frequency). The mechanical switch *MS* is permanently switched-off. Fig. 1.3 presents the bending vibration elongation evolution of the free end of the cantilever beam (the signal provided by accelerometer was converted in elongation). A short description of the vibration amplitude evolution is given in Table 1.1. If the electrical switch *ES* is switched-on (in A) then immediately after that (in B) the amplitude of vibrations starts to slowly increase; it is expected that the cantilever beam system should start to absorb more and more mechanical power and also to accumulate modal energy inside. In C the vibration amplitude and modal energy is maximal; the absorbed mechanical power is expected to be maximal and constant. In D the *ES* is switched-off, the excitation force drops to zero (as the absorbed mechanical power also does). In E the viscously damped free vibration is supplied by the mechanical modal energy stored inside the beam.

A	**B**	**C**	**D**	**E**
ES is switched on. Start harmonic excitation on 14.0056 Hz	The vibration amplitude slowly increases. It is presumed that the absorbed mechanical power increases.	Steady state regime with maximal amplitude. It is presumed that the absorbed mechanical power is maximal and constant.	*ES* is switched off. Stop excitation. The absorbed mechanical power becomes instantly zero.	Viscously low damped free vibration on 14.016 Hz (ξ = 0.5033%)

Table 1.1 – *A short description of the vibration amplitude evolution from Fig. 1.3.*

Let us consider a second experiment. Suppose that the actuation coil is permanently supplied as before (the same voltage and frequency values) with *ES* in switched-on status. Concerning Fig. 1.3 and A, B and C events, the same behaviour of the cantilever beam can be obtained using the mechanical switch *MS* (if it is switched-off in A). If *MS* is switched-on (in D) the vibration amplitude suddenly becomes zero, the motion is cancelled. It is expected that the absorbed mechanical power should also suddenly become zero. The mirroring of this second experiment in the evolution of the absorbed average mechanical power is given in Fig. 1.4(a). A short description of each event (A_1, B_1, C_1, D_1 and E_1) is given in Table 1.2.

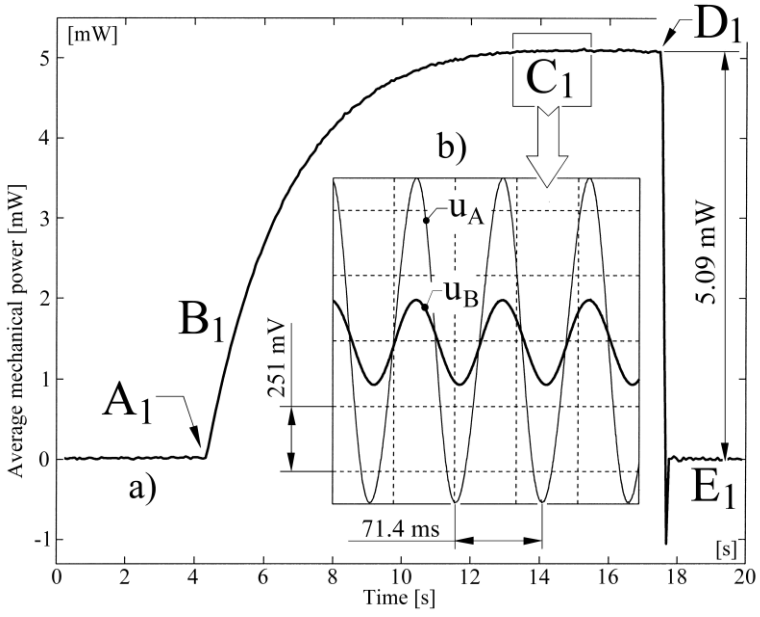

Fig. 1.4: *Experimental results:* ***a)*** *the evolution of absorbed average mechanical power at resonance,* ***b)*** *the evolution of u_A and u_B voltages.* (***see the chapter 1.12***)

The absorbed average mechanical power at resonance (steady-state regime) is 5.09 mW (the difference between levels in D_1 and E_1). In Eq. 1.14 was used these measurement parameters values: *n=218, Δt = 0.328 ms* and *m = 278*.

A1	**B1**	**C1**	**D1**	**E1**
MS is switched-off. The average mechanical power has null value. $\overline{P}_h = 19.6mW$. This is also the miroring of event A from Fig. 3.	The absorbed average mechanical power slowly increases. This is also the miroring of event B from Fig. 3.	Steady state regime. The absorbed average mechanical power has maximal and constant value, $\overline{N} = 5.09mW$. This is also the miroring of event C from Fig. 3.	*MS* is switched-on. Stop vibratory motion.The absorbed average mechanical power becomes zero.	Because *MS* is switched-on, the absorbed average mechanical power is nought.

Table 1.2 - *Short description of the evolution from Fig. 1.4*

In Fig. 1.4(b) are described also the evolution of u_A and u_B voltages used to calculate the average mechanical power in C_1. The phase angle φ is very small (6.5^o) because the coil inductance and the frequency of excitation have small values.

Thus it has proved that the measurement of the absorbed average mechanical power can be done with good accuracy. It is clear that the average mechanical power evolution is useful to describe the dynamics of the vibratory systems (see also next results).

According to Figs. 1.3 and 1.4 when the free end of the cantilever beam starts to be excited on resonance frequency (here the first flexural mode) the vibration amplitude and the modal mechanical power absorbed doesn't touch instantly the maximal values.

1.6 EXPERIMENTAL CONFIRMATION OF THE THEORETICAL PREDICTION

The theoretical model for the absorbed mechanical power established in Eq. 1.9 can be confirmed by the experimental measurements and data processing as it follows.

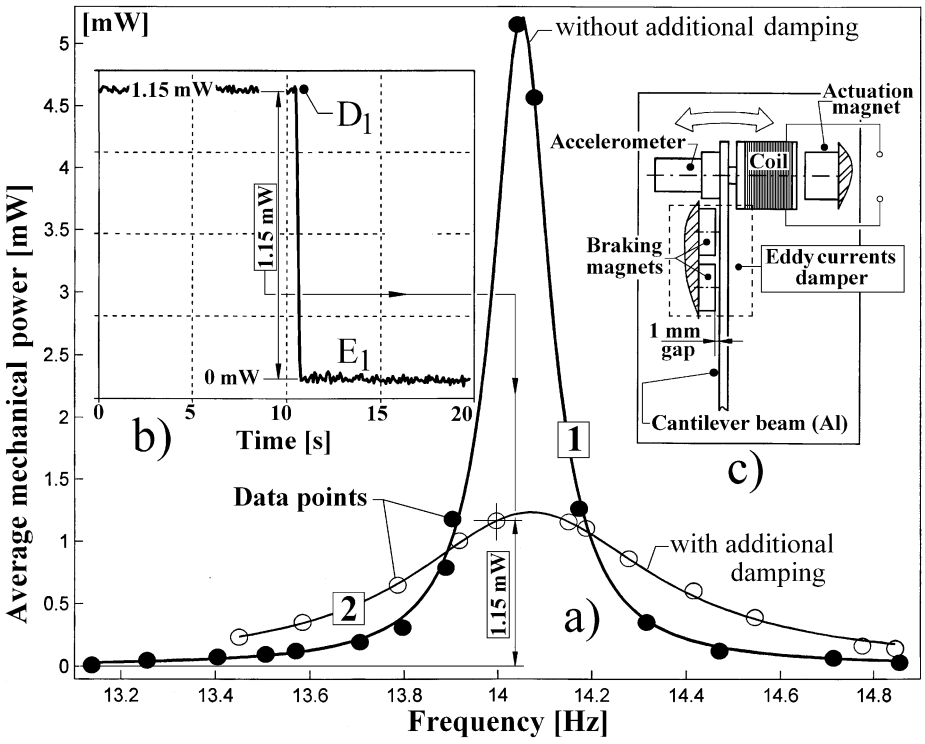

Fig. 1.5: *Experimental confirmation:* ***a)*** *curves fitting (average mechanical power versus frequency f_e),* ***b)*** *experimental measurement,* ***c)*** *passive damping technique at free end of the cantilever beam.*

By using the same set-up and measurement technique (U_{rms}*=418 mV* voltage), the absorbed average mechanical power for a narrow range of exciting frequencies around the resonant value (first bending/flexural mode of the free end of the cantilever beam) can be measured in the same way (the difference of power between D_1 and E_1 levels, see Fig. 1.4). Each measurement generates a data point. Using computer aided curve fitting, the experimental data points can be interpolated. Eq. 1.9 is used as fitting function (with $\omega=2\cdot\pi\cdot f_e$ the angular frequency). The objective of data interpolation is to find the values of the fitting parameters F^2/k, p and ξ. The graphical result is described in Fig. 1.5(a), curve #1.

The values of the fitting parameters are given in the first row of the Table 1.3. The first confirmation of the theoretical model of average mechanical power evolution is the shape of the curve #1 [8, 11] and the data point position on the curve.

	$\boldsymbol{F^2/k}$ *[N·m]*	$\boldsymbol{p}$ *[rad·s^{-1}]*	$\boldsymbol{\xi}$ *[rad $^{-1}$]*
Curve **#1**	$1.232\cdot10^{-6}$	88.2744 (**14.049 Hz**)	0.0052 (**0.52%**)
Curve **#2**	$1.234\cdot10^{-6}$	88.4182 (**14.072 Hz**)	0.0221 (**2.21%**)

Table 1.3 - *The values of the fitting parameters*

The second confirmation is given by the values of fitting parameters: $p/(2\cdot\pi)$ *= 14.049 Hz* frequency and ξ *= 0.0052* damping ratio (0.52%). These values are very close to those already found in Fig. 1.3 (viscously damped free vibration signal analysis, see the event E in Table 1.1).

The reliability of the mechanical power measurement technique and the theoretical prediction can also be confirmed by a new experiment. The damping in the cantilever beam system is increased using a passive damping technique based on eddy-curents [14], as it is described on Fig. 1.5(c). Two neodymium-iron-boron (NdFeB) permanent magnets are placed in the proximity of the free end of the cantilever beam (1 mm gap). The cantilever motion in magnetic field generates eddy-currents in the cantilever material (aluminium). The interaction between these currents and the magnetic field generates a viscous friction braking force. The experimental measurements of the absorbed average mechanical power and curve fitting data interpolation were done in the same condition as previously for curve #1. The graphical result is described on curve #2, Fig. 1.5(a). The values of the fitting parameters are described in the second row of the Table 1.3.

As expected, the absorbed average mechanical power at resonance is strongly reduced. According to Table 1.3 only the damping ratio is significantly changed: $\xi = 0.0221$ (2.21%).

It has been proved that the cantilever beam set-up works as a narrow-band-pass absorber for the mechanical modal power delivered by the actuation system. The amount of modal power absorbed at resonance depends on the damping ratio value. A single degree of freedom mass-spring-damper system has a minimal mechanical impedance[1] (or maximal mechanical admittance as well) on the resonance frequency. These are solid arguments to explain the behaviour of the passive dynamic absorbers (Ormondroyd [15]) also known as tune mass dampers. The actuating coil used here to excite the

cantilever beam transforms the mechanical impedance into electrical impedance.

1.7 EXPERIMENTAL CONDITIONS VALIDATION BY SIMULATION

The values of the fitting parameters which were found before can be used by computer assisted numerical simulation, to increase the confidence in the experimental conditions previously utilised. As an example, the experimental evolution from Fig. 1.3 can also be obtained by simulation. We already assumed that the cantilever beam can be approximated by a single degree of freedom mass-spring-damper system (for first flexural mode of vibration). The homogenous differential equation of this system (without additional damping) is described [13] as it follows:

$$\frac{d^2x}{dt^2} + 2 \cdot \xi \cdot p \cdot \frac{dx}{dt} + p^2 \cdot x = 0 \tag{1.17}$$

Using the values of the fitting parameters of the curve #1 (see Fig. 1.5 (a) and Table 1.3, first row) this equation can be written in the following manner:

$$\frac{d^2x}{dt^2} + 0.9180537 \cdot \frac{dx}{dt} + 7792.37 \cdot x = 0 \tag{1.18}$$

Based on this equation it is possible to generate the Simulink model of the experiment described in Fig. 1.3.

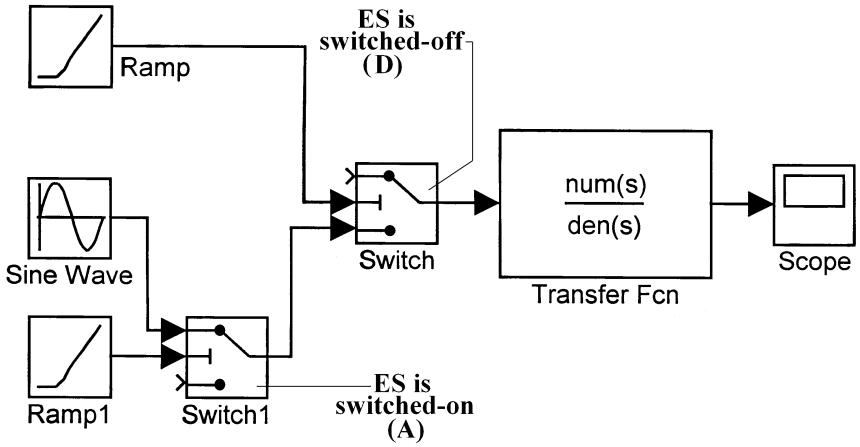

Fig. 1.6: *Simulink model of the experimental results described in Fig. 1.3.*

This model is shown in Fig. 1.6. The parameters used for each block in the model are described in Table 1.4.

Ramp block	Slope=0.6 Start time=0 Initial output=1
Ramp1 block	Slope=3 Start time=0 Initial output=1
Sine Wave block	Amplitude=0.030 Frequency (rad/s)=87.99
Switch block	u2>=Treshold Threshold=10
Switch1 block	u2>=Treshold Threshold=10
Transfer Fcn block	Numerator [0.9180537 7792.37] Denominator [1 0.9180537 7792.37]
Scope	Simulation time: Start time=0; Stop time=20;

Table 1.4 - *Block parameters used in the Simulink model (Fig. 1.6).*

The simulation done on this Simulink model gives a graphical result (available on the Scope block) which reproduces with high accuracy the experimental result described in Fig. 1.3.

1.8 NEGATIVE MECHANICAL POWER CONCEPT IN VIBRATION ENGINEERING

Usually, when a vibrating structure is excited, it is easy to understand what positive absorbed average mechanical power exactly means. An interesting question arises: *can absorbed average mechanical power be negative?* And if so, can negative power be useful in vibration engineering?

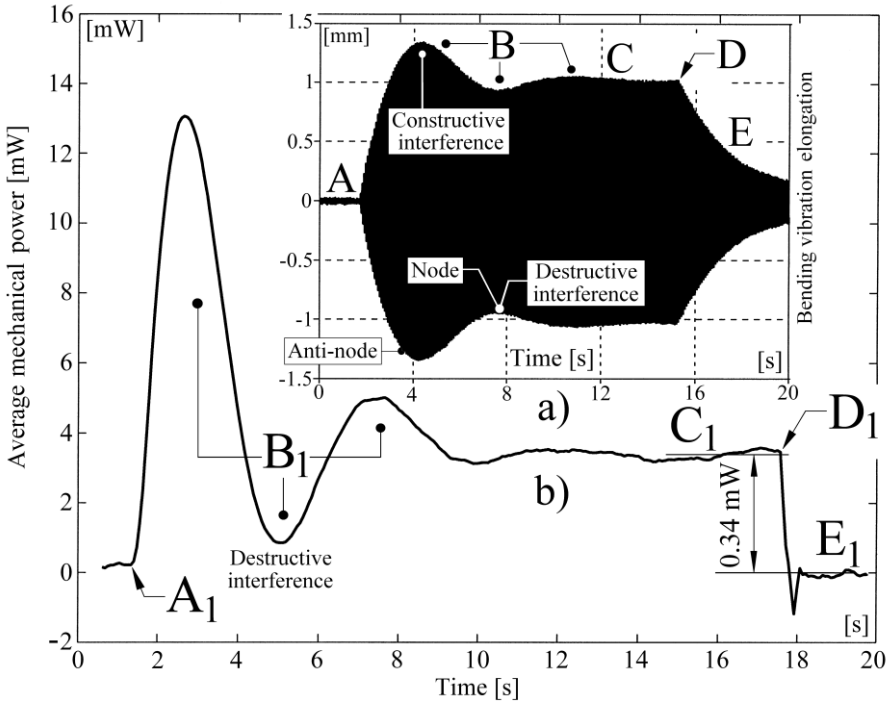

Fig. 1.7: *Self generated beat vibration:* ***a)*** *mirrored in elongation evolution,* ***b)*** *mirrored in average mechanical power evolution* ***(see the chapter 1.12).***

The negative absorbed average mechanical power has been experimentally observed during the transient regimes of excitation with beat vibration. Fig. 1.7(a) describes a first experiment with self generated beat vibration phenomenon; Fig. 1.7(b) describes the mirroring of beat vibration in the evolution of average mechanical power.

The experiments were done exactly in the same conditions previously used before for the experiment described in Figs. 1.3 (see Table 1.1) and 1.4 (see Table 1.2). The only difference consists in the frequency of the exciting force, *13.84 Hz*, lower than the resonance frequency of the first bending mode of the cantilever beam.

In Fig. 1.7(a) the variation of the amplitude in B area is connected to a beat vibration phenomenon. According to the vibration theory, when the electrical switch *ES* is switched-on (the event A) free and forced vibrations are generated in the cantilever beam. The viscously damped free vibrations are also generated if *ES* is switched-off (as indicated in E on Figs. 1.7(a) and 1.3). The viscously damped free vibrations (*14.005 Hz, ξ =0.0044*, according to Table 1.1) and forced vibrations (*13.84 Hz*) generates a transient regime with destructive and constructive interference, with nodes and anti-nodes (beat vibration). While in anti-nodes the resultant amplitude increases (zero phase-shift between free and forced vibrations, with constructive interference), in nodes the resultant amplitude decreases because the free and forced vibrations are out of phase (π phase-shift, with destructive interference). It is important to notice that the experimental evolution described in Fig. 1.7(a) can also be obtained by simulation,

using the model given in Fig. 1.6. Only the frequency of the Sine Wave block was changed (Frequency (rad/s) = 86.89, see Table 1.4).

On Fig. 1.7(b) it is evident that the transient phenomenon in B_1 is the mirroring of the beat vibration phenomenon previously described in B on Fig. 1.7(a). The absorbed mechanical modal power increases when the constructive interference of vibrations is produced and decreases when this interference is destructive.

Let us consider a second experiment with beat vibration phenomenon mirrored in vibration elongation and average mechanical power evolution, with the experimental results described in Fig. 1.8.

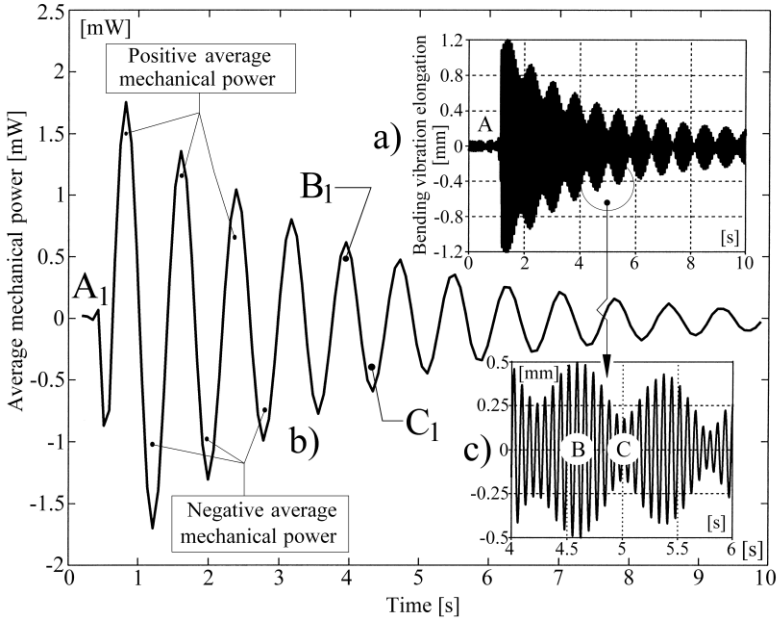

Fig. 1.8: *Beat phenomenon with negative average mechanical power:* ***a)*** *in elongation evolution,* ***b)*** *in average mechanical power evolution,* ***c)*** *zoom-in on elongation evolution* **(*see the chapter 1.12*).**

Exactly as before, the voice coil actuator is permanently electrically supplied, but the excitation frequency is smaller, *12.79 Hz* (lower than previously). In A *ES* switch is switched-on, *MS* switch is off. The cantilever beam vibrates with low amplitude (0.05 mm).

The first bending mode of the cantilever beam is mechanically excited with a step excitation (see the events A on Fig. 1.8(a) and A_1 on Fig. 1.8(b)). A viscously damped free vibration occurs. The beating vibration phenomenon which is generated (free and forced vibrations interference) is described on Fig. 1.8(a). Figure 1.8(c) presents a zoom of Fig. 1.8(a). An anti-node (in B) and a node (in C) are clearly indicated. The mirroring of the beating in the average mechanical power evolution is described in Fig. 1.8(b). There is an evolution with positive and negative peaks of the absorbed average mechanical power (as free damped oscillation of power).

The constructive interference generates anti-nodes, e.g. B on Fig. 1.8(c), and positive peaks of power, e.g. B_1 on Fig. 1.8(b). According to Eq. 1.8 ($\overline{N} = F_{rms} \cdot V_{rms} \cdot cos(\theta)$) the absorbed average mechanical power has maximum value if the phase-shift between the excitation force and the velocity of vibration motion is $\theta = 0$ (or, according to Eq. 1.7 the phase-shift between the excitation force and the elongation of vibration motion is $\alpha = \pi/2$). The voice coil actuator and the harmonic signal generator increase the modal energy stored inside the cantilever beam and the amplitude of the vibratory motion as well.

The destructive interference generates nodes, e.g. C on Fig. 1.8(c), and negative peaks of power, e.g. C_1 on Fig. 1.8(b). According to Eq. 1.8

($\overline{N} = F_{rms} \cdot V_{rms} \cdot cos(\theta)$) the power reaches its minimum value if the phase-shift between the excitation force and the velocity of vibration motion is $\theta = \pi$ (or, according to Eq. 1.7 the phase-shift between the excitation force and the elongation of vibration motion is $\alpha = 3 \cdot \pi/2$). Now the voice coil actuator and the harmonic signal generator work as an active damping system. It removes the modal energy stored inside the cantilever beam and reduces the amplitude of the vibratory motion. Moreover, it also works as an active negative mechanical modal power supply for the cantilever beam vibration mode (energy harvesting).

These conclusions are very useful in vibration engineering. To excite a vibratory structure means to actuate it with a positive mechanical modal power supply. To damp a vibratory motion in a structure means to actuate it with a negative mechanical modal power supply. A negative mechanical modal power supply generates a force directly proportional to the velocity (and π shift of phase between), or it generates a force directly proportional to the velocity and a force-displacement shift of phase of $3 \cdot \pi/2$. The damping can be active (active damping or synthetic damping as well, generated by an actuator and an electrical power supply) and passive (using a classical viscous damper or a passive dynamic absorber [15]). The active damping is briefly described in Fig. 1.9(a). We propose a conceptual technique, to generate active damping using a voice-coil actuator supplied by an active negative electrical modal power supply. In other words this power supply is used to absorb and to dissipate a maximum amount of modal energy delivered by the vibratory structure via the voice-coil

actuator. Of course, the negative modal power supply is a receiver and not a generator.

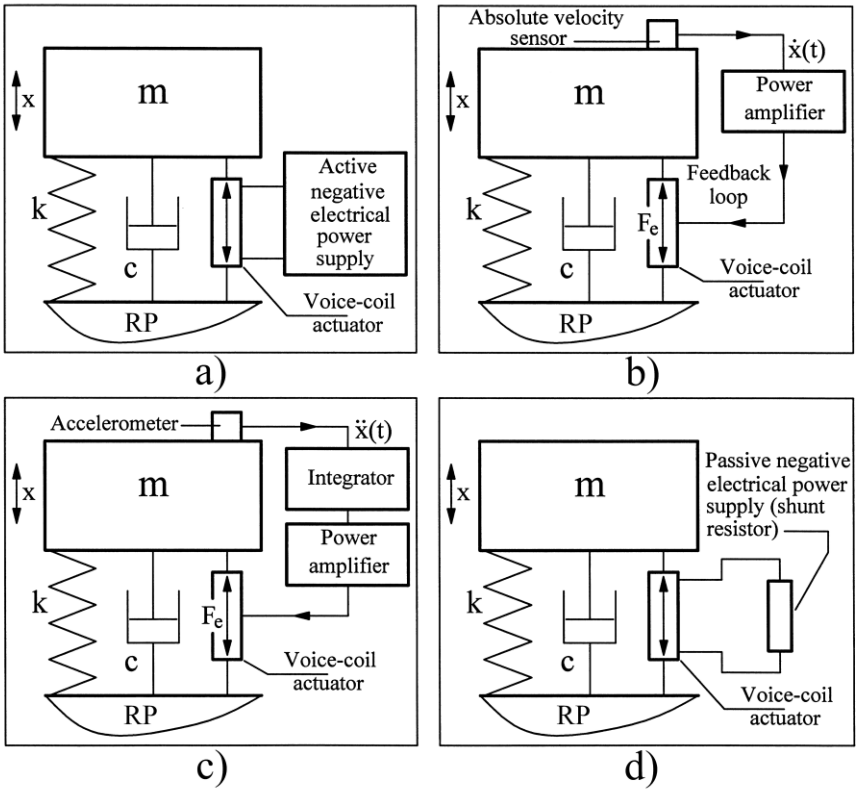

Fig. 1.9: *Synthetic damping with negative modal power supply :* ***a)*** *proposed technique,* ***b)*** *active damping with velocity-force feedback,* ***c)*** *active damping with acceleration-force,* ***d)*** *passive damping with shunt resistor*

A difficult first question arises: *how exactly can this special electrical power supply be obtained?* This is the greatest challenge of future work. We have already proved the availability of this technique in experimental condition (Fig. 1.8) and understood that the voice coil

actuator works as sensor and actuator as well. It seems that the active negative power supply should measure the voltage generated by the coil (velocity sensor) and to generate a current in the coil (hence an actuating Lorentz force).

A second question should also preoccupy us: *is it possible to create such a power supply*? The answer is yes, according to the scientific literature and Figs. 1.9 (b), 1.9 (c) and 1.9 (d).

A known technique in the field of vibration uses the active damping with negative feedback [16, 17]. A feedback loop whose input is velocity generates a proportional force. The force and the velocity have opposite directions.

According to Fig. 1.9 (b), this technique uses an absolute velocity sensor, a power amplifier and a voice-coil actuator. The sensor and the actuator must be collocated. The actuator generates an active damping viscous force $F_a=c_a \cdot dx/dt$ with $c_a<0$. If $c_a>0$ then the feedback is positive. In Fig. 1.9 (b) the active negative electrical power supply consists of a velocity sensor and a power amplifier. If an accelerometer is used as sensor, then an integrator should be used inside the feedback loop, as it is indicated in Fig. 1.9 (c). In comparison to Fig. 1.9 (a), both structures (Figs. 1.9 (b) and 1.9 (c)) need a sensor collocated with the actuator.

Based on a passive shunt placed as electric consumer on the voice coil actuator (de Marneffe [18]), an extremely simple solution to create a negative power supply can be found. In Fig. 1.9 (d) the passive shunt is a resistor. The vibratory motion generates a voltage in the coil (sensor behaviour). The voltage is proportional to the velocity. The voltage

generates a current. The current generates a damping force applied to the mass *m* (Lorentz force actuator behaviour). The force is directly proportional to the velocity, and inversely proportional to the ohmic resistance of the electrical circuit (coil and shunt resistor). The modal energy is removed and dissipated as heat produced by the resistor. Nevertheless, even if the shunt resistance is nought, the viscous force generated is not high enough because of the ohmic resistance of the coil.

1.9 HYPOTHESES FOR FUTURE RESEARCH

In a simplistic approach, the behaviour of the active negative electrical modal power supply (Fig. 1.9 (a)) can be obtained in the experimental conditions used in Fig. 1.8. Supposing that each time that the absorbed average mechanical power becomes positive (or $\overline{P}(t_s) > \overline{P}_h$) the electrical switch *ES* is switched-off. The electrical switch *ES* is switched-on only if this power is negative (or $\overline{P}(t_s) < \overline{P}_h$). If the vibratory system is mechanically excited then the beat vibration phenomenon occurs but only the destructive interference is used, so that a permanent damping has effect.

There is also another option based on the principle shown in Fig. 1.9 (d). Given R_c the voice-coil ohmic resistance value ($R_c>0$) and R_s the ohmic resistance value of the shunt resistor, the highest efficiency in damping is theoretically generated if $R_c+R_s \rightarrow 0$ so $R_s \rightarrow -R_c$. A negative shunt resistor (as electrical supplied electronic device or active shunt

[18]) should be an equivalent of the active negative electrical power supply. Nevertheless, for now, producing resistors with negative resistance (Wang [19]) seems to be a great technological challenge.
Last, but not least, there is a third option based on Eq. 1.8. The active negative electrical modal power supply should detect the velocity and the phase of the velocity of a mode of vibration and generate an exciting force directly proportional to the velocity and π shift of phase. The voice-coil is used as sensor and actuator.

1.10 CONCLUSIONS

The computer assisted measurement technique of the average mechanical power absorbed by an actuated vibratory system is a reliable tool in experimental research. The experimental set-up based on a cantilever beam actuated by a voice coil actuator assures credibility to the results of the research. The voice coil actuator is used as loading sensor for output mechanical power, based on the measurement of the input electrical power. The theoretical model for the evolution of the mechanical power versus the frequency of excitation was validated by the experimental results. The absorbed average mechanical power evolution can be used to describe the dynamic behaviour of the vibratory systems. The paper also performs an experimental research on a transient regime (beat vibration) with negative mechanical power absorbed from the actuator. Based on this research the paper proposes a conceptual technique to generate active damping using a voice-coil actuator supplied by an active negative

electrical modal power supply. In the future the research will focus on the synthesis of this power supply. Some research on power flows in dynamic systems actuated with piezoelectric actuators will also be carried out.

1.11 REFERENCES

1. Benassi, L., Elliot S. J., (2005), The equivalent impedance of power-minimising vibration controllers on plates, *Journal of Sound and Vibration*, Vol. 283, pp. 47-67, 2005.
2. Mak, C. M., Yun, Y., (2010), A study of power transmissibility for the vibration isolation of coherent vibratory machines on the floor of a building, *Applied Acoustics*, Volume 71, Issue 4, pp. 368-372, 2010.
3. Mandal, N. M., Rahman, A. R., Salman Leong, M. S., (2005), Experimental investigation of vibration power flow in thin technical orthotropic plates by the method of vibration intensity, *Journal of Sound and Vibration*, Volume 285, Issue 3, pp. 669-695, 2005.
4. Renji, K., Mahalakshmi, M., 2006, High frequency vibration energy transfer in a system of three plates connected at discrete points using statistical energy analysis, *Journal of Sound and Vibration*, Volume 296, Issue 3, pp. 539-553, 2006.
5. Howard, C. Q., Hansen, C. H., (2005), Six-Axis Vibrational Power Transducer for Active Vibration Isolation, *Proceedings of ACOUSTICS 2005*, 9-11 November 2005, Busselton, Western Australia.
6. Xie, S., Siu, Or, W., Chan, H. L.W, Choy, P. K., Liu, P. C. K., (2007), Analysis of vibration power flow from a vibrating machinery to a

floating elastic panel, *Mechanical Systems and Signal Processing*, Volume 21, Issue 1, January 2007, pp. 389-404.

7. Glynne-Jones, P., Tudor M. J., Beeby, S. P., White N.M., (2004), An electromagnetic, vibration-powered generator for intelligent sensor systems, *Sensors and Actuators A: Physical*, Volume 110, Issues 1-3, pp. 344-349, 2004.
8. Sari, I., Balkan, T., Kulah, H., (2008), An electromagnetic micro power generator for wideband environmental vibrations, *Sensors and Actuators A: Physical*, Volumes 145-146, pp. 405-413, 2008.
9. Stephen N.G., (2006), On energy harvesting from ambient vibration, *Journal of Sound and Vibration*, Volume 293, Issues 1-2, pp. 409-425, 2006.
10. Fujii, Y., Maru, K.,Jin, T., (2010), Method for evaluating the electrical and mechanical characteristics of a voice coil actuator, *Precision Engineering*, Volume 34, Issue 4, pp. 802-806, 2010.
11. Lewin, Walter, 8.03 Physics III: Vibrations and Waves, Fall 2004. (Massachusetts Institute of Technology: MIT OpenCourseWare), http://ocw.mit.edu/courses/physics/8-03-physics-iii-vibrations-and-waves-fall-2004/video-lectures/embed04/ (Accessed 31 Dec, 2009). License: Creative Commons BY-NC-SA
12. Paulitsch, C., P. Gardonio, P., Elliott, S.J., Sas, P., Boonen, R., (2004), Design of a Lightweight, Electrodynamic, Inertial Actuator with Integrated Velocity Sensor for Active Vibration Control of a Thin Lightly-Damped Panel," *Proceedings of ISMA. ISMA 2004: International Conference on Noise and Vibration Engineering*, Leuven, Belgium, ISMA Publications, pp. 239-254, 2004.

13. Thomas, M. and Laville, F., (2007), Simulation des vibration mécaniques par Matlab, Simulink et Ansys, Université du Québec, ISBN 978-2-9211-4562-6, 2007.
14. Sodano, A.H., Bae, J.S., Inman D.J., Belvin, K.V., (2006), Improved Concept and Model of Eddy Current Damper, In: Transactions of ASME, *Journal of Vibration and Acoustics*, Vol. 128, Issue 3, pp. 294-302, 2006.
15. Ormondroyd, J., den Hartog, J. P., (1928), The theory of the dynamic vibration absorber, *Transactions of the American Society of Mechanical Engineers, Journal of Applied Mechanics*, Vol. 50, Issue 7, A9-A22, 1928.
16. Preumont, A., (2002), Vibration Control of Active Structures: an Introduction," Kluwer, 2nd edition, 2002.
17. Abu Hanieh, A., (2003), Active Isolation and Damping of Vibrations via Stewart Platform," PhD thesis, Université Libre de Bruxelles, 2003.
18. de Marneffe, B., (2007), Active and Passive Vibration Isolation and Damping via Shunted Transducers, PhD Thesis, Université Libre de Bruxelles, 2007.
19. Wang, S., Chung, D.D.L., (1999), Apparent negative electrical resistance in carbon fiber composites, *Composite Part B: Engineering*, Vol. 30, Issue 6, pp. 579-590 (12), 1999.

1.12 A SUMMARY OF SOME EXPERIMENTAL FIGURES

Some experimental figures from this paper can be reproduced by any reader as it is indicated below. First please download the folder **Data paper 2** (see the download indications from preface).

Figure 1.3

Use the programs and the data files fromthe folder **Data Fig. 1.3.** Inside of this folder there are some programs and data files. You can run the Matlab program **fig13.m** in order to obtain the main parts of Figure 1.3.
It is possible to find-out the exactly value of the frequency of excitation in steady state regime (C area on Figure 1.3) by running the Matlab program **ident1**. This program finds out the characteristics of a theoretical harmonic curve which is the best fitting for the harmonic evolution of the vibration elongation in C area. The both curves (theoretical in blue and experimental in red) are drawed on the figure generated by the program. The value of frequency (already given in Table 1.1, first column) is written in the command window.
It is also possible to find out by numerical fitting the parameters of the free response of the cantilever beam from E area (Figure 1.3) by running the Matlab program **ident2**. It is suppose that this free response is described in theoretical terms by the following equation:

$$x(t) = a \cdot e^{-(\xi \cdot p \cdot t)} \cdot sin(p_1 \cdot t + \varphi) \qquad (1.19)$$

The program ident2 is able to find-out the best fitting curve which fit the experimental evolution and the values of the parameters involved in Eq. (1.19). You find the values of these parameters in the matrix d. You can see the both curves on the figure generated by the program (experimental curve in red and the fitting curve in blue). The both curves are very well fitted each other. This is an experimental confirmation that the theoretical shape of the free response from Eq. (1.19) is correct. The program ident2 is also useful to solve the task #3 from chapter 1.13.

The program generates in the command window the values of the damping ratio (%) and frequency of free response as it were also written on Figure 1.3 and Table 1.1 in last column.

Figure 1.4

You need the folder **Data Fig. 1.4.** Inside of this folder there is a program and a data file. You can run the Matlab program **desput** in order to obtain the main parts of Figure 1.4. The program also calculates the value of active electrical power absorbed by the cantilever beam in steady-state (5.09 mW).

Figure 1.7

Use the files from the folder named **Data Fig. 1.7.** Inside of this folder there is a program and some data files. You can run the Matlab program **desputa** in order to obtain the main parts of Figure 1.7.

Figure 1.8

Use the files from the folder named **Data Fig. 1.8.** Inside of this folder there is a program and some data files. You can run the Matlab program **desputa** in order to obtain the main parts of Figure 1.8.

1.13 THEORETICAL AND EXPERIMENTAL WORK TASKS

1. Perform the experimental setup described in Figs. 1.1 and 1.2. Use the oscilloscope PicoScope 4424 (4 channels) in order to acquire at the same time the voltages in the points A and B (Fig. 1.1) and the voltage delivered by the accelerometer (Fig. 1.2).

2. Perform the experiment described in Fig.1.3 in order to obtain the evolution of the voltage generated by accelerometer in two ways: using only the oscilloscope and via a Matlab program (with moving average numerical filtering of data).

3. Try to emulate a Matlab program in order to find out the parameters of free viscous response (E area from Fig. 1.3) by numerical interpolation (curve fitting). Here below is described an example of curve fitting applied on simulated data.

The program called simulation (listed below) simulates a free viscous response.

The program simulation

```
close all;clear all;tic;
k=1;a=10;e=2.718281828;n=0.54;p1=113.14;fi=1.234;
for i=0:0.0001:10
    x1(k)=i;y1(k)=0;
    if i>1;
y1(k)=a*e^(-n*x1(k))*sin(p1*x1(k)+fi);
%here above is a mathematical description of a free
%viscous response
    else end
k=k+1;
end
save x1;save y1;
```

The program ident (listed below) is used to find out with a good accuracy the values of the parameters *n*, *p1* and *fi* used before for the simulation of the free viscous response.

The program ident

```
close all;clear all;tic;
load x1;load y1;
dim=size(x1);l=dim(2);pasp=50;
nrpuncte=500;liminf=10000;limsup=liminf+pasp*nrpunct
e;x1=x1-x1(liminf);
j=1;for i=liminf:pasp:limsup-
1;y(j)=y1(i);x(j)=x1(i);j=j+1;end
```

```
rafinare=10;
min=99999999999;k=0;eroare=0;
aimin=5;aimax=15;stepai=(aimax-aimin)/rafinare;
nimin=0.30;nimax=2;stepni=(nimax-nimin)/rafinare;
p1imin=110;p1imax=120;stepp1i=(p1imax-
p1imin)/rafinare;
fiimin=0;fiimax=3;stepfi=(fiimax-fiimin)/rafinare;
run curvefit
%The listing of the program curvefit is given
%immediately below this program
for ncicli=1:30
min=99999999999;eroare=0;
aimin=c(1)-stepai;aimax=c(1)+stepai;stepai=stepai/2;
nimin=c(2)-stepni;nimax=c(2)+stepni;stepni=stepni/2;
p1imin=c(3)-
stepp1i;p1imax=c(3)+stepp1i;stepp1i=stepp1i/2;
fiimin=c(4)-
stepfi;fiimax=c(4)+stepfi;stepfi=stepfi/2;
run curvefit
end
d(1)=c(1);d(2)=c(2);d(3)=c(3);d(4)=c(4);
for i=1:nrpuncte;
   b(i)=d(1)* 2.718281828
^(-d(2)*x(i))*sin(d(3)*x(i)+d(4));
   t(i)=x(i);
end
close all
plot(t,y,'b','LineWidth',1.5);hold on;grid;
plot(t,b,'r');
toc
d
```

The program curvefit

```
for ai=aimin:stepai:aimax;
      for ni=nimin:stepni:nimax;
         for p1i=p1imin:stepp1i:p1imax;
           for fii=fiimin:stepfi:fiimax;
               for i=1:nrpuncte;
      b(i)=ai*2.718281828^(-
ni*x(i))*sin(p1i*x(i)+fii);
```

```
      %eroare=eroare+abs(abs((y(i)))-
abs((b(i))));k=k+1;
      eroare=eroare+abs(y(i)-b(i));k=k+1;
   end
   if
eroare<min;c(1)=ai;c(2)=ni;c(3)=p1i;c(4)=fii;min=ero
are;
      else end;eroare=0;
end
end
end
end
```

All three programs (simulation, ident and curvefit, also available in electronic format) should be placed in the same folder. First run the program simulation, then the program ident. The values of identified parameters are listed in the command window of Matlab. The last three values are *n*, *p1* and *fi*.

In order to find out the parameters of the free response from experimental evolution is necessary first to save the evolution of the voltage generated by accelerometer from oscilloscope in a data file (with extension .txt, named data.txt) in the same folder as the programs.

The header of this file should be removed (the file should contains just two columns of numbers). This file is imported by program ident. The first part of this program (marked with bold) should be replaced with these instructions:

```
close all;clear all;tic;
load data.txt;
%data.txt is the name of the file used to save the
%data from oscilloscope to computer
x1=data(:,1)/1;y1=data(:,2)/1;x1=x1-x1(1);
y1=y1+0.03;
```

```
%the instruction above removes the offset of the
%oscilloscope (this offset should be measured)
y1=smooth(y1,100);
%the instruction above makes the numerical filtering
%of data (moving average filter)
dim=size(x1);l=dim(1);pasp=50;
```

The program should be adapted in such a way the curve fitting procedure starts right in E area (Fig. 1.3). For this purpose is available the Matlab instruction `liminf=10000;` in program ident. The value of this variable should be changed appropriately.

4. Try to find out if the value of damping ratio ξ is strictly constant during the entire free response.

5. Perform the experiment described in Fig.1.4 in order to obtain the evolution of the average mechanical power absorbed by the cantilever beam. Also try to perform the experiment in order to find out the value of average mechanical power absorbed in steady state regime, for different values of frequency arround the resonance. The program listed below can be useful for this purpose:

The program desput

```
clear all;close all;
inreg=10;p=1;start=cputime;
load putporp1.txt;
l=size(putporp1);
timp1=putporp1(:,1);amplit=putporp1(:,2);
timp=timp1(1:l/2)/1000000;tens=amplit(1:l/2)/1000;
l1=l(1)/2+1;
curent=amplit(l1:l)/1900;
putinst=tens.*curent;
```

```
plot(timp,putinst)
sup=round(l(1)/(2*inreg*14.011416));%this last value
%is the value of frequency of the voltages
pk=1;lim=l1-sup;
for i=1:sup:lim;med=0;
   for j=1:sup;
      med=med+putinst(i+j);
   end
   med=med/sup;putact(pk)=med;
   timpputact(pk)=timp(i+round(sup/2));
   pk=pk+1;
end
plot(timpputact,putact,'k');

%rutina filtrare
d=size(putact);

k=1;
for i=1+p:d(2);
   a=putact(i-p+1:i);b=timpputact(i-
p+1:i);meda1=sum(a);meda2=sum(b);
   putactf(k)=meda1/p;timpf(k)=meda2/p;
   k=k+1;
end
 for i=1:p;putactf(i)=putactf(p+1);
   timpf(i)=timpf(p+1);
end
plot(timpf,putactf,'b','LineWidth',1.5)
stop=cputime;executie=stop-start
dim=size(timpf);dim1=dim(2);
lim1=14;lim2=17;lim3=18;lim4=20;med1=0;med2=0;k1=0;k
2=0;
for i=1:dim(2)
   if timpf(i)>lim1;if
timpf(i)<lim2;k1=k1+1;med1=med1+putactf(i);else end;
else end
   if timpf(i)>lim3;if
timpf(i)<lim4;k2=k2+1;med2=med2+putactf(i);else end;
else end
end
med1=med1/k1;
med2=med2/k2;
```

```
(med1-med2)
```

This program and the file **putporp1.txt** are also available in electronic format (see the chapter 1.12). Run the program and try to change the structure in order to achieve the proposed tasks.

6. Performed the experiment described in Figure 1.5. In order to find out the fitting parameters for each curve, the programs listed below (used to obtain Figure 1.5) can be useful.

The program curvefitting

```
clear all;close all;
%This section make the fitting of curve #1
load date3.txt;
x=date3(:,1);y=date3(:,2);
dim1=size(x);dim=dim1(1);

x1=x;y1=y;clear x;clear y;
start=cputime;
nrpuncte=dim;liminf=1;limsup=liminf+nrpuncte;
j=1;for i=liminf:limsup-
1;y(j)=y1(i);x(j)=x1(i);j=j+1;end
rafinare=30;
min=99999999999;k=0;eroare=0;
cmin=0.5000e-006;cmax=2.7000e-006;stepc=(cmax-
cmin)/rafinare;
pmin=87;pmax=89;stepp=(pmax-pmin)/rafinare;
zetamin=.004;zetamax=0.006;stepzeta=(zetamax-
zetamin)/rafinare;

run cfit
for ncicli=1:20
min=99999999999;eroare=0;
cmin=c(1)-stepc;cmax=c(1)+stepc;stepc=stepc/2;
pmin=c(2)-stepp;pmax=c(2)+stepp;stepp=stepp/2;
```

```
zetamin=c(3)-
stepzeta;zetamax=c(3)+stepzeta;stepzeta=stepzeta/2;
run cfit
end

d(1)=c(1);d(2)=c(2);d(3)=c(3);

inc=(x(dim)-x(1))/150;ku=1;
for i=x(1):inc:x(dim);i1=2*pi*i/p;
   b(ku)=d(1)*d(2)*d(3)*i1^2/((1-
i1^2)^2+4*i1^2*d(3)^2);
   absc(ku)=i;ku=ku+1;
end
hold on;
%plot(x,y,'k','LineWidth',1.5);
plot(absc,b,'b','LineWidth',1.5);hold on

d,k
stop=cputime;executie=stop-start

x=x1;y=y1;
for j=1:dim;
for i=.1:.1:3;k=1;scalex=0.006;scaley=0.00002;
   for teta=0:.01:2*pi+.1;

absc(k)=(x(j)+i*cos(teta)*scalex);ord(k)=y(j)+i*sin(
teta)*scaley;
      k=k+1;
   end
   plot(absc,ord,'r');clear absc;clear ord;hold on
end
end

%This section make the fitting of curve #2

load date2.txt;;
x=date2(:,1);y=date2(:,2);
dim1=size(x);dim=dim1(1);

x1=x;y1=y;clear x;clear y;
start=cputime;
nrpuncte=dim;liminf=1;limsup=liminf+nrpuncte;
```

```
j=1;for i=liminf:limsup-
1;y(j)=y1(i);x(j)=x1(i);j=j+1;end
rafinare=30;
min=99999999999;k=0;eroare=0;
cmin=0.5000e-006;cmax=2.7000e-006;stepc=(cmax-
cmin)/rafinare;
pmin=87;pmax=89;stepp=(pmax-pmin)/rafinare;
zetamin=.01;zetamax=0.03;stepzeta=(zetamax-
zetamin)/rafinare;
run cfit
for ncicli=1:20
min=99999999999;eroare=0;
cmin=c(1)-stepc;cmax=c(1)+stepc;stepc=stepc/2;
pmin=c(2)-stepp;pmax=c(2)+stepp;stepp=stepp/2;
zetamin=c(3)-
stepzeta;zetamax=c(3)+stepzeta;stepzeta=stepzeta/2;
run cfit
end

d1(1)=c(1);d1(2)=c(2);d1(3)=c(3);

inc=(x(dim)-x(1))/150;ku=1;
for i=x(1):inc:x(dim);i1=2*pi*i/p;
   b(ku)=d1(1)*d1(2)*d1(3)*i1^2/((1-
i1^2)^2+4*i1^2*d1(3)^2);
   absc(ku)=i;ku=ku+1;
end
hold on;

plot(absc,b,'r','LineWidth',1.5);hold on
axis([13.1 14.9 -0.0001 0.0053])
d1,k
stop=cputime;executie=stop-start
 x=x1;y=y1;
for j=1:dim;
for i=.1:.1:3;k=1;
   for teta=0:.01:2*pi+.1;
absc(k)=(x(j)+i*cos(teta)*scalex);ord(k)=y(j)+i*sin(
teta)*scaley;
      k=k+1;
   end
   plot(absc,ord,'b');clear absc;clear ord;hold on
```

```
end
end
```

The program cfit

```
for ci=cmin:stepc:cmax;
   for p=pmin:stepp:pmax;
      for zeta=zetamin:stepzeta:zetamax;
         for i=1:nrpuncte;
            pulsrel=2*pi*x(i)/p;
      b(i)=ci*p*zeta*pulsrel^2/((1-
pulsrel^2)^2+4*pulsrel^2*zeta^2);
      eroare=eroare+abs(abs((y(i)))-
abs((b(i))));k=k+1;
   end
   if
eroare<min;c(1)=ci;c(2)=p;c(3)=zeta;min=eroare;
      else end;eroare=0;
end
end
end
```

The file date3.txt

```
14.85557  0.000030219
14.71360  0.000067708
14.47028  0.00012467
14.31600  0.00035309
14.17322  0.0012653
14.07710  0.0045669
14.04056  0.0051522
13.90310  0.00118
13.88880  0.00078782
13.79662  0.00031057
13.70580  0.0001949
13.56990  0.00012563
13.5064   0.000096958
13.40482  0.00007615
```

13.2555 0.000048298
13.1371 0.00001086

The file date2.txt

14.846200 0.000143
14.775700 0.00016464
14.545400 0.00039199
14.415376 0.00060452
14.278150 0.0008617
14.188100 0.0011062
14.150900 0.0011579
13.996800 0.0011650
13.917500 0.0010048
13.785790 0.00064934
13.584117 0.000353
13.450590 0.00023394

The both programs and both data files should be placed in the same folder. Run the program curvefitting and you will obtain the curves from Figure 1.5.

7. Perform the Simulink simulation described in Fig. 1.6 and Table 1.4 in order to obtain the result given in Figs. 1.3 and 1.7 (a).

8. Perform the experiment described in Figs. 1.7 and 1.8.

Paper 2

DYNAMIC CHARACTERIZATION OF A PIEZOELECTRIC ACTUATED CANTILEVER BEAM USING ENERGETIC PARAMETERS

ABSTRACT

This paper aims to examine in experimental terms some new research opportunities on the dynamic behaviour of the mechanical systems with piezoelectric actuation, using the energetic parameters evolution (especially the electric active power or real power as well) captured from the supply circuit of the actuator. The study is carried out on an experimental setup which consists of an aluminium cantilever beam having two small thickness PZT piezoelectric plate transducers glued close-by the rigidly fixed end on each side of the beam. Using some new theoretical and experimental approaches, developed for these purposes, there is undertaken the computer assisted monitoring of the energetic parameters from the piezoelectric transducers supply circuit. The transducers are used as sensors and actuators as well. The research focuses on the possibility to describe some essential dynamic phenomena such as: vibration modes characterization, resonance, modal damping

using negative power actively and passively generated and the dynamics of transient regimes. Some results are similar to those already obtained on a cantilever beam actuated with a voice-coil (Lorentz force) actuator.

Keywords: Vibration engineering, cantilever beam, piezoelectric actuation, energetic parameters, negative power

2.1 INTRODUCTION

The piezoelectric actuation and sensing using the inverse and direct piezoelectric effect is well known in mechanical structures vibration engineering [1, 2]. The same piezoelectric device, called transducer, works as actuator and sensor. Generally the actuation is used to excite mechanical structures in order to produce vibrations or small static displacements. The sensing is used to describe the dynamics of the structures (in terms of the voltage measured on the electrodes [3]) and, actually, for power harvesting [4, 5, 6] in order to convert the environmental mechanical vibration energy into storable electrical energy and to damp the vibrations as well. During the last two decades the vibration engineering focussed on a new challenge: active and passive vibration damping in mechanical structures using piezoelectric transducers. The active vibration damping [1, 2, 7, 8, and 9] generally uses a negative velocity-force feedback loop with collocated sensor and actuator. With a feedback loop it is also possible to change some modal frequencies of mechanical structures. The passive damping techniques [8, 9, and 10] use the piezoelectric transducer as sensor and actuator. Using a resistance-inductance (R-L) series shunt placed on the transducers electrodes, the mechanical modal

energy is converted into electrical energy and dissipated as heating on the resistor. The inductance is used to cancel the capacitive reactance of the piezoelectric transducer on the frequency of the vibration mode in order to have minimal electrical impedance, or to have a damping R-L-C electrical resonating circuit in co-resonance with the mechanical structure. For each mode of vibration it is necessary to use an R-L series shunt. Because the piezoelectric transducer has a small capacity value, the damping of the low frequencies modes needs very high values for the inductance (hundreds or even thousands of Henries) and small resistance. That is why in this case it is used a synthetic inductance [9, 11].

The dual behaviour of the transducers is also exploited in new mechatronic devices: the piezoelectric alternating voltage transformers [12].

The characterization of a mechanical structure from the dynamic point of view using the power flow through the piezoelectric actuator was done in a theoretical manner in [13, 14]. Some considerations in theoretical and experimental terms are presented in [15]. There are many unexploited resources on the piezoelectric actuation topics research. A good opportunity is to use the computer assisted measurement of the energetic parameters from the actuation system, especially the absorbed active power from the electrical supply circuit. On this subject, the paper aims to propose a technique to evaluate the dynamics of a piezoelectric actuated cantilever beam.

2.2 THE EXPERIMENTAL SETUP

In vibration engineering of the piezoelectric actuated (powered) mechanical systems, the use of the energetic parameters evolution acquired on the actuator electrical supply circuit is not completely brought out and seems to be limited to the description of the dynamic phenomena associated with the power harvesting of the modal energy of the environmental mechanical vibrations.

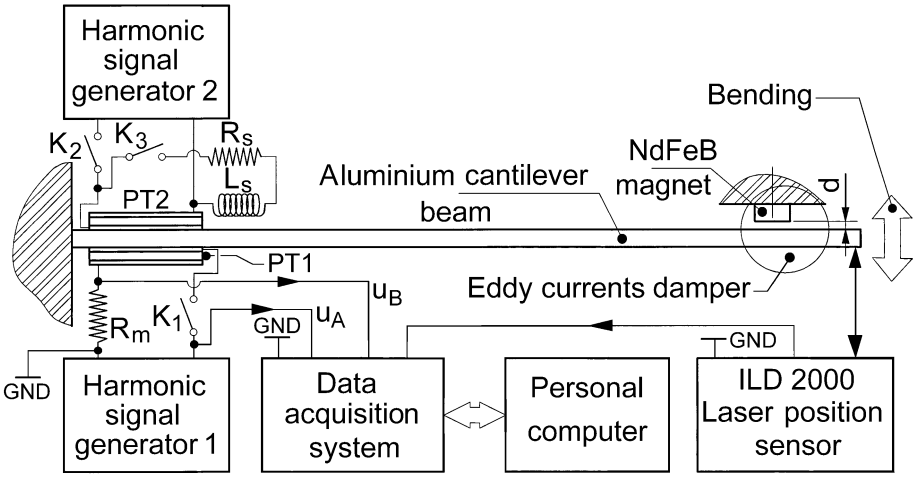

Fig. 2.1: *Description of the experimental setup.*

The research resources on this direction are underused. However this paper aims to demonstrate the efficiency of the computer assisted monitoring of the energetic parameters evolution, using a simple setup conceptually described in Figure 2.1, based on an aluminium cantilever beam (AlMgSi1 alloy, 300 x 25 x 2 mm). Close by the rigidly fixed end of the beam (2 mm distance), two PZT (lead zirconate titanate) patches transducers PT1 and PT2 (40 x 25 x 0.5mm, SensorTech BM500 type, with deformation in length mode), with d_{31}

polarization (d_{31}=-175·10^{-12} m/V), are glued with an epoxy glue (UHU plus endfest 300). The transducers can be used as actuators, if they are electrically supplied with a harmonic signal generator (with tunable voltage and frequency) for each one (using the K_1 and K_2 on-off switches).

If a resistor R_m is placed in series in PT1 transducer supply circuit then the voltage $u_B(t)$ describes the current inside the transducer ($i(t)=u_B(t)/R_m$, due to Ohm's law). Using the voltages $u_A(t)$ and $u_B(t)$, (acquired, converted in numeric format and transmitted to a personal computer, with a data acquisition system based on an oscilloscope PicoScope Technology ADC 212/50), and some computer programmes (written in Matlab), it is possible to describe the evolution of the energetic parameters in time and frequency domain, for all the dynamic regimes of the cantilever beam actuated (excited) by the transducer PT1.

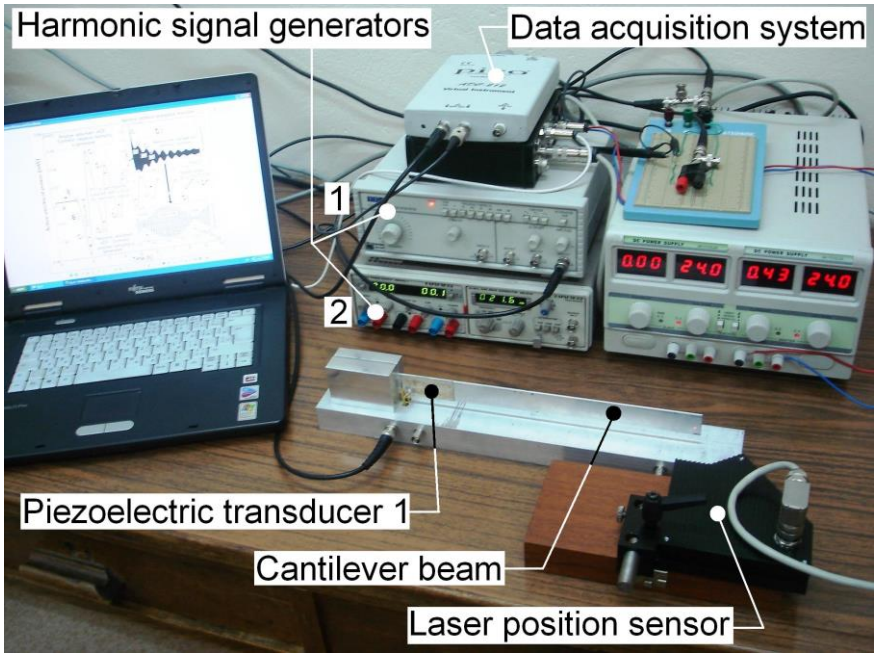

Fig. 2.2: *A view of the experimental setup.*

A laser position sensor ILD 2000 is used to describe the vibration of the free end of the beam for the first flexural mode (bending). The damping ratio ζ of the first mode can be tuned using an eddy-currents passive damper built with an NdFeB (neodymium-iron-boron) permanent magnet placed in the proximity of the free end of the beam.

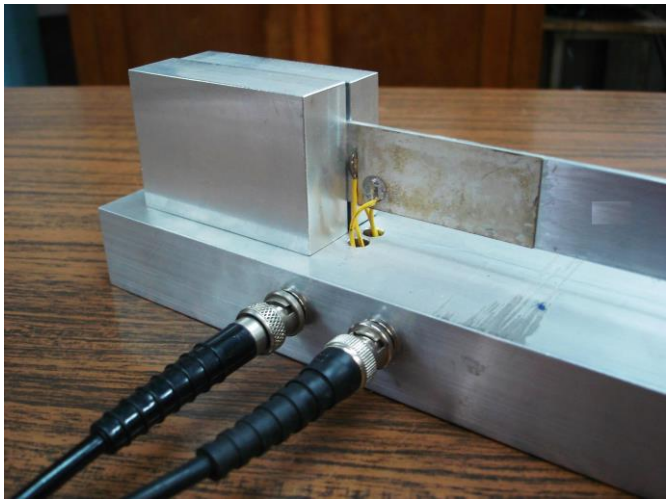

Fig. 2.3: *A view on the rigidly fixed end of the cantilever beam with the transducer PT1.*

The damping ratio value ζ depends by the distance *d*. If the switch K_3 is switched-on and K_2 is switched-off, then the transducer PT2 is placed in a close circuit with a R_s-L_s (resistance-inductance) shunt, the system works as a passive dynamic absorber [9, 11] used to damp the high frequency flexural modes excited by PT1 transducer (which works as actuator). The behaviour of this passive dynamic absorber is mirrored in the active power absorbed by PT1.

Figure 2.2 presents a view on the experimental setup. Figure 2.3 presents a view on the rigidly fixed end of the cantilever beam with PT1 transducer. The PT2 transducer is glued on the opposite side of the cantilever beam.

2.3 COMPUTER ASSISTED ENERGETIC PARAMETERS MONITORING

If the switch K_1 is switched-on, then the instantaneous electrical power generated by the harmonic signal generator 1 and delivered to the transducer PT1 (which actuates in dynamic regime the cantilever beam) is given by:

$$P(t) = u(t) \cdot i(t) \tag{2.1}$$

as the result of the multiplication of the instantaneous voltage $u(t) = \sqrt{2} \cdot U_{rms} \cdot sin(\omega \cdot t)$ and the instantaneous current $i(t) = \sqrt{2} \cdot I_{rms} \cdot sin(\omega \cdot t - \varphi)$ delivered by the supply circuit. Here $\omega = 2 \cdot \pi \cdot f$ is the angular frequency of the excitation and f is the frequency, φ is the phase angle, U_{rms} and I_{rms} are the root mean square values of the voltage and current, $\sqrt{2} \cdot U_{rms}$ and $\sqrt{2} \cdot I_{rms}$ are the amplitudes of voltage and current.

The active electric power is calculated as the average value of the instantaneous power on a semi-period $T/2 = 1/(2 \cdot f)$:

$$\overline{P} = \frac{2}{T} \cdot \int_0^{\frac{T}{2}} P(t) \cdot dt = \frac{2}{T} \cdot \int_0^{\frac{T}{2}} u(t) \cdot i(t) \cdot dt = U_{rms} \cdot I_{rms} \cdot cos(\varphi) \tag{2.2}$$

This is the real part of the apparent electric power which is absorbed and converted by the transducer PT1 (acting as actuator) in heating and mechanical work or mechanical power in order to excite the cantilever beam to vibrate on flexural mode on the frequency f. Here $cos(\varphi)$ is called also power factor.

Taken into account the voltages $u_A(t)$ and $u_B(t)$ from Figure 2.1, converted into numerical format, and the first part of Eq. (2), the evolution of the active electric power can be described as:

$$\overline{P}(t_s) \approx \frac{2}{R_m \cdot n} \cdot \sum_{j=n\cdot l+1}^{n\cdot(l+1)} [u_A(t_j) - u_B(t_j)] \cdot u_B(t_j) \qquad (2.3)$$

With $l = 0, 1, 2, ..., k$

Here $u_A(t_j)$ and $u_B(t_j)$ are the numerical values (samples) of the voltages u_A and u_B, acquired at the time $t_j = j \cdot \Delta t$, with Δt the sampling interval, $n = T/(2 \cdot \Delta t)$ is the number of samples on a semi-period (as an integer) and $t_s = l \cdot T/2 = l \cdot n \cdot \Delta t$ is the time coordinate of the active power (sampling time), with $t_s = 0, T/2, \ldots l \cdot T/2, ..., k \cdot T/2$. If $\Delta t \rightarrow 0$ then in Eq. (2.3) the sign ≈ becomes =. In Eq. (2.3) the instantaneous current sample is described by: $i(t_j) = u_B(t_j)/ R_m$ and the instantaneous voltage sample is given by: $u(t_j) = [u_A(t_j) - u_B(t_j)]$, as voltage applied on the transducer PT1. The evolutions of the root mean square values U_{rms} and I_{rms} are described by:

$$U_{rms}(t_s) = \frac{max|u_A(t_j)| - max|u_B(t_j)|}{\sqrt{2}} \quad , \quad I_{rms}(t_s) = \frac{max|u_B(t_j)|}{R_m \cdot \sqrt{2}} \qquad (2.4)$$

$$j = (n \cdot l + 1) \div [n \cdot (l + 1)] \qquad l = 0, 1, 2, ..., k$$

The evolution of the apparent power is described by:

$$\overline{S}(t_s) = U_{rms}(t_s) \cdot I_{rms}(t_s) \qquad (2.5)$$

The evolution of the electrical impedance of the transducer PT1 is described by:

$$Z(t_s) = \frac{U_{rms}(t_s)}{I_{rms}(t_s)} \qquad \text{if} \qquad Z(t_s) >> R_m \tag{2.6}$$

Using the Eqs. (2.2), (2.3) and (2.5), the phase angle evolution is described as follows:

$$\varphi(t_s) \approx a\cos[\frac{\overline{P}(t_s)}{\overline{S}(t_s)}] \tag{2.7}$$

And the evolution of the reactive power is given by:

$$\overline{Q}(t_s) \approx \overline{S}(t_s) \cdot sin[\varphi(t_s)] \tag{2.8}$$

The sampling frequency of the energetic parameters in this last equations, except Eq. (2.1), is *2·f Hz.*

The common sense indicates that the dynamic behaviour of the cantilever beam excited by the transducer PT1 (if it is supplied with a harmonic voltage) should have a high influence on the evolution of these energetic parameters. As an example, the excitation at resonance on a flexural (bending) mode of the cantilever beam should imply the increasing of the mechanical power delivered by PT1, so the increasing of the active power absorbed from the electrical supply source (harmonic generator 1). And of course, the absorbed active power should be strongly dependent on the value of the excitation frequency [17].

From the monitoring point of view, the transducer PT1 works as excitation system (actuator) and loading sensor.

This paper tries to illustrate the resources of the computer aided research of the mechanical structures dynamics using the energetic parameters evolution acquired in the electric supply circuit of a piezoelectric transducer used for actuation.

2.4 EXPERIMENTAL RESULTS AND DISCUSSION

2.4.1 Characterization of the First Flexural Vibration Mode.

In this regard, a first approach can be the experimental description of the cantilever beam dynamic behaviour when it is excited with a frequency (*f=21.0085 Hz*) which is very close to the first flexural (bending) vibration mode.

The transducer PT1 is used as actuator, supplied with a voltage u_A which has a peak to peak amplitude by 8.52 V (or 3.012 V_{rms} as well). Figure 2.4 presents the evolution of the vibration elongation of the free end of the cantilever beam after the moment (marked with A) when the switch K_1 is switched-on.

The vibration amplitude starts to increase slowly (as indicates a zoom-in to the area marked with B) up to a maximum peak to peak value of 2.762 mm in C (steady-state forced response). In D the switch K_1 is switched-off; the excitation source is suddenly removed. The free end of the beam continues to vibrate as a viscously damped free

vibration, using the modal energy stored inside (in E area, the frequency of the motion is 21.1647 Hz, the damping ratio $\zeta = 0.275\%$).

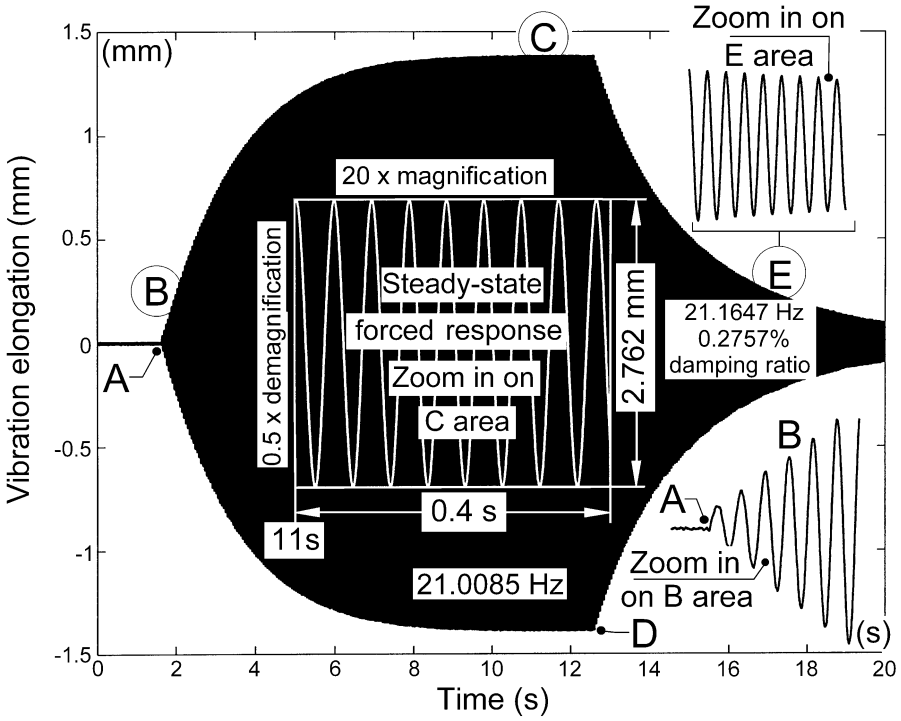

Fig. 2.4: *Temporal evolution of the flexural vibration elongation, excited on the resonance frequency of the first mode (start in A, stop in D,* ***see also the chapter 2.7****).*

The same experiment was performed and the evolution of the active electrical power absorbed by the transducer PT1 was calculated and plotted as it is described in Figure 2.5. Here the Eq. (2.3) was used for computer calculus, based on the acquired values of the voltages $u_A(t_j)$ and $u_B(t_j)$. A measurement resistor with $R_m=1021\ \Omega$ value was used according to Figure 2.1. It is absolutely clear that after the moment A the absorbed active power increases progressively starting

from zero, becomes maximal in C area and suddenly drops to zero in the moment D.

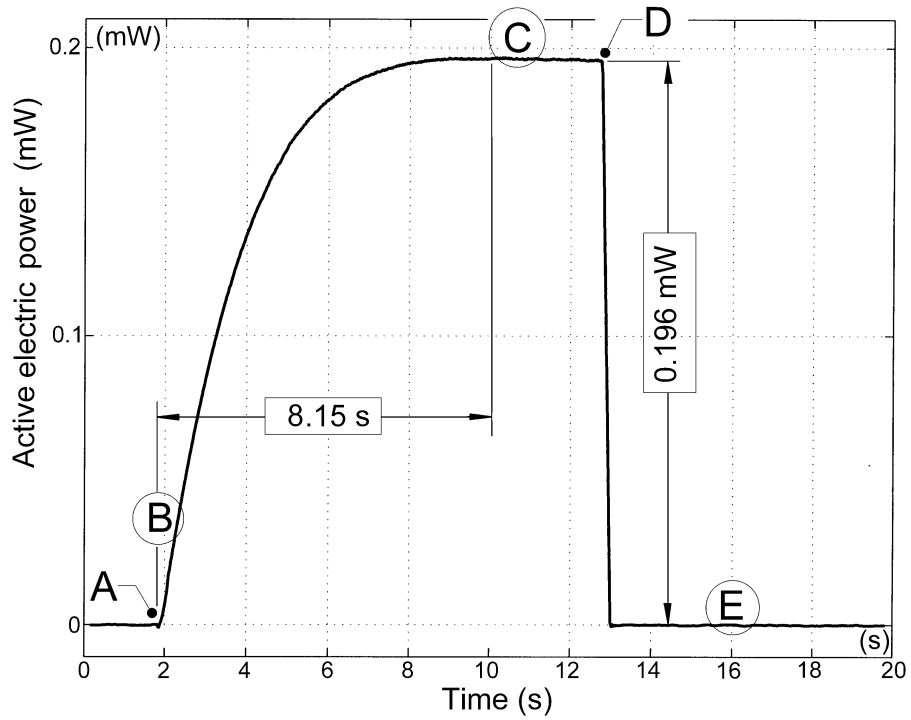

Fig. 2.5: *The evolution of the absorbed active power in the experiment described in Figure 2.4 (**see also the chapter 2.7**).*

There is a first conclusion drawn from Figures 2.4 and 2.5: the mechanical system of the cantilever beam needs time to accumulate modal energy inside and to increase the vibration amplitude.

There is a second conclusion drawn from Figure 2.5: as it is expected [17], the evolution of the active power absorbed by the transducer PT1 is strongly dependent by the dynamics of the cantilever beam (resonant behaviour of a low damped vibration mode).

The amount of the absorbed active power at excitation on 21.00 Hz frequency is 196 μW (steady state absorbed power). A part of this power is converted into real mechanical power, delivered to the cantilever beam and used to produce mechanical work (finally dissipated as heating).

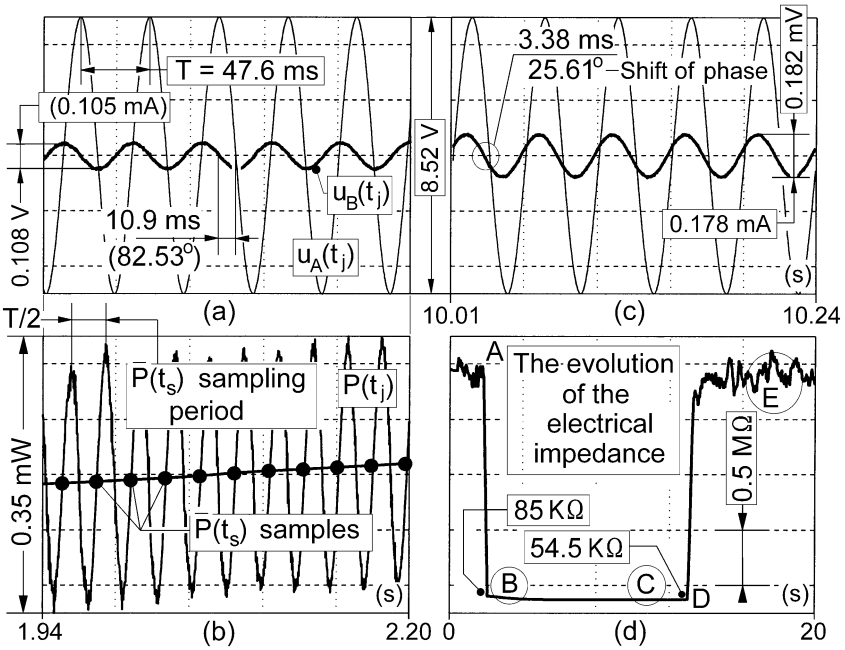

Fig. 2.6: ***(a)*** *Instantaneous voltage and current in area B from Figure 2.5;* ***(b)*** *Instantaneous and active power in area B;* ***(c)*** *Instantaneous voltage and current in area C from Figure 2.5;* ***(d)*** *The evolution of the electrical impedance of the transducer PT1 in the experiment described in Figure 2.4 (**see also the chapter 2.7**).*

Figure 2.6 (a) describes the evolutions of the voltages $u_A(t_j)$ and $u_B(t_j)$ corresponding to the B area from Figure 2.5. Using these two voltages the evolution of the instantaneous electrical power $P(t_j)$ and active electric power $\bar{P}(t_s)$ are calculated and plotted as described in

Figure 2.6 (b). Figure 2.6 (c) describes the evolutions of the voltages $u_A(t_j)$ and $u_B(t_j)$ corresponding to the C area from Figure 2.5. In comparison with Figure 2.6 (a) the increasing of the amplitude of $u_B(t_j)$ and the decreasing of the shift of phase between $u_A(t_j)$ and $u_B(t_j)$ are clearly indicated. The increasing of the active electrical power is produced essentially by the current inside the transducer PT1 and the angle of phase φ between the instantaneous current and voltage (according also to Eq. 2.2).

Figure 2.6 (d) describes the evolution of the electrical impedance of the transducer PT1 during the experiment described in Figure 2.5. Before the moment A and after the moment D the impedance is theoretically infinite (the switch K_1 is off, the current is zero). Practically, according to Figure 2.1, in the measurement circuit of the voltage $u_B(t_j)$ the resistor R_m works as an antenna, the current is extremely small but not zero. When K_1 is switched-on, the electrical impedance drops to 85 KΩ and after that decreases slowly to the minimal value of 54.5 KΩ because of the dynamic behaviour of the cantilever beam (the mechanical impedance also decreases).

There is a third conclusion associated with Figures 2.4, 2.5 and 2.6 (d). The experiment is very well described using the vibration elongation, it is well described using the electrical power evolution but it is poorly described in the electrical impedance evolution.

The vibration theory [17, 13] indicates that, around the resonance, the absorbed mechanical power is strongly dependent on the excitation frequency and the damping ratio values.

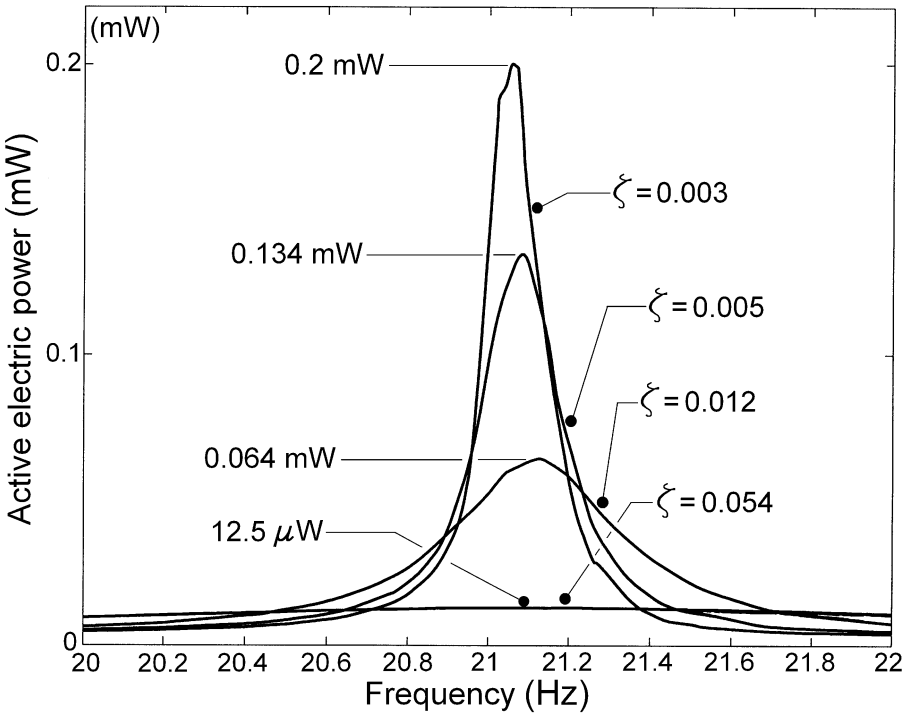

Fig. 2.7: *The absorbed active power evolution in frequency domain (first flexural vibration mode) for different values of the damping ratio.*

Normally we should find the same dependence on the evolution of the electrical absorbed active power, as is indicated in the experimental results shown in Figure 2.7. In Figure 2.7 there is plotted the experimental evolution of the absorbed active electric power in frequency domain around the resonance, for different values of damping ratio. According to Figure 2.1 the value of damping ratio ζ is changed by tuning the proximity distance d between the magnet and the cantilever beam in the eddy-currents damper.

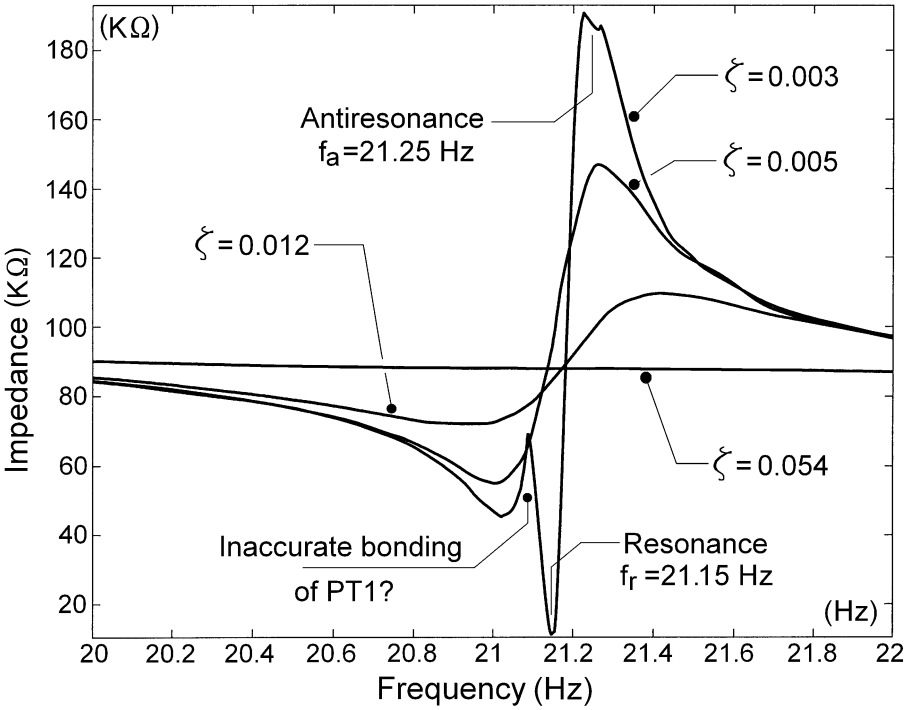

Fig. 2.8: *The electrical impedance evolution plotted in the experimental conditions from Figure 2.7.*

The experimental evolutions described in Figure 2.7 are perfectly similar with the theoretical simulation done according to the researches described in [13]. The results described in Figure 2.7 prove that on each mode of vibration the cantilever beam works as a narrow band frequency mechanical modal energy absorber (less than 1 Hz bandwidth, here). This is an important conclusion useful in synthesis of the passive dynamic vibration absorbers (or tune mass dampers as well [19]).

According to Eq. (2.6) it is possible to plot the experimental evolution of the electrical impedance of the transducer PT1 in

frequency domain, in the same experimental conditions from Figure 2.7, as it is shown in Figure 2.8. This type of evolution of the impedance for undamped structures was already described in the literature [8]. There are two peaks, the minimal amplitude peak correspond to the resonance frequency f_r (21.15 Hz), the maximal amplitude peak correspond to the antiresonance frequency f_a (21.25 Hz). The experimental evolution of the impedance presented by the undamped cantilever beam is useful to calculate the generalized electromechanical coupling coefficient K_{31}^{PT1} of the transducer PT1 for first flexural mode, using the formula [8, 16]:

$$K_{31}^{PT1} = \sqrt{\frac{f_a^2 - f_r^2}{f_r^2}} = 0.097 \tag{2.9}$$

The value of this coefficient [10] is a measure of the percentage of total system modal strain energy converted into electrical energy by the piezoelectric transducer PT1 when it is used as sensor. The generalized electromechanical coupling coefficient K_{31}^{PT1} is smaller than the electromechanical coupling coefficient [10]. According to [10] the generalized coupling coefficient reflects the fact that the piezoelectric transducer is glued to the cantilever beam and is in parallel with some other stiffness, and thus a smaller fraction of the system strain energy is converted in electrical energy.

An interesting result of the experimental research is the evolution of the phase angle φ between the instantaneous voltage and

current (calculated with Eq. (2.7)) in the same experimental conditions, as it is indicated on Figure 2.9.

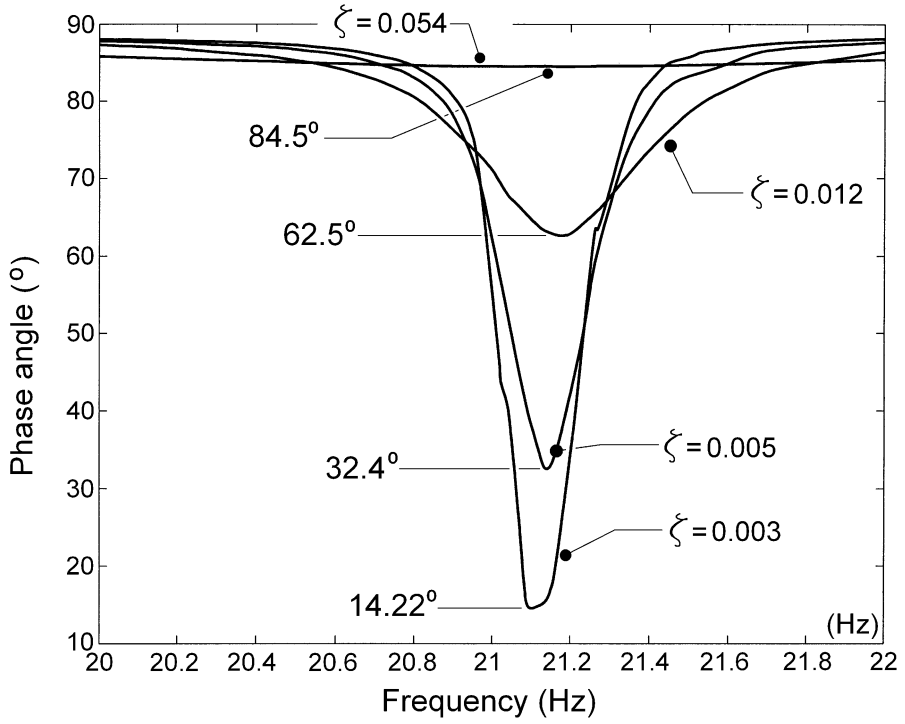

Fig. 2.9: *The evolution of phase angle φ in frequency domain under the experimental conditions from Figure 2.7.*

It is clear that at resonance the phase angle φ is strongly decreased (the power factor $\cos(\varphi)$ evolution has the biggest influence on the active electric power evolution). According to Figure 2.9, the easiest way to detect the resonance of the low damped vibration modes is to evaluate the angle of phase evolution between the instantaneous voltage and the instantaneous current evolutions.

Figure 2.10 describes the evolution of the reactive power, calculated according to the Eq. (2.8). As it is clearly illustrated here and

in Figure 2.8, the peak to peak amplitude decreases when the damping ratio increases.

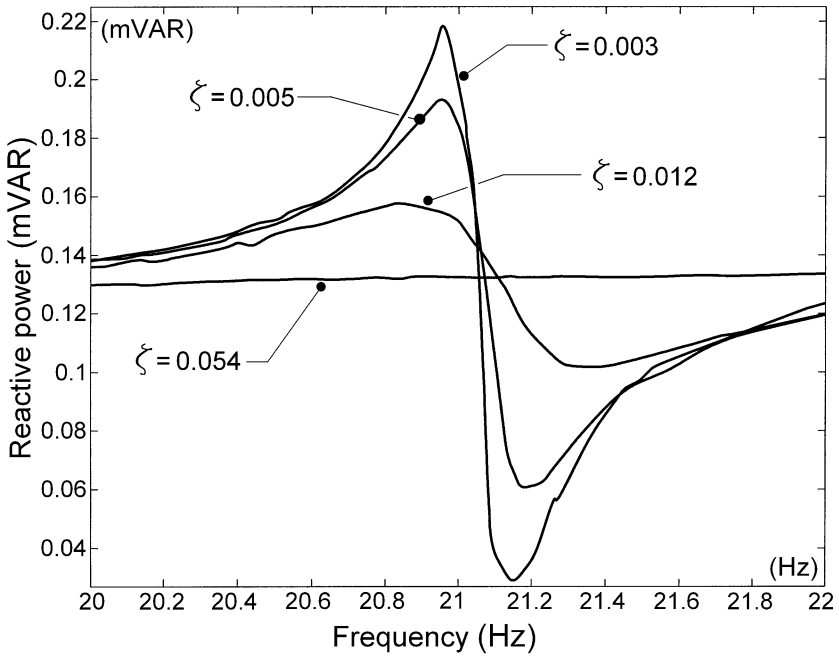

Fig. 2.10: *The evolution of the electric reactive power in frequency domain under the experimental conditions from Figure 2.7.*

There is another example which proves the trustworthiness of the experimental research using computer assisted monitoring of the active electric power, according to the experimental results described in Figure 2.11. It is well known from the literature [16] that the calculus of the generalized electromechanical coupling coefficient K_{31}, for a piezoelectric transducer placed on a mechanical structure can also be done using the resonance frequency values (on a certain mode of vibration) of the mechanical structure when the transducer is placed in

open circuit (resonance frequency f_o) and short circuit (resonance frequency f_s) with formula [10, 16]:

$$K_{31} = \sqrt{\frac{f_o^2 - f_s^2}{f_s^2}} \tag{2.10}$$

This is a formula with the same structure with Eq. (2.9). Eq. (2.10) can be used for the experimental evaluation of K_{31}^{PT2} coefficient for the transducer PT2.

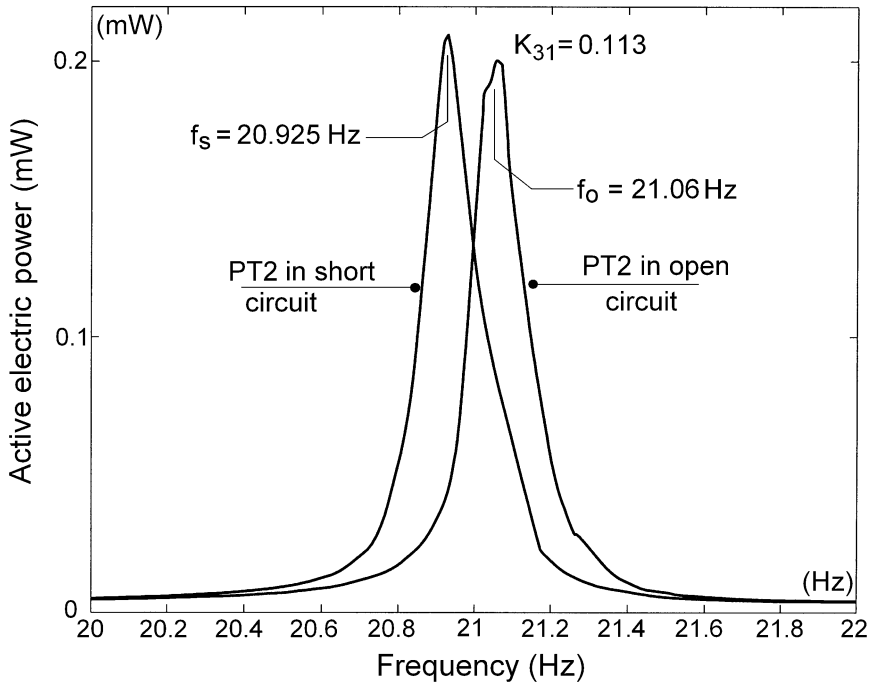

Fig. 2.11: *The evolution of the electric active power in the supply circuit of the transducer PT1 with the transducer PT2 in open and short circuit.*

The values of the resonant frequency of the beam (first flexural mode of vibration) in these two circumstances can be found using the evolution of the active electrical power in frequency domain in the supply circuit of the transducer PT1, according to the results shown in Figure 2.11. The resonant frequency of the first flexural mode when the transducer PT2 is in short circuit is $f_s=20.925\ Hz$, the resonant frequency in open circuit is $f_o=21.06\ Hz$. Using these two values of frequency, the generalized electromechanical coupling coefficient K_{31}^{PT2} for the transducer PT2 (measured on first flexural mode of the cantilever beam) is calculated using Eq. (2.10), with the result: $K_{31}^{PT2}=0.113$.

This is a value close to the value calculated for PT1 transducer ($K_{31}^{PT1}=0.097$, based on Eq. (2.9)) but using a different procedure. When the PT2 transducer is placed in short circuit, the modal stiffness is decreased, as it is clearly indicated on Figure 2.11.

These results prove that some characteristics of the piezoelectric actuated cantilever beam dynamics on low frequency modes can be described using the evolution in frequency domain for the energetic parameters of actuation, with a simple experimental setup.

2.4.2 Characterization of Some Transient Regimes of Vibration on First Flexural Mode

Let us look now a new experiment under the same conditions used before in Figures 2.4 and 2.5, but with the harmonic signal

generator 1 tuned on 20.8 Hz frequency, smaller than the resonance frequency of the first flexural mode of the cantilever beam. The same U_{rms} voltage (8.52 V) is used.

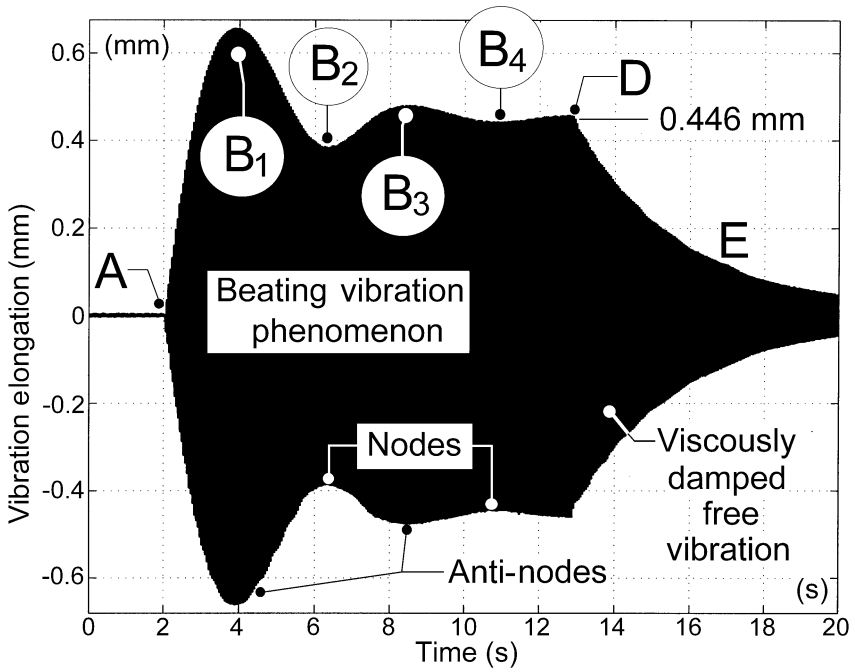

Fig. 2.12: *Transient regime generated by the transducer PT1, mirrored in vibration elongation evolution (sub-resonant harmonic excitation, start in A, stop in D,* ***see also the chapter 2.7****).*

Figure 2.12 presents the evolution of the elongation of the vibratory motion of the free end of the cantilever beam. Figure 2.13 presents the evolution of the absorbed active electrical power.

The phenomenon of low frequency variation of the vibration amplitude from Figure 2.12 marked with B_1, B_2, B_3 and B_4 is described also as the phenomenon of low frequency variation of the absorbed active electrical power from Figure 2.13.

According to the vibration theory, this phenomenon is absolutely normal. When the excitation starts (in A, the switch K_1 is switched-on, the transducer PT1 is electrically supplied) two vibration components occur. The first component is the forced vibration response (20.8 Hz frequency) and the second component is the viscously damped free vibration (21.164 Hz frequency, as it is described also in E area from Figure 2.12 and Figure 2.4).

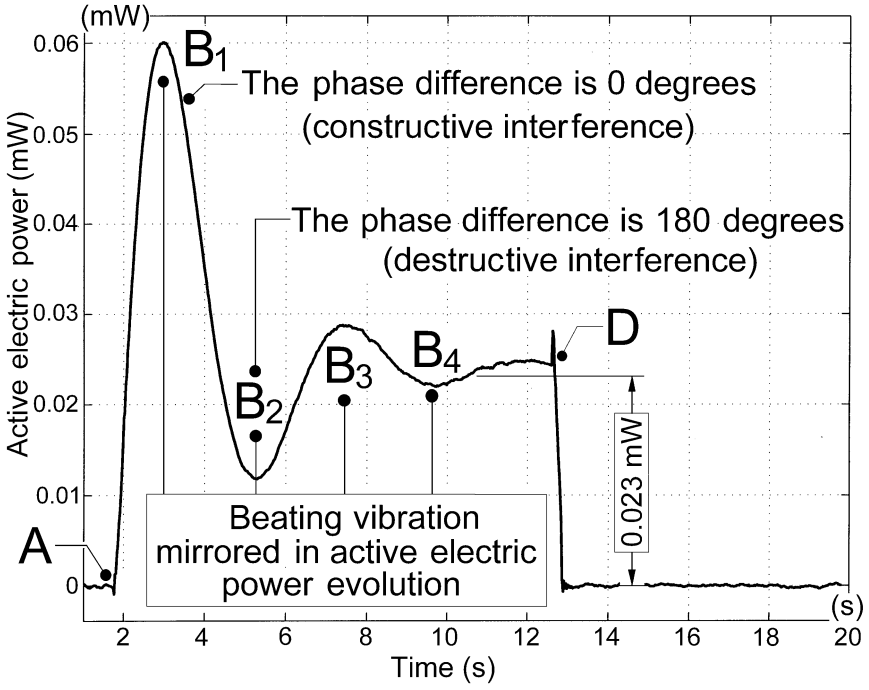

Fig. 2.13: *The mirroring in the active power evolution for the transient regime described in Figure 2.12 (**see also the chapter 2.7**).*

The addition of these two response components with different frequencies generates a beating phenomenon with nodes (minimal vibration amplitude) when the components are out of phase (180^o angle of phase, destructive interference), and anti-nodes (maximal vibration

amplitude) when the phase angle between these two components is zero (constructive interference).

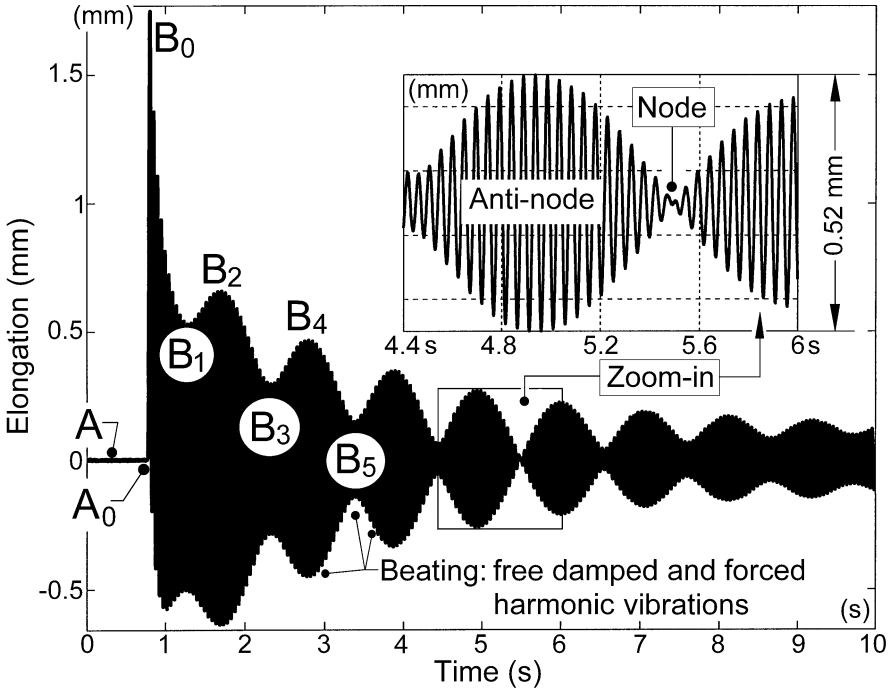

Fig. 2.14: *The description of a transient regime with beating phenomenon mirrored in vibration elongation evolution (**see also the chapter 2.7**)*

The beating phenomenon is very well described in the evolution of the absorbed active power on PT1 supply circuit, with maximal peaks in anti-nodes (B_1, B_3, here the increasing of the vibration amplitude is produced by the increasing of the absorbed power) and minimal peaks in nodes (B_2, B_4, here the decreasing of the vibration amplitude is produced by the decreasing of the absorbed power).

2.4.2.1. Negative Active Power

The results of a more eloquent experiment, with important practical implications, are described in Figure 2.14. The transducer PT1 is permanently supplied with a harmonic signal with the same voltage U_{rms} as before, but with a frequency of 20.2 Hz (smaller than the resonance frequency), thus there is generated a permanently forced vibration.

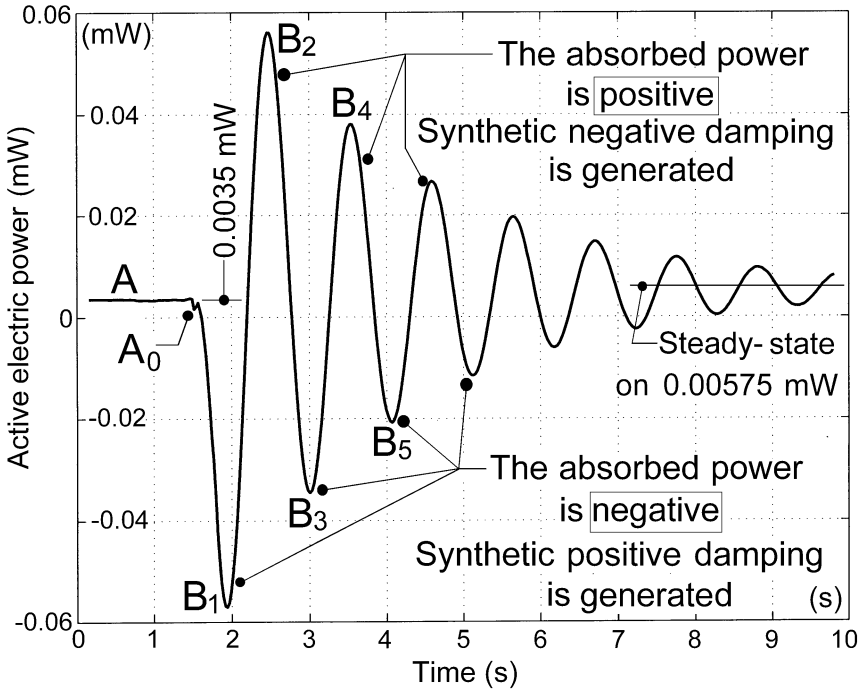

Fig. 2.15: *The mirroring in the active power evolution (negative and positive) for the transient regime described in Fig. 2.14 (**see also the chapter 2.7**).*

In A the free end of the cantilever beam is manually locked. At the moment A_0 the free end of the cantilever beam is manually excited with a step mechanical excitation. As a result a free viscous damped response vibration component occurs (21.164 Hz frequency). The addition between this vibration and the forced vibration component (20.2 Hz frequency) produces a beating phenomenon, described in Figure 2.14 as vibration elongation evolution.

The same experiment was performed once again; the evolution of the absorbed electrical active power is described in Figure 2.15. The beating phenomenon is clearly mirrored here. A relevant fact is that in anti-nodes due to the constructive interference the absorbed active electrical power is positive (e.g. the peaks B_2, B_4 etc.), and in nodes due to the destructive interference the power is negative (e.g. the peaks B_1, B_3, B_5, etc.). On Figure 2.14 the peak B_0 is generated because the DC (direct current) signal component delivered by the laser position sensor is removed by filtering in the oscilloscope (used as data acquisition system).

If the absorbed active electrical power is negative as well, the mechanical power delivered by PT1 to the cantilever beam is negative. There is a question here: how could the mechanical power be negative?

Suppose that F_{rms} is the root mean square of the instantaneous harmonic force produced by the transducer PT1. Suppose that this force is applied in a point on the cantilever beam which has a velocity v_{rms} (root mean square value of the instantaneous harmonic velocity). The average value of the mechanical power generated by PT1 is described by:

$$\overline{N} = F_{rms} \cdot v_{rms} \cdot cos(\theta) \tag{2.11}$$

Here θ is the phase angle between the actuation force and the velocity. The mechanical power delivered by the transducer PT1 is negative if the phase angle between force and velocity has a value described by: $\pi/2<\theta<3\cdot\pi/2$. The mechanical power has a minimum value, negative, if $\theta = \pi$ (180 degrees out of phase between force and velocity). The transducer PT1 works as modal energy absorber (energy consumer), the vibration amplitude decreases.

The mechanical power delivered by the transducer PT1 is positive if the phase angle between force and velocity has a value described by: $-\pi/2<\theta<\pi/2$. The mechanical power has a maximum value, positive, if $\theta = 0$. The transducer PT1 works as modal power supply, the vibration amplitude increases.

According to Eq. (2.2), ($\overline{P} = U_{rms} \cdot I_{rms} \cdot cos(\varphi)$, which has the same structure with Eq. (2.11)), the absorbed active electrical power can be negative only if the power factor $cos(\varphi)$ is negative, so the phase angle is $\pi/2<\varphi<3\cdot\pi/2$. For the negative peak B_1 on Figure 2.15 the phase angle is $\varphi = 0.62\cdot\pi$ (or 112.4 degrees). When the absorbed electrical active power is negative (in nodes), because of the direct piezoelectric effect the transducer PT1 works as a mechanical to electrical energy converter (modal energy absorber). It absorbs the mechanical modal strain energy of the cantilever beam. A part of this mechanical energy is converted into electrical energy delivered to the harmonic generator 1 where it is dissipated as heating. The transducer

PT1 works as an electrical power supply (actuated with mechanical strain power) and the harmonic generator 1 works as a consumer (or as a negative modal power supply) which eliminate the modal energy stored in the cantilever beam.

Also, according to Eq. (2.2), the absorbed active electrical power is positive if $cos(\varphi)>0$, so if $-\pi/2<\varphi<\pi/2$. For the positive peak B_2 on Figure 2.15 the phase angle is 66.6 degrees. When the absorbed electrical active power is positive, because of the inverse piezoelectric effect, the transducer PT1 works as an energy converter from electrical to mechanical. It absorbs the electrical energy delivered by the harmonic generator 1. A part of this electrical energy is converted into mechanical strain energy delivered to the cantilever beam and used to supply the forced vibration. The transducer PT1 works as an electrical power consumer and the harmonic generator 1 works as an electrical positive power supply.

The negative power in the mechanical system of the beam is associated with the occurrence of the active damping phenomenon. Positive synthetic damping is generated. It is thus experimentally shown a possible technique for correcting the resonant amplification of the mechanical systems using a negative modal power supply. The forcing of the current-voltage phase angle at values $\pi/2<\varphi<3\cdot\pi/2$ ensures this behavior of the transducer PT1.

The absorbed electrical active power is proportional with the transducer conductance. The conductance is the real part of the admittance. The admittance is the inverse of the impedance. The electrical impedance of the piezoelectric transducers is widely used in

the literature [8, 10 and 16] for the dynamic characterization. Figure 2.16 presents the evolution of the electrical impedance of the transducer PT1 (calculated according to Eq. (2.6)) during the experiment of beating previously described in Figure 2.15. A comparison between Figures 2.15 and 2.16 proves that is easiest to describe, understand and exploit a transient regime with beating vibration using the evolution of the absorbed electrical active power.

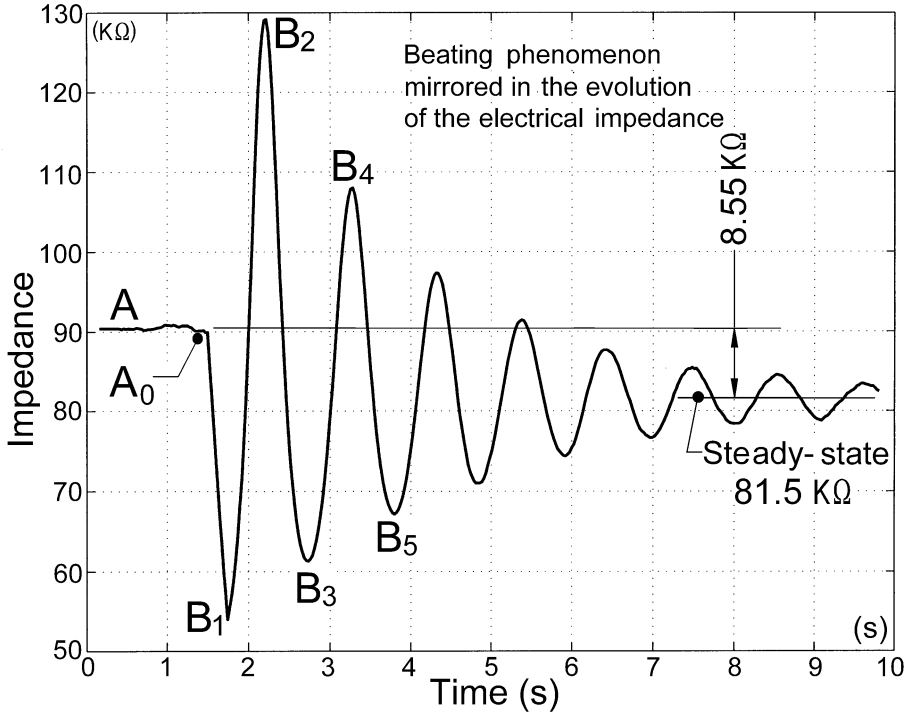

Fig. 2.16: *The mirroring in the electrical impedance evolution for the transient regime described in Figure 2.14.*

In the definition of the electrical impedance are involved only the voltage and the current. In the definition of the electrical active power are involved the voltage, the current and, very important, the

phase angle φ between the instantaneous current and voltage. If the voltage applied to the transducer is constant then the electrical impedance depends only by the current but the electrical active power depends by the current and the phase angle. It is better to use the active power to obtain information about some dynamic phenomena (e. g according to Figure 2.15, to detect if the transducer PT1 introduces or eliminates modal energy in the cantilever beam).

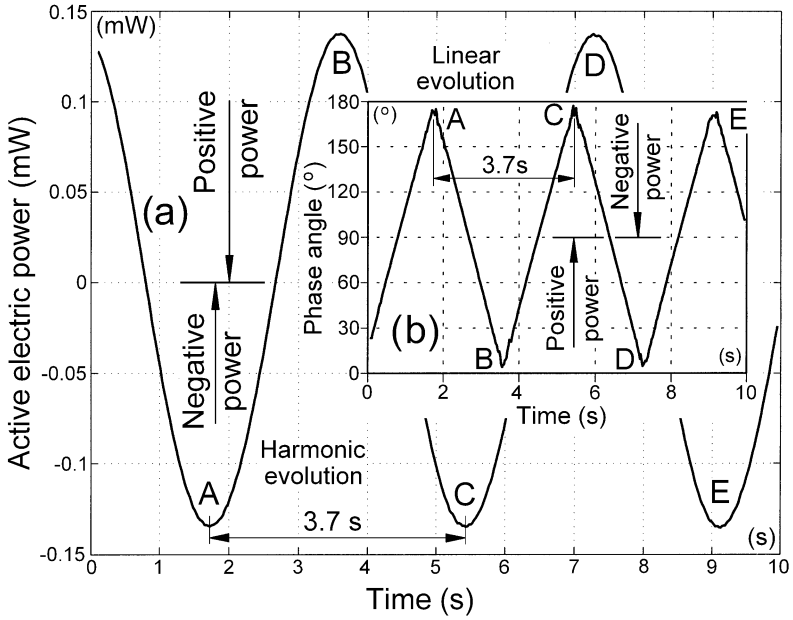

Fig. 2.17: *Transient regime with harmonic evolution of the active electric power absorbed by the transducer PT1 (negative and positive power).*

A transient regime with negative absorbed active power can be also illustrated by the following experiment, with the results shown in Figure 2.17. On the experimental setup formally described in Figure 2.1 the switches K_1 and K_2 are switched-on (K_3 is off), each of the two

transducers PT1 and PT2 being powered with harmonic signals with two different frequencies, close to each other and to the resonance frequency of the first flexural mode of vibration. The voltage and frequency applied on the transducer PT1 by the harmonic generator 1 are: $u_{PT1}=1.27\ V_{rms}$ and $f_{PT1}=21.024\ Hz$, the voltage and frequency applied on the transducer PT2 by the harmonic generator 2 are: $u_{PT2}=3.15\ V_{rms}$ and $f_{PT2}=20.75\ Hz$. Thus the cantilever beam is excited in such a manner that a permanent beating vibration phenomenon occurs. The beating is mirrored in the evolution of the active electric power absorbed by the transducer PT1, according to Figure 2.17 (a). The power has a harmonic evolution, with the same frequency with the frequency f_{BV} of the beating vibration nodes being:

$$f_{BV} = f_{PT1} - f_{PT2} = 0.274\ Hz \tag{2.12}$$

This frequency corresponds to a period of $T_{BV}=3.64\ s$, a very close value to the one experimentally revealed in Figures 2.17 (a) and 2.17 (b).

The evolution of power with maximum (positive) and minimum (negative) values can be explained using the same arguments as those presented in the physical horizon of Figures 2.14 and 2.15. The negative electrical active power in the dynamic systems represents an interesting result experimentally revealed here.

As already anticipated, the negative active power is determined by the value of the current-voltage phase angle φ, by the character of its evolution. Figure 2.17 (b) describes the evolution of phase angle φ,

with regular ramp-slope excursion, linearly variable between 0 and π, with the same frequency as that of the power, given in Figure 2.17 (a). This type of evolution has a very interesting explanation: the current from the supply circuit of the transducer PT1 has the same frequency with the voltage from the supply circuit of the transducer PT2. There is a practical example of an AC (alternating current) supplying circuit with different frequencies values for voltage and current.

The results described in Figure 2.17 reinforce the conclusion that forcing the absorption of negative power (with an effect in reducing of the vibrations' amplitude) is done by forcing the voltage-current phase shift to values higher than $\pi/2$ (or $\pi/2<\varphi<3\cdot\pi/2$). Of course this is possible only if the cantilever beam vibrates; the negative power used for actuation always means damping.

The implications of this approach are probably useful in what concerns the synthesis of a new procedure of active damping of vibrations based on modal negative power input actively generated supplying a piezoelectric transducer. A piezoelectric transducer placed on a vibrating structure works as an active damper if it is supplied with a negative electrical power supply. If the structure where the transducer is placed vibrates then the negative power supply should be able to self generate an instantaneous current and an instantaneous voltage with 180 degrees out of phase between, on the frequency of each excited mode of vibration simultaneously if necessary. Of course there are some difficult issues concerning this procedure. The biggest future

challenge is to find a simple way to produce a cheap negative power supply unconditionally stable on a wideband of frequency.

A resistance-inductance (R-L) series circuit (shunt) placed on the transducer electrodes produces passive damping [8, 9, 10] if the inductance is tuned properly. The R-L series circuit works as a narrowband passive negative electrical power supply.

The active damping with negative power actuation is already available [1, 2, 7, 8 and 15], but it uses two transducers, a piezoelectric sensor collocated with a piezoelectric actuator and a feedback loop in between. The sensor is used to drive an electronic circuit which is able to supply the actuator with negative active power on some modes of vibration. For the time being this is the most efficient technique of active damping.

A classical negative velocity force feedback damping system [7, 9] with collocation of the sensor and actuator generates an actuating force in opposite direction with the velocity, so according to Eq. (2.11), a negative mechanical power is generated. If the feedback is positive then the power generated by the actuator is positive, the system may starts to vibrate and become unstable (synthetic negative damping is generated).

There is also known a technique of active damping [18] based on a single piezoelectric transducer placed on a mechanical structure but using the self-sensing principle (the transducer works as sensor and actuator, naturally collocated) and feedback as before. A bridge circuit is connected to the electrodes of the transducer. The circuit is used to distinguish the actuating voltage from the sensing voltage and to

control the actuating voltage. For active damping the power produced by the piezoelectric transducer and absorbed by the structure should be negative.

2.4.3 Characterization of a High Frequency Mode of Flexural Vibration

The approach to characterize the dynamic behavior of the cantilever beam based on the evolution of the energetic parameters within the supply circuit of the transducer PT1 (used as actuator) may be completed by studying the other modes of flexional vibration on the same setup described in Figure 2.1.

As an example, there are presented some experimental results related to a flexural vibration mode of the cantilever beam that has a frequency of 1039.75 Hz. For this vibration mode it will also be studied the effects of a well-known technique of passive damping [8, 9 and 10], the using of the transducer PT2 as passive dynamic modal energy absorber. An R_s-L_s (resistor-inductor) series shunt is placed on the electrodes of the transducer PT2 (in Figure 2.1 the switch K_1 is switched-on, the switch K_2 is off, and the switch K_3 is on).

Formally, this absorber works just like a tune mass passive dynamic damper [19]. The resonant frequency of the flexural mode should be close to the resonance frequency within the electric circuit of the transducer PT2 (which acts like a series circuit of resistor-inductor-capacitor). The inductive reactance is used to cancel the capacitive reactance of the transducer PT2 on the frequency of the mode in such a

way that the electrical impedance of the circuit is minimal (the impedance is equal with the resistance). If the cantilever beam vibrates on this mode (the transducer PT1 is used for actuation) then the transducer PT2 converts a part of the mechanical modal strain energy of the cantilever beam into active electrical energy which is dissipated as heating on the resistor. The transducer PT2 works as a modal damper, passive absorber (consumer) or passive negative mechanical power supply as well.

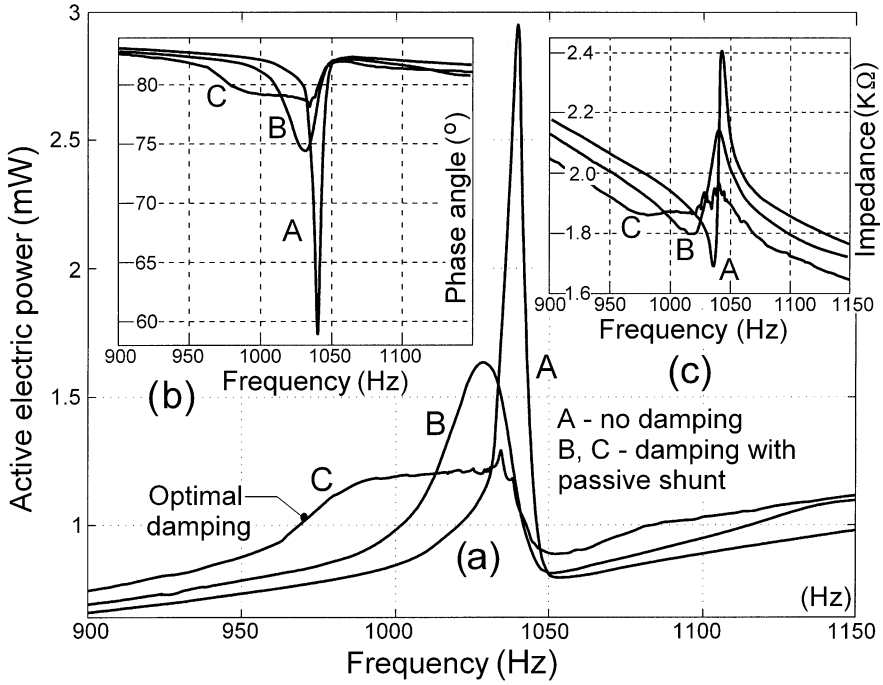

Fig. 2.18: *The characterization in frequency domain of a high frequency vibration mode with and without modal passive damping (R_s-L_s shunt):* ***(a)*** *The active absorbed power evolution;* ***(b)*** *The evolution of current-voltage phase angle φ;* ***(c)*** *The evolution of the electrical impedance.*

A series of experimental results is presented in Figure 2.18. Figure 2.18 (a) describes the evolution of the electrical active power absorbed by the transducer PT1, in frequency domain, when it excites the cantilever beam around the frequency of this vibration mode. On the setup described in Figure 2.1 a measurement resistor $R_m = 56\ \Omega$ is used. The curve marked with A refers to the evolution when the transducer PT2 is in open circuit (K_3 is switched-off). As it was already proved, there is a peak of power absorption on resonance frequency.

The curves marked with B and C refer to the evolution when PT2 and the external R_s-L_s shunt works as a passive absorber (K_3 is switched-on). For the evolution described with curve B the shunt uses the values: $R_s=100.4\ \Omega$ and $L_s=0.2584\ H$. As it is clearly indicated, the shunt reduces the peak amplitude, but the effect is non-optimal. The measured capacity of the transducer PT2 is $C_{PT2}=80.1\ nF$, the resonance frequency f_{RLC} of the resistor-inductor-capacitor series circuit is given by:

$$f_{RLC} = \frac{1}{2 \cdot \pi \cdot \sqrt{L_s \cdot C_{PT2}}} = 1106.26\,Hz \qquad (2.13)$$

A very similar behaviour to the optimal attenuation is described on curve C (with $R_s=100.9\ \Omega$ and $L_s=0.2997\ H$). The resonance frequency of the resistor-inductor-capacitor series circuit calculated with Eq. (2.13) is $f_{RLC}=1027.21\ Hz$, close to the frequency of the flexural vibration mode of the cantilever beam (1039.75 Hz).

Figure 2.18 (b) shows the evolution of the current-voltage phase angle φ in the supplying circuit of the transducer PT1, Figure 2.18 (c)

shows the evolution of the PT1 electrical impedance, in the same three experimental circumstances (A, B and C), for the same frequency domain. The influence of the electric resonance frequency value of the resistor-inductor-capacitor series circuit on the modal attenuation is very well described in power evolution (Fig. 2.18 (a)) and in phase angle evolution (Fig. 2.18 (b)).

The R_s-L_s series shunt works as a negative passive electrical power supply. This damping technique is useful to damp high frequency modes of vibration. In order to damp a low frequency mode it is necessary to use a very high inductance (electronically generated [9]). According to Eq. (2.13), it is possible to achieved the damping of the first flexural mode (on 21.164 Hz frequency) with an R_s-L_s shunt with an inductance L_s*=706.012 H.*

2. 5 CONCLUSIONS

The evolution of the energetic parameters of actuation is useful in the experimental research of the mechanical structures dynamics, which are excited with piezoelectric actuators. For that purpose, this paper presents a series of experimental results obtained with simple research facilities, based on computer assisted techniques of data acquisition and processing. There was used a simple setup based on an aluminium cantilever beam and two PZT piezoelectric transducers PT1 and PT2, glued near the rigid fixed end was used. Each piezoelectric transducer can be used as actuator if it is electrically supplied (e.g with

a harmonic signal generator) or as sensor. The evolution in time and frequency domain of the energetic parameters (active electric power, phase angle, impedance and reactive electric power) in the supplying circuit of the transducer PT1 (working as actuator and sensor) is used to describe some dynamic characteristics of the cantilever beam. Two instantaneous voltage signals acquired in the electrical supplying circuit and some specific computer programs written in Matlab are used to describe the evolution of the energetic parameters. For first flexural (bending) vibration mode of the cantilever beam (21.164 Hz frequency) a few different regimes was evaluated in experimental terms (e.g. the excitation at resonance, the behaviour as narrowband frequency mechanical modal energy absorber, beating vibration phenomena with positive and negative absorbed active electrical power, passive damping). There were done some researches on a high frequency vibration mode (1039.75 Hz). The efficiency of a well known passive damping technique of modal damping (resistor-inductor series shunt placed on the transducer PT2) was evaluated using the energetic parameters evolution in frequency domain.

There are emphasized a series of results, precursors of subsequent developments, among which we propose the concept of vibration damping with negative modal power actively generated. This concept -as a big challenge for our future researches- can be used probably to damp some modes of a mechanical structure using a piezoelectric transducer placed on the structure and a negative active power supply. This power supply should be able to detect the frequency and the phase of each excited mode of vibration (using the transducer

as sensor) and to push the transducer (used as actuator) to deliver negative strain mechanical power on those modes, simultaneously if necessary. This is possible if, for each excited mode, the transducer is electrically supplied with an instantaneous voltage and an instantaneous current with π angle of phase between (180^o out of phase), both having the same frequency with the vibration mode.

Some unpublished experimental research provides similar results in the evaluation of the dynamic behaviour of a cantilever beam actuated with an electrodynamic actuator (Lorentz force generator).

The computer aided energetic parameters evaluation technique can be used for experimental researches purposes of all electrically actuated systems supplied with alternating current.

2.6 REFERENCES

20. J. N. Reddy, (1999), *On laminate composite plates with integrated sensors and actuators*, Engineering Structures, vol. 21, pp. 568–593, 1999.
21. V. Piefort, (2001), *Finite Element Modeling of Piezoelectric Active Structures*, Ph.D. thesis, Université Libre de Bruxelles, Brussels, Belgium, 2001.
22. L. Dalessandro L, D. Rosato, (2005), *Finite-Element Analysis of the Frequency Response of a Metallic Cantilever Coupled With a Piezoelectric Transducer*, IEEE Transactions on

Instrumentation and Measurement, vol. 54, no. 5, pp. 1881-1890, 2005.

23. T. Eggborn, (2003), *Analytical Models to Predict Power Harvesting with Piezoelectric Materials*, Master degree thesis, Virginia Polytechnic Institute and State University, 2003.
24. Y. P. Liu1, Y. P. Vasic, D. F. Costa, W. J. Wu, C. K. Lee, (2009), *Velocity-Controlled Piezoelectric Switching Energy Harvesting Device*, ICREPQ'09 2009, Proceedings of International Conference On Renewable Energies And Power Quality. Valencia, Spain, 2009.
25. H. A. Sodano, D. J. Inman, G. Park, (2004), *A Review of Power Harvesting from Vibration using Piezoelectric Materials*, Shock and Vibration Digest, vol. 36, no. 3, pp. 197-205, 2004.
26. A. Preumont, (2002), *Vibration Control of Active Structures: an Introduction*, 2nd ed., pp. 37-88, Kluwer, Dordrecht, The Netherlands, 2002.
27. B. de Marneffe, (2007), *Active and Passive Vibration Isolation and Damping via Shunted Transducers*, Ph.D. thesis, Université Libre de Bruxelles, Brussels, Belgium, 2007.
28. S. O. R. Moheimani, (2003), *A Survey of Recent Innovations in Vibration Damping and Control Using Shunted Piezoelectric Transducers*, IEEE Transactions on Control Systems Technology, vol. 11, no. 4, pp, 482-494, 2003.
29. N. W. Hagood, A. von Flotow, (1991), *Damping of Structural Vibrations with Piezoelectric Materials and Passive Electrical*

Networks, Journal of Sound and Vibrations, vol. 146, no. 2, pp. 243-268, 1991.

30. A. J. Fleming, S. Behren, S. O. R. Moheimani, (2000), *Synthetic Impedance for Implementation of piezoelectric shunt-damping circuit*, Electronics Letters., vol. 36, no. 18, pp. 1525-1526, 2000.
31. Yu-Hsiang Hsu, Chih-Kung Lee, Wen-Hsin Hsiao, (2003), *Optimizing Piezoelectric Transformer for Maximum Power Transfer*, Smart Materials and Structures, vol. 12, no. 3, pp. 373-383, 2003.
32. S. Chandrasekaran, D. K. Lindner, (2000), *Power Flow Through Controlled Piezoelectric Actuators*, Journal of Intelligent Material Systems and Structures, vol. 11, no. 6, pp. 469-481, 2000.
33. C. Liang, F. P. Sun, C. A. Rogers, (1994), *Coupled Electro-Mechanical Analysis of Adaptive Material Systems-Determination of the Actuator Power Consumption and System Energy Transfer*, Journal of Intelligent Material Systems and Structures, vol. 5, no. 1, pp.12-20, 1994.
34. D. J. Warkentin, (1995), *Power Amplification for Piezoelectric Actuators in Controlled Structures*, Ph.D. thesis, Massachusetts Institute of Technology, 1995.
35. A. Preumont, (2006), *Mechatronics: Dynamics of Electromechanical and Piezoelectric Systems*, pp. 95-190, Springer, 2006.

36. Lewin, Walter, 8.03 Physics III: Vibrations and Waves, Fall 2004. (Massachusetts Institute of Technology: MIT OpenCourseWare), http://ocw.mit.edu/courses/physics/8-03-physics-iii-vibrations-and-waves-fall-2004/video-lectures/embed04/ (Accessed 31 Dec, 2009). License: Creative Commons BY-NC-SA
37. J. J. Dosch, D. J. Inman, E. A. Garcia, (1992), *Self-Sensing Piezoelectric Actuator for Collocated Control*, Journal of Intelligent Material Systems and Structures, vol. 3, no. 1, pp. 166-185, 1992.
38. J. P. Den Hartog, (1985), *Mechanical Vibrations*, Fourth edition, McGraw-Hill, London, 1956, Reprinted by Dover, New York, 1985.

2.7 A SUMMARY OF SOME EXPERIMENTAL FIGURES

Some experimental figures from this paper can be reproduced by any reader as it is indicated below. First please download the folder **Data paper 2** (see the download indications from preface).

Figure 2.4

You need the folder **Data Fig. 2.4.** In order to obtain this figure please have a look on the task #2 (in chapter 2.8). The reader is invited to observe that Figures 2.4 and 1.3 are very similar.

It is possible to find-out the exactly value of the frequency of excitation in steady state regime (C area on Figure 2.4) by running the Matlab program **ident2** (available in the folder **Data Fig. 2.4**). This program finds out the characteristics of a theoretical harmonic curve which is the best fitting for the harmonic evolution of the vibration elongation in C area. The both curves (theoretical in blue and experimental in red) are drawed on the figure generated by the program. The value of frequency (21.0085 Hz, already written on Figure 2.4) is written in the command window.

It is also possible to find out by numerical fitting the parameters of the free response of the cantilever beam from E area (Figure 2.4) by running the Matlab program **ident3** (available also in the folder **Data Fig. 2.4**). It is suppose that this free response is described in theoretical terms by the Eq. (1.19), written in the chapter 1.12. The program **ident3** is able to find-out the best fitting curve which fit the experimental evolution and the values of the parameters involved in Eq. (1.19). You find the values of these parameters in the matrix d. You can see the both curves on the figure generated by the program (experimental curve in red and the fitting curve in blue). The both curves are very well fitted each other.

This experiment also confirms that the theoretical description (1.19) of the free response of the cantilever beam is correct.

The program generates in the command window the values of the damping ratio (%) and frequency of free response as it were also written on Figure 2.4.
Try to increase the precision of the determination of the parameters involved in Eq. (1.19) by numerical fitting.

Figure 2.5

In order to obtain this Figure using Matlab please have a look on task #3 (in chapter 2.8). The reader is invited to observe that Figures 2.5 and 1.4 are very similar. This proves that two different actuation systems act identical by the point of view of the absorbed active electrical power during the same dynamic phenomenon.

Figure 2.6

Use the programs from the folder **Data Fig. 2.6.** In order to obtain the main parts of Figure 2.6 the reader should run the Matlab program **fig26.m** from this folder.

Figure 2.12 and 2.13

You need the folder **Data Fig. 2.12-2.13**. If you run the Matlab program **fig21213.m** you should obtain a figure which contains Figure 2.12 and 2.13. This describes the behaviour of the cantilever beam very similar to those already decribed in Figure 1.7. Notice that here are

involved two different types of actuators. In Figure 1.7 b) the beating phenomenon is described by the evolution of active power absorbed by a voice-coil actuator. Here (and in Figure 13 too) the beating phenomenon is described by the active power absorbed by a piezoelectric actuator.

Figure 2.14

Use the folder **Data Fig. 2.14.** Run the Matlab program **fig214.m**. You should obtain the main part of Figure 2.14.

Figure 2.15

You need the folder **Data Fig. 2.15.** Run the Matlab program **fig215.m** placed in this folder. You should obtain the main part of Figure 2.15. This figure is very similar those already shown as Figure 1.8.

2.8 THEORETICAL AND EXPERIMENTAL WORK TASKS

1. Perform the experimental setup described in Figs. 2.1 and 2.2. Use the oscilloscope PicoScope 4424 (4 channels) in order to acquire at the same time the voltages u_A and u_B and the voltage delivered by the laser position sensor.

2. Perform the experiment described in Fig. 2.4 in order to obtain the evolution of the voltage generated by laser position sensor in two ways:

   - using only the oscilloscope;

   - using a Matlab program which converts the voltage in displacement of the free end cantilever beam;

In order to solve these tasks please have a look on the Matlab program **fig24**.m presented below. Running this program leads to getting the Figure 2.4. The file **datfig24.txt** and the program **fig24.m** are available in electronic format (in the folder **Data Fig. 2.4**).

Program fig24

```
clear all;close all;durata=20;
load datfig24.txt;
x=datfig24(:,1)/1000000;
y=datfig24(:,2)*1.93548-8.5;
%the constant value 1.93548 mm/mV transforms the
voltage %delivered by laser sensor in displacement
p=5;dim1=size(y);dim=dim1(1);k=1;
for i=1+p:dim;
   medy=0;
   for j=1:p;
      medy=medy+y(i-j)/p;
   end
   yfts(k)=medy;
   xfts(k)=k*durata/dim;
   k=k+1;
end
%the above part of the program (marked with bold)
%perform the filtering of %data (moving average
filter)
%p is the parameter of filtering

plot(xfts,yfts,'k','LineWidth',1.5);hold on
```

```
k=1;for i=4821:5950;abs(k)=xfts(i)*13-6;
ord(k)=yfts(i)*3-900;
k=k+1;end;plot(abs,ord,'k','LineWidth',1);clear
abs;clear ord;
k=1;for i=53096:54317;abs(k)=xfts(i)*10-159;
ord(k)=yfts(i)*1.7+950;
k=k+1;end;plot(abs,ord,'k','LineWidth',1);clear abs;
clear ord;
k=1;for i=34482:35703;abs(k)=xfts(i)*20-222;
ord(k)=yfts(i)/2;
k=k+1;end;plot(abs,ord,'w','LineWidth',1.5);
clear abs;clear ord;
```

The file **datfig24.txt** is saved from oscilloscope. First column describes the time (in microseconds), the second column describe the voltage (millivolts) delivered by the laser position sensor ILD 2000 (see Figures 2.1 and 2.2)

3. Perform the experiment described in graphical terms in Figure 2.5. You should acquire the voltages u_A and u_B during the experiment and to use a Matlab program similar to the one shown below. The file **datefig25.txt** and the Matlab program **fig25.m** are available in electronic format (in the folder **Data Fig. 2.5**).

Program fig25

```
   clear all;close all;inreg=20;p=10;
load datefig25.txt;
   l=size(datefig25);
   timp1= datefig25 (:,1);amplit= datefig25 (:,2);
   timp=timp1(1:l/2)/1000000;
   tens=amplit(1:l/2)/1000;
   l1=l(1)/2+1;curent=amplit(l1:l)/(1000*1020);
```

```
%this value (1020) is the resistive shunt
putinst=tens.*curent;

%Here below it is calculated the value of
frequency of the harmonic signal
k=0;
for i=1:l1-2;
   prod=tens(i)*tens(i+1);
   if prod<0;k=k+1;flag2(k)=i;else end
   if k==1;flag1=i;else end
   end
   frecv=k/(2*(timp(flag2(k))-timp(flag1)))
   for i=1:k-1
      dif=flag2(i+1)-flag2(i);pont=0;
      if dif<5;pont=1;else end;
   end;pont
%if pont > 0 this means that the calculus of
%frequency is wrong (please explain that) you
should perform once again %the experiment
incr=1*(l(1)/(2*inreg*frecv));
sup=round(incr);per=inreg/(l1-1)*incr;
   fil=5;
   ji1=size(flag2);ji=ji1(2);
   medt1=0;for i=1:ji-1;
    timpef(i)=i*per/2;
   end;
   for i=1:ji-1;max=-1000;medp=0;
       for k=flag2(i):flag2(i+1);
         medp=medp+putinst(k);
       end;
     putactf1(i)=medp/(flag2(i+1)-flag2(i));
    end
matdefil=putactf1;d=size(matdefil);k=1;
for i=1+p:d(2);
   a=matdefil(i-p+1:i);b=timpef(i-
p+1:i);meda1=sum(a);meda2=sum(b);
   matfil(k)=meda1/p;timpeff(k)=meda2/p;k=k+1;
```

```
   end
   for i=1:p;matfil(i)=matfil(p+1);
   timpeff(i)=timpeff(p+1);end;
   putactff1=matfil;clear matdefil;clear matfil;
plot(timpeff,putactff1,'k','LineWidth',1.5);
axis([0 20 -.00001 0.0002])
```

The instructions marked with bold characters allow determining the value of frequency of voltages u_A and u_B.

In order to find by calculus the value of active electrical power absorbed by PZT actuator in steady-state between the levels D and E (on Figure 2.5) it is useful to run immediately after the program **fig25** this section of program:

```
dim=size(timpeff);dim1=dim(2);
increment=1/(timpeff(dim1)/dim1);
limtime1=9.5;limtime2=12.5;
limtime3=14;limtime4=17;
med1=0;k=0;
limtime1a=round(limtime1*increment);
limtime2a=round(limtime2*increment);
 for i=limtime1a:limtime2a;
    med1=med1+putactff1(i);k=k+1;
end
med1=med1/k;med2=0;k=0;
limtime3a=round(limtime3*increment);
limtime4a=round(limtime4*increment);
for i=limtime3a:limtime4a;
    med2=med2+putactff1(i);k=k+1;
end
med2=med2/k;med1-med2
```

The result (1.9617e-004 W) is already written on figure 2.5. This is the active electrical power absorbed by PZT actuator when it is supplied on the resonance frequency on first flexural mode of the free

end of the cantilever beam. In the same manner it is possible to find the value for any other frequency of excitation. Of course it is possible to add the last section to the program fig25.

4. Based on the discussion from task #3 you are invited to perform the experiments which allows you to draw something similar to Figure 2.7 and 2.11. Note that experiments should be made in such a way to avoid the transient regimes. For each frequency you should put K_1 switch (see Figure 2.1) in position on. Wait a while until the transient regimes (see Figures 2.11 and 2.13) disappears. Start the data acquisition (on the oscilloscope) and after that switch-off the K_1 switch. Use the program fig25 in order to find out the active power absorbed. Of course you should set the temporal limits from the program, see previously the instructions:

```
limtime1=9.5;limtime2=12.5;
limtime3=14;limtime4=17;
```

5. Based on the discussion from task #2 performs the experiments which led to the results of the graphs shown in Figures 2.12 and 2.14.

6. Based on the discussion from task #3 performs the experiments which led to the results of the graphs shown in Figures 2.13 and 2.15.

7. Optionally the reader can try creating programs that allow to find out the evolution of impedance (Figure 2.8), phase shift between voltage and current (Figure 2.9) and reactive power (Figure 2.10).
8. Perform the experiment described in Figure 2.14 (beating phenomenon mirrored in the evolution of the elongation of first flexural mode) and Figure 2.15 (the same phenomenon

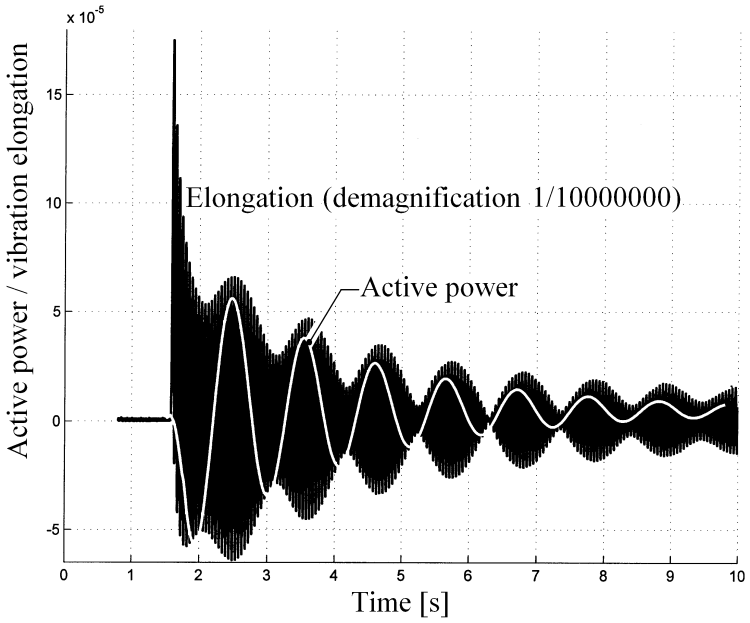

Fig. 2.19: *Beating phenomenon mirroring in the evolution of the vibrations of the free end of the cantilever beam and the active electrical power.*

mirrored in the evolution of the active electrical power absorbed by the piezoelectric actuator). Both evolutions should be registered in the same time. Put on the same figure

the both evolutions. You must obtain something that looks like the figure 2.19 (in order to obtain Figure 2.19 ask to the teacher the folder **Data Fig. 2.19** and run the Matlab program DESPUT2b1). Try to formulate a hypothesis about the shift of phase between evolutions. As it is clearly indicated, the positive and negative peaks of the active power are shifted related to the anti-nodes and the nodes of the elongation.

Paper 3

A STUDY ON ACTUATION POWER FLOW PRODUCED IN AN ACTIVE DAMPING SYSTEM

ABSTRACT

This paper aims to present some new features of the experimental research in dynamics of a closed-loop actively controlled mechanical system with collocated PZT sensor and actuator and a proportional-derivative regulator. The evolution of active electrical power absorbed by the actuator is mainly used. A fraction of this power is converted into mechanical real power and delivered by the actuator to the mechanical system. This paper highlights the fact that derivative gain in the regulator produces a directly proportional synthetic damping (positive or negative) in the mechanical system, due to the fact that a directly proportional flow of active electrical power (negative or positive) absorbed by the actuator is generated. The paper proves that the active power flow evolution is very useful to describe the behavior of the actuator for some dynamic regimes (more useful than the magnitude of the electrical impedance).

The research was done on a setup that consists of an aluminium cantilever beam equipped with two PZT collocated transducers -rectangular laminar design- closely glued by the rigidly fixed end of the beam. The feedback between sensor and actuator is provided by a regulator which produces a tunable phase difference between input and output (equivalent to a proportional-derivative feedback). The electrical current and the voltage generated by the regulator and applied to the actuator are used for finding the values of the active electrical power absorbed by the actuator, the magnitude of the electrical impedance and the values of some dynamic parameters of the cantilever (e. g. damping ratio, damped modal frequency, etc.) due to an external excitation of first bending mode. A computer assisted data acquisition system and some new data processing techniques are used for these purposes.

Keywords: Vibration, cantilever beam, piezoelectric actuation, negative modal power, synthetic damping.

Nomenclature

a	Slope of linear regression of the synthetic damping [$rad^{-1} \cdot mW^{-1}$]
α	Shift of phase angle between input and output voltage of the regulator [^{o}]
b	Intercept of linear regression of the synthetic damping [rad^{-1}]
C_d	Derivative gain [s/rad]
C_p	Proportional gain []
C_v	Voltage gain []
C_{sd}	Synthetic damping constant [rad^{-1}]
C_{ss}	Synthetic stiffness constant [rad^2/s^2]

d_{31}	Transverse piezoelectric coefficient [m/V]
Δt	Sampling interval [s]
f_0	Undamped modal natural frequency of the first bending mode [Hz]
φ	Shift of phase angle between the instantaneous current and voltage [^{o}]
i	Instantaneous current [A]
I_{rms}	Root mean square current [A]
K_{31}	Generalized electromechanical coupling coefficient []
k_{ss}	Synthetic modal stiffness [N/m]
k_m	Open-loop modal stiffness [N/m]
m_m	Open-loop modal mass [Kg]
n	Number of samples [ ]
ω	Angular frequency of harmonic excitation [rad/s]
ω_0	Undamped natural modal angular frequency of the first bending mode [rad/s]
ω_1	Damped natural nodal angular frequency of the first bending mode [rad/s]
ω_m	Open-loop undamped natural modal angular frequency of the first bending mode [rad/s]
ω_{ss}	Undamped synthetic angular frequency [rad/s]
p	Parameter of the moving average filter []
$P_{el,act}$	Active electrical power [W]
$P_{el,inst}$	Instantaneous electrical power [W]
$P_{el,react}$	Reactive electrical power [Var]
$P_{mec,real}$	Mechanical real power delivered by piezoelectric

	actuator [W]
$P_{mec,dis}$	Mechanical dissipated power [W]
$P_{mec,mod}$	Power flow generated by the modal energy stored in the cantilever beam [W]
P_{pv}	Power peak active electrical power [W]
P_{ss}	Steady-state active electrical power [W]
R_m	Measuring resistance [Ω]
T	Period of the alternating current [s]
θ_a	Phase angle of origin of time for the voltage u_a [°]
θ_B	Phase angle of origin of time for the voltage u_B [°]
θ_s	Phase angle of origin of time for the voltage u_s [°]
u_a	Instantaneous voltage applied to the piezoelectric actuator PA [V]
u_A	Instantaneous voltage delivered by the regulator [V]
u_B	Instantaneous drop of voltage on the measuring resistor [V]
u_s	Instantaneous voltage generated by the piezoelectric sensor PS [V]
$U_{a,rms}$	Root mean square of u_a voltage [V]
U_s	Amplitude of u_s voltage [V]
U_a	Amplitude of u_a voltage [V]
U_B	Amplitude of u_B voltage [V]
Z	Electrical impedance [Ω]
Z_c	Steady-state impedance [Ω]
ζ	Damping ratio [rad^{-1}]
ζ_1	Damping ratio of active electrical power [rad^{-1}]

ζ_n Synthetic damping ratio [rad^{-1}]

ζ_{sd} Natural damping ratio [rad^{-1}]

3.1 INTRODUCTION

The correction of the dynamic behavior of flexible mechanical structures with distributed mass through automated systems based on negative feedback from a sensor to an electric actuator using an electronic regulator is well known [1, 2, 3]. It seems that this type of correction has first been proposed in [4]. These systems are often used to eliminate or to reduce vibration amplitude on some resonant frequencies modes of the mechanical structures by active damping and isolation [5, 6]. The aforementioned active systems are able to generate and to deliver positive synthetic damping through the actuator to the mechanical structure.

An obvious question is in order: how should the actuator be powered in order to produce synthetic positive damping in the mechanical structure? The first answer is provided by a long practice in vibration engineering: the actuator should be powered in such a way that the force generated and applied in a point of the mechanical structure is opposed to the velocity of that point. The actuator acts as a viscous friction force generator. In consequence, a damping technique called direct velocity feedback control [7, 8, 9 and 10] was defined. If the sensor and the actuator are collocated (decentralized control [5]), the dynamic stability is guaranteed and the regulator has a very simple

task: to generate a negative feedback with proportional gain (the signal delivered by the velocity sensor is inverted and amplified before powering the actuator).

The same technique of vibration damping with collocated sensor and actuator is available if a displacement sensor is used. The regulator should produce a negative derivative feedback (the signal delivered by the displacement sensor is differentiated, inverted and amplified before powering the actuator). The same type of regulator is used for active vibration damping of mechanical structures (e. g. thin beams and plates) with PZT (lead-zirconate-titanate) laminar piezoelectric collocated sensor and actuator [11], as is illustrated in this paper. A piezoelectric sensor acts as a dynamic mechanical strain sensor. This strain is a description of relative deformation (displacement) of the mechanical structure.

Let us consider once again the previous question: how should the actuator be powered in order to produce synthetic positive damping in the mechanical structure? Starting from the conclusion that damping signifies that the system dissipates modal energy it results that the actuator should contribute to this goal. According to previous discussions, this paper claims and intends to prove experimentally that the actuator should absorb and dissipate mechanical modal energy. It works as an active damping device and acts as a negative mechanical modal real power supply. It provides a force opposed to the velocity (or at least a force with phase shift between $\pi/2$ and $3\cdot\pi/2$ relative to the velocity, [12]), therefore a negative mechanical real power. This negative real power is delivered to the mechanical structure. In order to

produce a negative mechanical modal real power the actuator should be electrically powered exclusively by a negative active electrical power. This means that the active damping can be done in open-loop system with an actuator and a negative active electrical modal power supply (without any sensor). This electrical power supply absorbs and dissipates the mechanical modal real power from mechanical structure (previously converted by the actuator in active electrical power). The active electrical power flows from the actuator to the electrical power supply. The dynamic stability is guaranteed due to the fact that the actuator cannot be supplied with positive active electrical modal power. It is obvious nowadays that this type of active electrical power supply exists but it should be reminded that it uses a sensor placed on the mechanical structure. In a closed-loop damping system with collocated sensor-actuator and negative derivative feedback [7, 8, 9 and 10], the sensor and the regulator play the role of the negative active electrical modal power supply. In the self sensing damping technique [13, 14] the electronic device placed on the electrodes of the PZT transducer (acting as sensor and actuator) should work as a negative active electrical power supply. A passive shunt damping circuit [15, 16, 17, 18, 19, 20, 21, 22 and 23], an adaptive shunt damping circuit [24] or an energy harvesting circuit [25] placed on the electrodes of a piezoelectric transducer works as a negative active electrical power supply on the modal frequency. The transducer acts both as a sensor and as an actuator.

Any system which is built for vibration suppression by damping (active, passive, semi-active [18, 26] or hybrid system [27]) and using

electrical actuators must ensure their supply with negative active electrical modal power. Therefore the evolution of the active electrical power flow absorbed by the actuators appears to be an important topic of research (this is useful for the study of vibration damping). The aforementioned topic is mainly considered in this paper.

Several results adjacent to the matter have already been reported in the literature regarding the use of active electric power (energy). They are related to the research concerning dynamical systems driven by transducers. Some papers investigate the power requirements for control law and actuation in order to decrease the energy consumption [28, 29, 30 and 26], to select a control strategy [9], to maximize the power transferred to the mechanical system [31], and to maximize the synthetic damping [32, 30 and 26]. The latter is a very important aspect which must not be overlooked. Others papers deal with energy harvesting [25, 33] or self powered damping systems [34] using piezoelectric transducers. An interesting theoretical study on the flow of active and reactive electrical power to the piezoelectric actuator inside a closed-loop system for active damping of mechanical structures is presented in [35]. The paper [19] focuses on the treatment of the electrical energy produced by piezoelectric transducers using a network of passive electrical elements. A new method of passive damping is described in [21 and 22]. It is based on the generalized principle of virtual power.

The work presented below aims to investigate experimentally the evolution of active electrical power absorbed by the actuator inside a closed-loop feedback system for active damping with PZT

piezoelectric sensor and actuator (collocated, laminar rectangular design, closely bonded by the rigidly fixed end of a cantilever beam). A phase shifter with adjustable phase is used as regulator inside the closed-loop. This type of regulator was already proposed in [36 and 37]. It will later be shown in the current paper that a phase shifter works as proportional and derivative regulator.

This paper especially illustrates the operating regimes with positive and negative active electrical power absorbed by the actuator (generated by positive and negative derivative feedback) and their influence on the dynamics of the beam (negative and positive synthetic damping is generated). A study on the evolution of the magnitude of the electrical impedance of the actuator and the evolution of the mechanical synthetic stiffness generated by proportional feedback was also performed. The paper highlights some new features concerning the usage of the active electric power evolution in terms of characterization and understanding the dynamics of mechanical structures actively controlled.

3.2. THE EXPERIMENTAL SETUP

The research was done on an experimental setup conceptually described in Figure 3.1, with a picture shown in Figure 3.2. The mechanical system consists of a cantilever beam 1 (300 x 25 x 2 mm, made of aluminium alloy AlMgSi1). A piezoelectric actuator 10 (PA) and a piezoelectric sensor 11 (PS) are glued -as collocated transducers- in close proximity of the rigidly fixed end, on each side of the beam.

The sensor and the actuator are identical, made of PZT (lead-zirconate-titanate), laminar rectangular design, 40 x 25 x 0.5mm, SensorTech BM500 type, with deformation in length mode, d_{31} polarization (d_{31}=-*175·10^{-12} m/V*) and opposite poling directions.

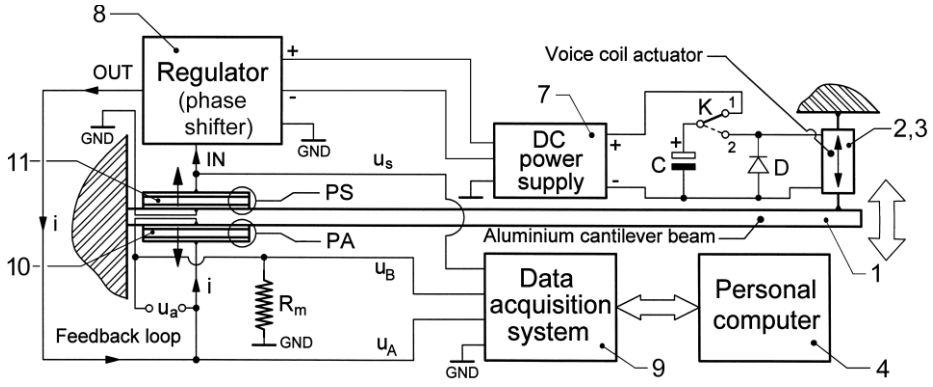

Fig. 3.1: *A description of the experimental setup.*

According to [12] the generalized electromechanical coupling coefficient of the sensor is $K_{31} = 0.113$ (the ratio between the real parts of input mechanical power and output electrical power) and of the actuator is $K_{31} = 0.097$ (the ratio between the real parts of input electrical power and output mechanical power). This type of setup (with surface-bonded piezoelectric transducers) is commonly used in experimental research [24, 17, 30, 26, 12, 36 and 10] and suggestions for usage in some industrial applications have already been made [38].

The voltage u_s generated by the sensor (if a bending mode of the beam is excited) is used as input signal in a regulator 8. The regulator generates a voltage u_A and a current i. The current flowing through a series circuit consists of the actuator PA and a measuring resistor R_m (12 KΩ) to the electrical ground (GND). This way the feedback loop is

closed. The regulator (an electronic device manufactured in the laboratory, supplied by a DC power supply 7) performs the functions of a phase shifter with manual phase adjustment between output and input voltages. The voltage drop u_B across the resistor R_m is used to measure the current i ($i=u_B/R_m$ due to the Ohm's law). The voltage drop u_a across the actuator PA is calculated as follows: $u_a=u_A-u_B$. The voltages u_s, u_A and u_B are collected by a data acquisition system 9 (a PicoScope 4424 oscilloscope with 12 bits resolution, 1% accuracy) and delivered in numerical format to a personal computer 4. These voltages are used for computer aided calculus (using Matlab) of the active electrical power absorbed by the actuator PA and for finding out some dynamic characteristics of the free response of the beam excited on the first bending mode of vibration (e.g. the damped modal frequency and damping ratio). A simple voice coil actuator placed on the free end of the beam is used in order to excite the first bending mode of vibration. It consists of a fixed coil (marked with 2 on Figure 3.2) and a permanent magnet (3 on Figure 3.2, neodymium-iron-boron, with axial magnetization) placed on the beam. The magnet is placed without physical contact inside the coil, centered [12]. The interaction between the current flow in the coil and the magnetic field generates a Lorentz force used to actuate the cantilever beam. The coil is supplied by a charged electrolytic capacitor C (1500 μF) when a switch K is switched from position 1 to position 2. In position 1 the capacitor is electrically charged (via the DC power supply 7). If the switch K is switched in position 2 the electric charges accumulated in the capacitor generates a short pulse of current in the coil. A pulse excitation of the cantilever

beam is generated. The voice coil actuator can also be used to produce a harmonic force if the coil is supplied with a harmonic voltage (the diode D should be removed).

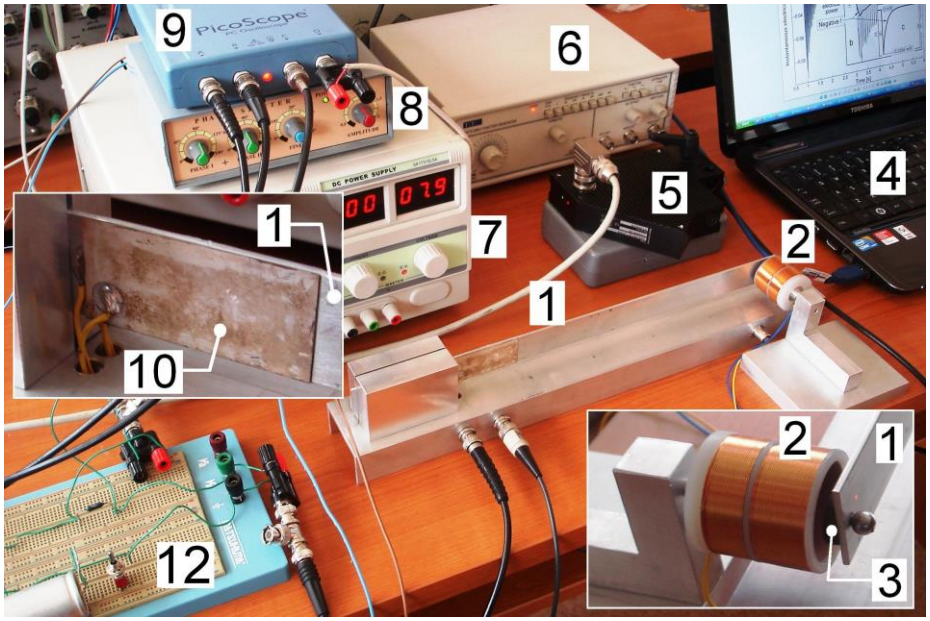

Fig. 3.2: *A picture of the experimental setup with zoom-in on the actuator and the voice coil.*

Figure 3.2 shows a picture of the experimental setup. Number 1 marks the cantilever beam, 2 marks the fixed coil, 3 - the permanent magnet placed on the free end of the beam, 4 - the computer, 5 - a laser position sensor ILD 2000 (useful for bending vibration elongation measurement [12]), 6 - a harmonic signal generator, 7 - the DC power supply, 8 - the regulator, 9 - the data acquisition system, 10 - the piezoelectric actuator PA (the piezoelectric sensor PS marked with 11 on Figure 3.1 is glued on the opposite side of the beam), 12 - a solderless breadboard (here are placed the resistor R_m, the capacitor C,

the switch K and some connecting wires).

3.3 THE EXPERIMENTAL PROCEDURE

3.3.1 Short overview of the experimental procedures.

The monitoring of the active electrical power absorbed by the actuator uses the instantaneous values of voltage $u_a(t)$ and current $i(t)$. These values are calculated using the voltages $u_A(t)$ and $u_B(t)$, collected and converted in numerical format by the data acquisition system and stored inside the computer. The instantaneous electrical power is the mathematical product of $u_a(t)$ and $i(t)$ [12, 39]. The active electrical power (also called real power) is usually obtained as a mean value of the instantaneous electrical power [12, 39]. This paper proposes a new method of calculating the active power: numerical filtering of the instantaneous power using a moving average filter (band-stop filter).

The active power flow in the actuator is created by the mechanical excitation of the cantilever beam and the regulator (due to the derivative feedback). By the above described means mainly the first bending mode of vibration it is excited (impulse excitation). The free response of the cantilever beam (mirrored in the evolution of $u_a(t)$, $u_s(t)$ and $i(t)$) is used for experimental research. The shift of phase generated by the regulator (between $u_a(t)$ and $u_s(t)$) determines the character of free response of the beam (the damped modal natural frequency and the

damping ratio). The phase shifting is equivalent to a proportional and derivative feedback control law between the sensor and the actuator.

The proportional gain of the feedback loop generates synthetic mechanical modal stiffness (revealed experimentally in the evolution of the frequency of the free response). The derivative gain of the feedback loop generates synthetic mechanical modal damping (revealed experimentally in the evolution of the damping ratio of the free response). It will be experimentally demonstrated that in order to create synthetic modal damping (positive or negative) the actuator absorbs active electrical power (negative or positive), generated by a positive or a negative derivative gain in the feedback closed-loop (the poling direction of actuator and sensor are opposite). The viscously damped free response of the cantilever beam is described by the evolution of the voltage $u_s(t)$ delivered by the sensor, or by the supplying voltage $u_a(t)$ of the actuator or by the evolution of the current $i(t)$. A computer aided method for signals fitting was developed in order to find out the amplitude, the frequency the damping ratio and the angle of the phase related to the origin of time for $u_a(t)$ and $i(t)$. The value of the shift of phase between $u_a(t)$ and $i(t)$ and the active electrical power can be used to calculate the reactive electrical power delivered to the actuator.

3.3.2 Some considerations on the behavior of the regulator.

Let us consider that the voltage $u_s(t)$ generated by the sensor PS has a harmonic evolution, written as: $u_s=A\cdot sin(\omega\cdot t)$. This voltage is generated if the voice coil actuator (Figures 3.1 and 3.2) is supplied

with a harmonic voltage having the angular frequency ω (the diode D should be removed). A bending vibration is generated. The voltage drop u_a on the actuator PA can be written as:

$$u_a = C_v \cdot A \cdot sin(\omega \cdot t + \alpha) \tag{3.1}$$

Here α is the shift of phase generated by the regulator and C_v is the voltage gain (in the experiments revealed in this paper $C_v \approx 1$, it has a light variation depending on α, because of the measuring resistor R_m). The voltage drop u_a can be rewritten as it follows:

$$u_a = C_p \cdot u_s + C_d \cdot \frac{d(u_s)}{dt} \text{ with } C_p = C_v \cdot cos(\alpha) \text{ and}$$

$$C_d = \frac{C_v}{\omega} \cdot sin(\alpha) \tag{3.2}$$

According to Eq. (3.2) the phase shifter works as a proportional and derivative regulator with proportional gain C_p and derivative gain C_d (both gains depending on α). Taking into account the fact that the sensor and the actuator have different poling directions, the following observations can be made. If $C_p > 0$ (or $C_p < 0$) the proportional feedback is negative (positive); it will generate a synthetic positive (negative) mechanical stiffness. If $C_d > 0$ (or $C_d < 0$) the derivative feedback is negative (positive); it will also generate a synthetic positive (negative) mechanical damping. The regulator behaves identically if the input $u_s(t)$ is an exponentially damped periodic voltage due to an impulse excitation of the first bending mode of vibration of the

cantilever beam. All these considerations are fully confirmed in this paper.

3.3.3 A strategy for monitoring the active electrical power.

As it has been said before the instantaneous electrical power delivered to the actuator PA is written as:

$$P_{el,inst}(t) = u_a(t) \cdot i(t) = \frac{1}{R_m} \cdot [u_A(t) - u_B(t)] \cdot u_B(t) \qquad (3.3)$$

Suppose that in the same conditions as those discussed above for the regulator, the instantaneous voltage drop on the actuator $u_a(t)$ and the current $i(t)$ are described as:

$$u_a(t) = \sqrt{2} \cdot U_{a,rms} \sin(\omega \cdot t) \text{ and } i(t) = \sqrt{2} \cdot I_{rms} \sin(\omega \cdot t - \varphi) \qquad (3.4)$$

Here $U_{a,rms}$ and I_{rms} are the root mean square values of the voltage and current [12], $\sqrt{2} \cdot U_{a,rms}$ and $\sqrt{2} \cdot I_{rms}$ are the amplitudes of voltage and current, φ is the shift of phase between instantaneous voltage and current.

If the angular frequency ω is constant, then the active electrical power $P_{el,act}$ is described as the average value of the instantaneous power calculated on a semi-period $T/2 = 2\pi/\omega$ as follows:

$$P_{el,act}(t_k) = \frac{2}{T} \cdot \int_{t=k\cdot\frac{T}{2}}^{(k+1)\cdot\frac{T}{2}} P_{el,inst}(t) \cdot dt = \frac{2}{T} \cdot \int_{t=k\cdot\frac{T}{2}}^{(k+1)\cdot\frac{T}{2}} u_a(t) \cdot i(t) \cdot dt \tag{3.5}$$

In Eq. (3.5) $k = 0, 1, 2, \ldots\ldots, n$, with n the total number of samples, $t_k = k \cdot T/2$ is the time value of the sample, $T/2$ is also the sampling interval, or $2/T$ is the sampling rate.

By solving the integral from Eq. (3.5) for the semi-period k the following result is obtained:

$$P_{el,act}(t_k) = U_{a,rms}(t_k) \cdot I_{rms}(t_k) \cdot cos[\varphi(t_k)] \tag{3.6}$$

In Eq. (3.6) $cos[\varphi(t_k)]$ is called power factor. This relationship helps to explain the concept of positive and negative active electrical power. $U_{a,rms}(t_k)$ and $I_{rms}(t_k)$ are positive quantities and this brings up the fact that if the power factor is negative the active electrical power $P_{el,act}$ is negative. This means that $P_{el,act}$ flows from actuator to regulator. If the power factor is positive $P_{el,act}$ is positive, flowing from regulator to the actuator.

Using a technique for determining the values $\varphi(t_k)$, the reactive electrical power absorbed by the actuator PA can be written as:

$$P_{el,react}(t_k) = P_{el,act}(t_k) \cdot tan[\varphi(t_k)] \tag{3.7}$$

It is relative difficult to calculate the active electrical power using Eq. (3.6). In [12] a numerical method of calculus of $P_{el,act}$ based

on Eq. (3.5) was introduced. This method has a disadvantage: the sampling rate of $P_{el,act}$ is small, only $2/T\ s^{-1}$.

A new numerical method is described here. It is mathematically proved (also by numerical simulation) that the instantaneous electrical power $P_{el,inst}$ from Eq. (3.3) (with $u_a(t)$ and $i(t)$ given in Eqs. (3.4)) has two components.

A first component is constant or has a low speed variation: this is the active electrical power $P_{el,act}$. A second component [12] is periodical, it has the angular frequency $2\cdot\omega$. This new method of calculus of $P_{el,act}$ consists of a complete removal of the second component by numerical filtering of $P_{el,inst}$ using a band-stop filter. The active electrical power is calculated using a simple moving average filter (which also works as a band-stop filter) as it follows:

$$P_{el,act}(t_j) = \frac{1}{p} \cdot \sum_{i=j-p}^{j} P_{el,inst}(t_i) \text{ with } j = p+1, p+2, \ldots .n \qquad (3.8)$$

In Eq. (3.8) $P_{el,act}(t_j)$ is the current numerical value (sample) of the active electrical power (the output of the filter), $P_{el,inst}(t_i)$ is the current numerical value (sample) of the instantaneous electrical power written according to Eq. (3.3), $t_j=j\cdot\Delta t$ and $t_i=i\cdot\Delta t$, are the time coordinates, Δt is the sampling interval, n is the number of samples. The filter parameter p is defined as the integer part of the ratio $T/(2\cdot\Delta t)$.

The sampling rate of numerical description of active electrical power, instantaneous electrical power, instantaneous voltage u_a and current i is the same: $1/\Delta t >> 2/T$.

The filter described in Eq. (3.8) can be implemented using the Matlab instruction: `pelact=smooth(pelinst,p);` with a good approximation.

Here `pelact` and `pelinst` are the names of a single column matrix which contains the numerical values of $P_{el,act}$ and $P_{el,inst}$ and p is the value of filter parameter previously defined.

The real mechanical power $P_{mec,real}$ delivered by the actuator to the cantilever beam is only a small part of the active electrical power $P_{el,act}$ absorbed by the actuator. The ratio $K_{31}=P_{mec,real}/P_{el,act}$ is the generalized coupling coefficient of the actuator ($K_{31}=0.097$, according to [12]). Therefore all dynamic phenomena reflected in the evolution of mechanical power absorbed by the cantilever beam via the actuator PA can be investigated using the active electrical power monitoring. All these theoretical considerations remain valid if the voltage and current have periodic non-harmonic time evolution.

3.3.4 Experimental resources of the signals generated in the closed-loop feedback system as result of the free response of the cantilever beam.

The majority of experimental research results are based on the resources offered by the evolution of u_s, u_a and u_B voltages generated as a consequence of the viscous damped free responses on the first mode of vibration of the cantilever beam. These responses are generated by the impulse excitation produced by the voice coil actuator. Different

values of shift of phase α generated by the regulator are used. Figure 3.3 (a) presents an experimental evolution of these voltages for $\alpha=85.33^{o}$. Figure 3.3 (b) presents a zoom in on A area, close to the excitation moment. Figure 3.3 (c) presents a zoom in on B area. According to Figure 3.3 (b) there is a supplementary mode excited, but it is very quickly damped. Finally the free responses are related only to the first bending mode (according to Figure 3.3 (c)). All three voltages are used to find out the active electrical power evolution by calculus (Eqs. (3.5) or (3.8)).

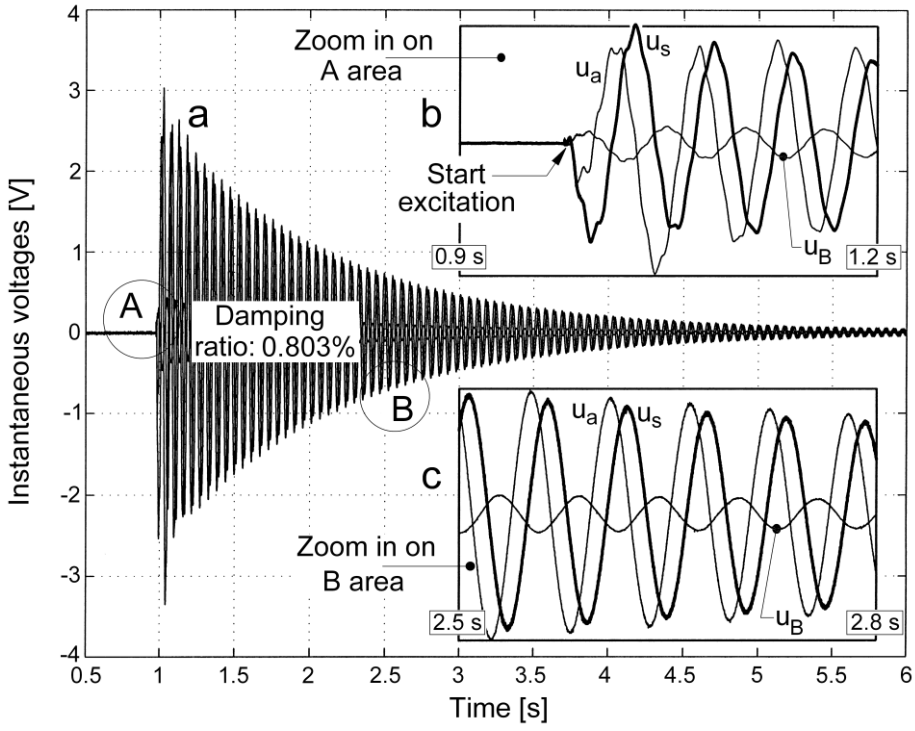

Fig. 3.3: ***(a)*** *A free viscous damped response on first bending mode mirrored in time evolution of u_s, u_a and u_B voltages ($\alpha=85.33^{o}$, negative derivative feedback);* ***(b)*** *A zoom in on A area;* ***(c)*** *a zoom in on B area (**see also the chapter 3.7**).*

All three voltages have a well known theoretical description written bellow as instantaneous numerical values:

$$u_s(t_i) = U_s \cdot e^{-\zeta \cdot \omega_0 \cdot t_i} \sin(\omega_1 \cdot t_i + \theta_s)$$
$$u_a(t_i) = U_a \cdot e^{-\zeta \cdot \omega_0 \cdot t_i} \sin(\omega_1 \cdot t_i + \theta_a)$$
$$u_B(t_i) = U_B \cdot e^{-\zeta \cdot \omega_0 \cdot t_i} \sin(\omega_1 \cdot t_i + \theta_B) \quad (3.9)$$

Here U_s, U_a and U_B are the amplitudes at $t_i=0$, ζ is the modal damping ratio, ω_0 is the undamped modal natural angular frequency, $\omega_1 = \omega_0 \cdot \sqrt{1-\zeta^2}$ is the damped modal natural angular frequency, θ_s, θ_a and θ_B are the values of phase angle at origin of time ($t_i=0$). The parameters ζ, ω_0 and ω_1 are evidently the same for all three voltages, $\omega_0 \approx \omega_1$ because ζ has a very small value. In order to have a pure viscous damped response of the cantilever beam on the first bending mode, the origin of time ($t_i=0$) involved in Eqs. (3.9) is delayed with $t_d=0.15$ s from the moment of start of excitation.

A numerical method of computer aided data processing (curve fitting of experimental evolution for u_s, u_a and u_B voltages from Figure 3.3) was developed in order to find out with good accuracy the values of the parameters used in Eqs. (3.9). The values of these parameters are useful to calculate: the values of ω_1 and ω_0, the phase shift and the gain generated by the regulator ($\alpha=\theta_a-\theta_s$ and $C_v=U_a/U_s$, useful to find the values of proportional gain $C_p=C_v \cdot \cos(\alpha)$ and derivative gain $C_d= C_v \cdot \sin(\alpha)/\omega_1$), to prove experimentally that the proportional gain C_p

produces synthetic modal stiffness (ω_0 depends on C_p), to prove experimentally that the derivative gain C_d produces synthetic modal damping (ζ depends on C_d), to determine the active electrical power flow in the actuator PA, to calculate the phase shift φ between instantaneous voltage $u_a(t_i)$ and current $i(t_i)$ applied on the actuator ($\varphi=\theta_B-\theta_a$), and to calculate also the value of filter parameter p involved in Eq. (3.8)).

3.4. EXPERIMENTAL RESULTS AND DISCUSSION

3.4.1 Negative active electrical power flow towards actuator generated in the closed-loop feedback system

As already anticipated, a negative active electrical power flow between regulator and actuator occurs if the derivative gain C_d is positive ($0<\alpha<\pi$) and if the cantilever beam is excited in order to vibrate on the first bending mode.

Using the evolution of the voltages u_a and u_B already described in Figure 3.3 due to an impulse excitation ($\alpha=85,33^o$, $C_v=1.07$, $\omega_1=110.25$ *rad/s*, $\zeta=0.00803$ rad^{-1}(or *0.803%)*, C_d is closed to the maximum value, C_p is closed to zero), it is easy to determine by calculus the evolutions of the instantaneous electrical power (Eq. (3.3)) and electrical active power (Eq. (3.8)). Figure 3.4 (a) presents the evolution of the instantaneous electrical power absorbed by the actuator

as a result of impulse excitation of the cantilever beam in the conditions mentioned above. Figure 3.4 (b) presents a zoom in on A area with the instantaneous electrical power and active electrical power evolution. Figure 3.4 (c) presents the evolution of the active electrical power as a result of numerical filtering of the instantaneous electrical power given in Figure 3.4 (a) (with $\omega_1 = 2 \cdot \pi \cdot 17.54$ *rad/s*, $\Delta t = 0.1$ *ms*, $p = 282$). In order to remove the influence of the second mode excited on the active electrical power evolution (Figure 3.3 (b)), the instantaneous electrical power is filtered using the Matlab instructions: `pelact = smooth(pelinst, 2*p);pelact=smooth(pelact,2*p);`

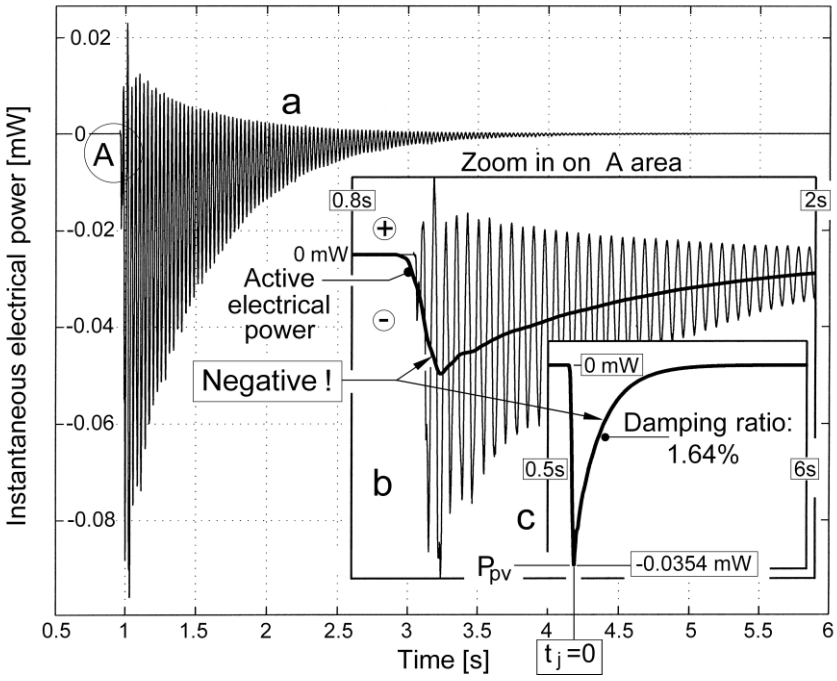

Fig. 3.4: ***(a)*** *Time evolution of instantaneous electrical power absorbed by the actuator during the experiment described in Figure 3.3;* ***(b)*** *A zoom in on A area;* ***(c)*** *Time evolution of the active negative electrical power (**see also the chapter 3.7**).*

It is obvious that the active electrical power absorbed by the actuator is negative (the power factor is negative: $cos(\varphi)=-0.723$, $\varphi=136.35^{o}$). There is a negative peak value of electrical active power $P_{pv}= -35.4\ \mu W$. After the peak the active electrical power should theoretically have an exponential evolution to zero (taking into consideration Eqs. (3.9), (3.3) and (3.8)), described as:

$$P_{el,act}(t_j) = P_0 \cdot e^{-\zeta_1 \cdot \omega_0 \cdot t_j} \qquad \zeta_1 = 2 \cdot \zeta \tag{3.10}$$

This is observed with good accuracy in the graphic result given in Figure 3.4 (c). The curve fitting of experimental evolution produces the values of the parameters involved in Eq. (3.10): $\zeta_1=0.0164\ rad^{-1}$ ($\zeta=0.00803\ rad^{-1}$) with $\zeta_1 \approx 2 \cdot \zeta$, and $P_0 = -32.04\ \mu W$ (with $P_0 \approx P_{pv}$). This also proves that the phase shift φ and the magnitude of the electrical impedance of the actuator are constant (as we shall see later).

A negative power flow towards the actuator means that the actuator works as a damper: it generates positive synthetic mechanical modal damping. A simple experiment can prove this. In conditions similar to those used above, the voice coil actuator (Figure 3.1) is supplied with a pure harmonic voltage on 17.58 Hz frequency (practically the frequency of first bending mode of the cantilever beam). The elongation of the vibration of the free end of the beam is measured with a laser position sensor ILD 2000 (marked with 5 on Figure 3.2). Figure 3.5 (a) presents the evolution of the vibration elongation with the feedback loop opened (no synthetic damping). In A

the supplying circuit of the voice coil actuator is switched-on (the amplitude of forced vibrations increases slowly, the cantilever beam needs time to accumulate modal energy). In B the supplying circuit is switched-off. Afterwards, the modal energy stored in the beam is eliminated during the free viscous damped vibrations (described in C area).

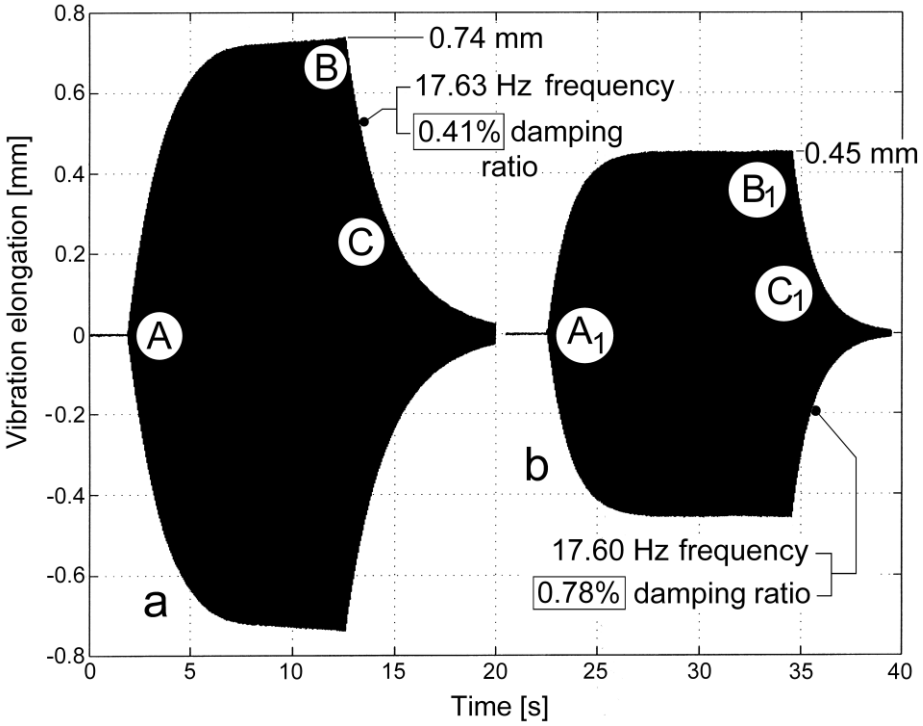

Fig. 3.5: ***(a)*** *Forced vibration (A and B areas) generated by harmonic excitation on the frequency of resonance, free damped response in C area (open-loop);* ***(b)*** *The same experiment in closed-loop feedback (α=85.33º)* ***see also the chapter 3.7****.*

Figure 3.5 (b) presents the evolution of the vibration elongation in the same conditions (see A_1, B_1 and C_1 marks) but with the feedback derivative loop being closed (a positive synthetic damping is

generated). The maximum amplitude of forced vibration (lateral displacement) at resonance is smaller in Figure 3.5 (b) because of the positive synthetic damping. The damping ratio ζ of the first bending mode can be deduced experimentally by free response data fitting (the elongation evolution from C and C_1 areas). It has the value $\zeta = 0.41\%$ (or $0.0041\ rad^{-1}$), in Figure 3.5 (a) (natural mechanical damping) and $\zeta = 0.78\ \%$ (or $0.0078\ rad^{-1}$) in Figure 3.5 (b) (natural and synthetic damping). Because C_p is close to zero (no synthetic stiffness), the frequency of the free responses is practically the same.

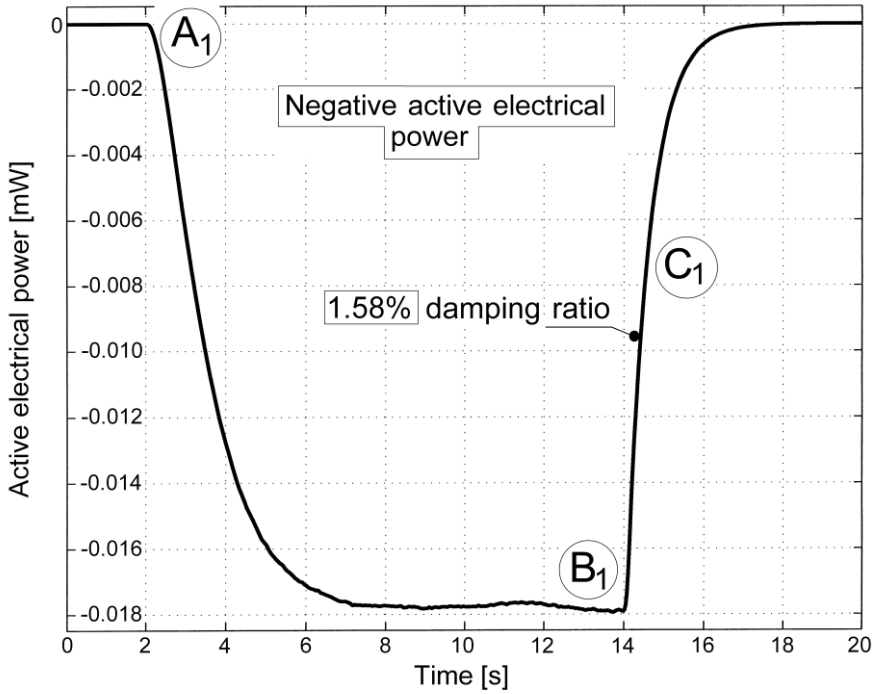

Fig. 3.6: *Time evolution of the active electrical power absorbed by the actuator during the experiment described in Figure 3.5 (b).*

The evolution of the active electrical power absorbed by the actuator during the experiment described in Figure 3.5 (b) is presented

in Figure 3.6. As expected, the active electrical power is permanently negative. The DC power supply 7 and the regulator 8 works as a negative modal power supply driven by the piezoelectric sensor 11. As expected, in C_1 area (free response of the cantilever beam mirrored in the active electrical power evolution) the active electrical power has an exponential evolution with $\zeta_1 = 1.58\ \%$ (with $\zeta_1 \approx 2 \cdot \zeta$, the same result as before). The evolution of power between A_1 and B_1 should be correlated with the evolution of power absorbed by the voice coil actuator [39]. A part of the modal power delivered by the voice coil actuator to cantilever beam is eliminated by the piezoelectric actuator PA.

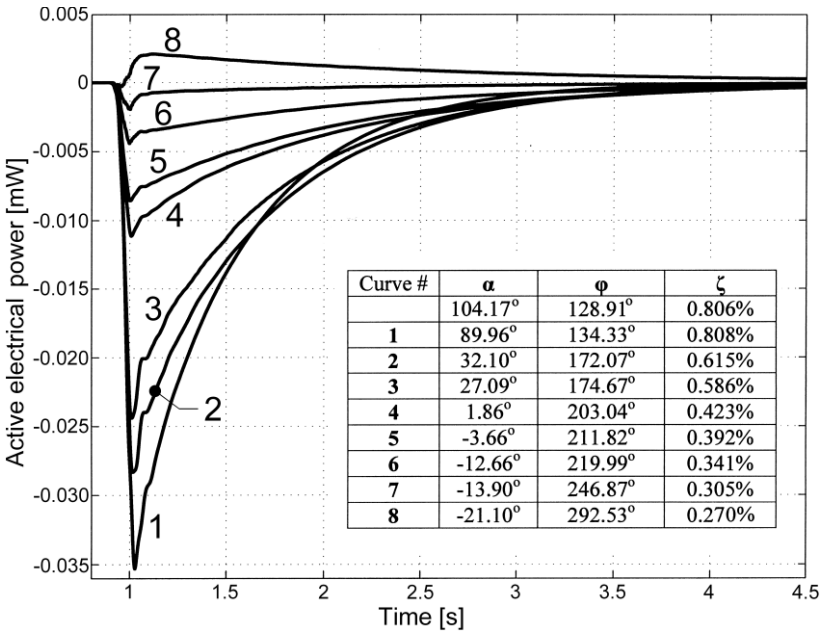

Curve #	α	φ	ζ
	104.17°	128.91°	0.806%
1	89.96°	134.33°	0.808%
2	32.10°	172.07°	0.615%
3	27.09°	174.67°	0.586%
4	1.86°	203.04°	0.423%
5	-3.66°	211.82°	0.392%
6	-12.66°	219.99°	0.341%
7	-13.90°	246.87°	0.305%
8	-21.10°	292.53°	0.270%

Fig. 3.7: *Time evolutions of active electrical power for several values of shift of phase α, due to an impulse excitation of the first bending mode (negative derivative feedback),* ***see also the chapter 3.7****.*

According to Eq. (3.2), if $0<\alpha<\pi$ then $C_d > 0$ and the regulator works as a negative active electrical modal power supply. This power is converted by the actuator in negative mechanical modal power supply delivered to the cantilever beam. The experimental results (Figure 3.7) partially confirm the theory. Figure 3.7 presents the evolution of the active electrical power (numerical filtered) due to the impulse excitation of the cantilever beam for several different values of shift of phase α. The table drawn in Figure 3.7 indicates the values of α, φ and damping ratio ζ for each curve. For each of the curve, excepting the curve #8, the absorbed active electrical power is negative. For curves #5, #6 and #7, even if $\alpha<0$ ($C_d<0$, the absorbed active power should be positive, φ should be bigger than $3\pi/2$) however $\varphi<3\pi/2$ and the absorbed power is negative (because $\cos(\varphi)<0$). We didn't find an explanation of this phenomenon yet. Moreover, the absorbed power should be positive because a positive power produces a negative synthetic damping and the damping ratio decreases. This happened for curves #5, #6 and #7 the damping ratio being smaller than $\zeta=0.41\%$ (the open-loop damping ratio value revealed in Figure 3.5 (a)).

3.4.2 Positive active electrical power flow towards PA actuator generated in the closed-loop feedback system.

There is a first condition for generating a positive active electrical power flow between the regulator and the actuator: a positive derivative feedback between the sensor and the actuator. This means that the derivative gain C_d is negative. There is a second condition: the

cantilever beam vibrates on the first bending mode (free or forced response) due to an external excitation. Due to a positive active electrical power flow a negative synthetic modal damping is generated, the modal damping ratio ζ of the first bending mode decreases.

It is possible to obtain a negative derivative gain C_d if the phase shift generated by the regulator is located between the limits $\pi<\alpha<2\pi$.

The regulator works as a positive active electrical modal power supply ($-\pi/2<\varphi<\pi/2$ with $cos(\varphi)>0$, see a first example: the curve #8 on Figure 3.7), converted by actuator into positive mechanical modal power supply delivered to the cantilever beam.

3.4.2.1 Positive active electrical power flow with dynamic stability

Due to the positive derivative feedback, the cantilever beam keeps or does not keep the dynamic stability. A dynamic system actuated in closed-loop is stable if it is able to completely eliminate all the modal energy stored inside after any external perturbation ceases. If the negative synthetic damping does not cancel the natural (structural) damping completely the cantilever beam keeps the dynamic stability.

An experimental example is described below. Figure 3.8 (a) presents the evolution of u_s, u_a and u_B voltages generated due to an impulse excitation when the shift of phase of the regulator is tuned on $\alpha = -52.33^o$ ($C_d < 0$).The damping ratio of the first mode is now very small: $\zeta = 0.083\ \%$ (compared to the value of the damping ratio without feedback: $\zeta = 0.41\ \%$, revealed in Figure 3.5 (a)). There are two details

of Figure 3.8 (a): a zoom in on A area (described in Figure 3.8 (b)) and a zoom in on B area (described in Figure 3.8 (c)). In Figure 3.8 (b) we highlighted the fact that an excited second mode of vibration (105 Hz frequency) is very quickly damped. In Figure 3.8 (c) the shift of phase relationships between the voltages u_s, u_a and u_B is highlighted (a comparison with Figure 3.3 (c) is indicated). The dynamic system of the cantilever beam is stable because all three voltages finally becomes zero.

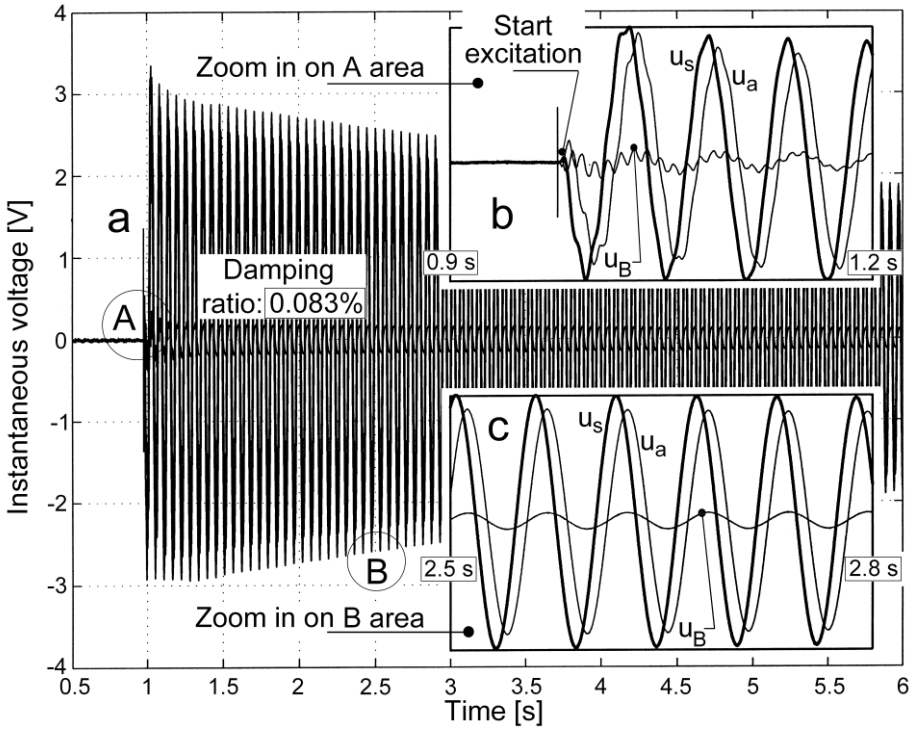

Fig. 3.8: ***(a)*** *A free viscous damped response on first bending mode mirrored in time evolution of u_s, u_a and u_B voltages (α=-52.33^o, positive derivative feedback);* ***(b)*** *A zoom in on A area;* ***(c)*** *a zoom in on B area* ***(see also the chapter 3.7).***

Figure 3.9 (a) describes the evolution of the instantaneous and active electrical power flow to the piezoelectric actuator during the previous experiment. Figure 3.9 (b) describes a zoom in on A area. Figure 3.9 (c) presents only the evolution of the active electrical power. As expected, the active electrical power absorbed by the actuator is positive (the power factor is positive: $cos(\varphi)=0.98$, $\varphi=-10.78^{o}$) and it has an exponential evolution to zero ($\zeta_1=0.166$ % with $\zeta_1=2\cdot\zeta$) with a peak value $P_{pv}=+21\mu W$.

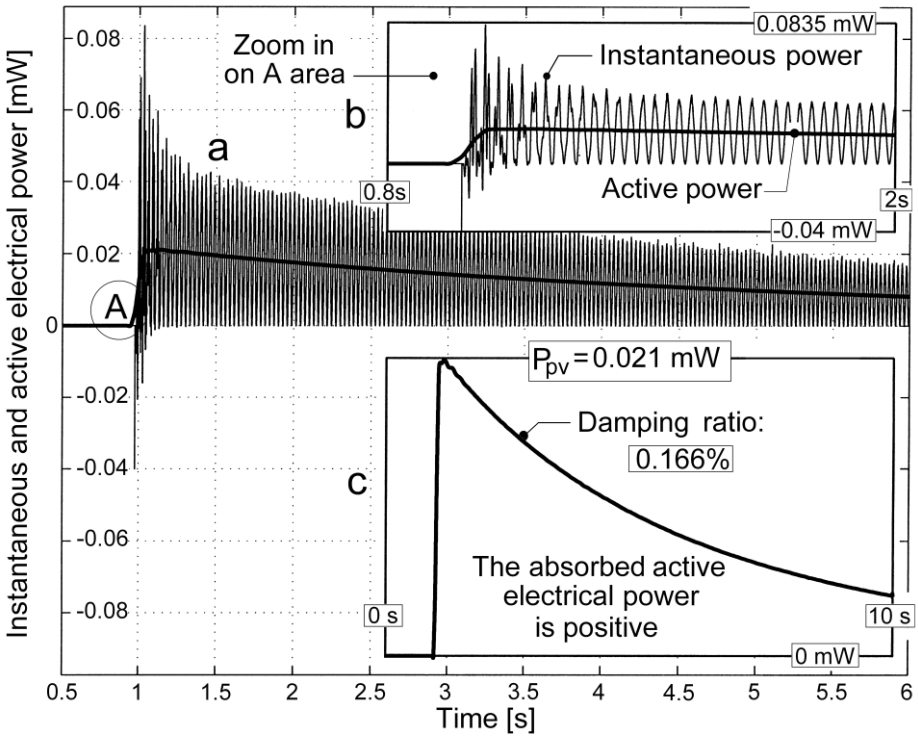

Fig. 3.9: ***(a)*** *Time evolution of instantaneous electrical power absorbed by the actuator during the experiment described in Figure 3.8;* ***(b)*** *A zoom in on A area;* ***(c)*** *Time evolution of the active positive electrical power* ***(see also the chapter 3.7).***

Figure 3.10 presents the evolution of the active electrical power (always positive) due to an impulse excitation for several different values of the angle α (that decreases), in order to have a progressively decreased negative derivative gain $C_d=C_v \cdot sin(\alpha)/\omega_1$. A table drawn in Figure 3.10 indicates the values for α, φ and ζ for each curve (from #8 to #14).

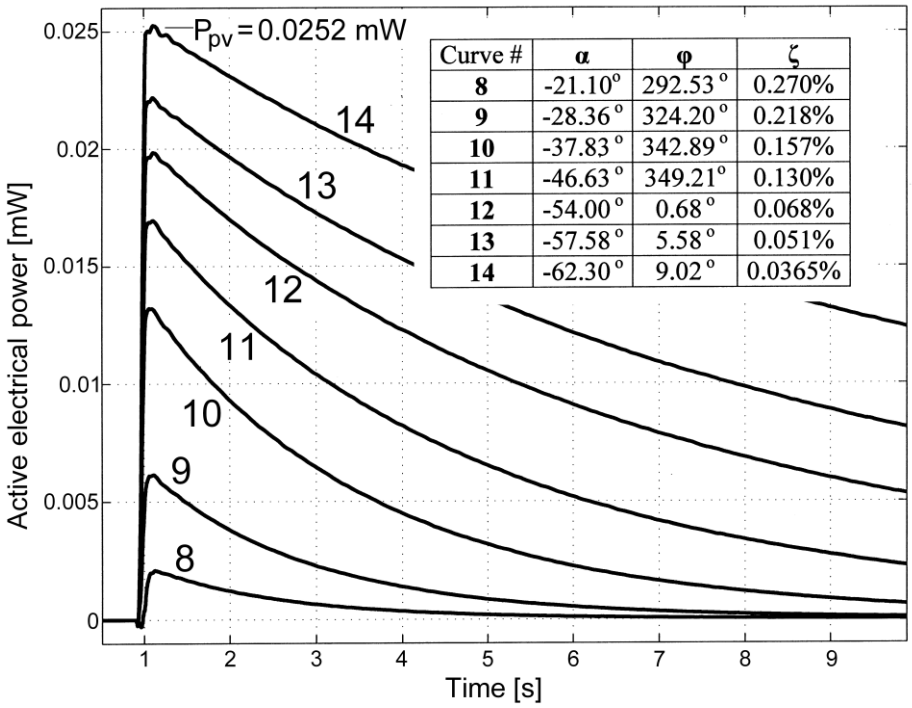

Curve #	α	φ	ζ
8	-21.10°	292.53°	0.270%
9	-28.36°	324.20°	0.218%
10	-37.83°	342.89°	0.157%
11	-46.63°	349.21°	0.130%
12	-54.00°	0.68°	0.068%
13	-57.58°	5.58°	0.051%
14	-62.30°	9.02°	0.0365%

Fig. 3.10: *Time evolution of the active positive electrical power for several values of shift of phase α, due to a pulse excitation of the first bending mode (positive derivative feedback),* ***see also the chapter 3.).***

It is clear that the damping ratio ζ decreases, and the maximum value P_0 (Eq. 3.11) value increases. There is a stability limit ($\alpha \approx -64^o$). Below this limit the system becomes unstable.

3.4.2.2 Positive active electrical power flow with dynamic instability

If the derivative gain C_d further decreases (because the shift angle α decreases more), the negative synthetic modal damping completely cancel the natural damping. The dynamic system of the cantilever beam becomes unstable.

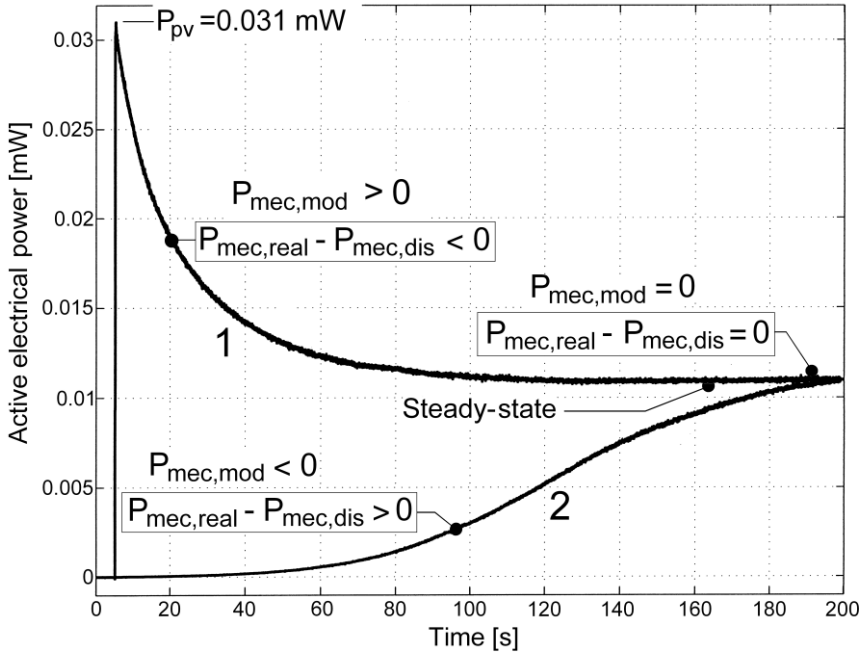

Fig. 3.11: *Dynamic instability due a positive derivative feedback mirrored in time evolution of active electrical power;* ***#1*** *- free response of the cantilever due an impulse excitation;* ***#2*** *- evolution generated by self excited vibratory regime* ***(see also the chapter 3.7).***

If a pulse excitation is produced as before, the evolution of the active electrical power absorbed by the actuator has a maximum peak but does not evolve to zero. This is revealed in Figure 3.11, curve #1, for a shift of phase $\alpha = -67.74^{o}$ and $P_{pv}=31\ \mu W$. The absorbed active electrical power has an asymptotic (exponentially) trend to a constant value, positive, as steady-state value P_{ss} (here $P_{ss}=10.95\ \mu W$). This means that finally, in steady-state, the cantilever beam vibrates with constant amplitude. The dynamic system of the cantilever beam is self excited in order to vibrate on the frequency of the first bending mode. The energy needed to power self excited vibration is provided by the DC power supply 7 via the regulator 8 (on Figures 3.1 and 3.2). There is a constant flow of positive active power to actuator, with value P_{ss}.

The dynamic system of the cantilever beam has an interesting behavior: when the feedback loop is closed (the same shift of phase as we previously experienced) it starts to vibrate apparently without any external excitation. In fact even an extremely small dynamic perturbation from the environment is able to initiate the vibratory behavior. It is expected that due to the positive derivative feedback the amplitude of vibration increases more and more. The evolution of the active electrical power absorbed by the actuator (revealed in Figure 3.11, curve #2) is asymptotic starting from zero and also has an asymptotic trend to a constant, positive, steady-state value, very close to that of curve #1. This also means that finally, in steady-state, the cantilever beam vibrates with constant amplitude.

The evolution of the amplitude of vibration in time depends on the balance of input and output mechanical power. The input power is

the mechanical real power $P_{mec,real}$ produced by the actuator (the active electrical power is converted into mechanical real power). This power depends on α, C_v and K_{31}. The output power is the modal mechanical dissipated power $P_{mec,dis}$ (as heating, due to friction inside the beam and air friction). This power depends on the modal damping ratio of the cantilever beam. Both powers also depend on the vibration amplitude. The $P_{mec,dis}$ can be seen as a negative input power. If $P_{mec,real} - P_{mec,dis} < 0$ the vibration amplitude decreases exponentially (and the absorbed active electrical power too, see curve #1 on Figure 3.11) to a steady-state value. The cantilever beam system loses some modal mechanical energy stored inside. If we assume that $P_{mec,mod}$ is the power flow generated by the modal mechanical energy, before steady-state, this relationship can be written: $P_{mec,real} - P_{mec,dis} + P_{mec,mod} = 0$ (here $P_{mec.mod}$ is a positive power flow).

If $P_{mec,real} - P_{mec,dis} > 0$ the amplitude of vibration increases to the steady-state value (also the absorbed active electrical power, see curve #2). The modal energy stored in the cantilever system increases. Therefore, before steady-state, this relationship can be written: $P_{mec,real} - P_{mec,dis} - P_{mec,mod} = 0$ (here $P_{mec.mod}$ is a negative power flow).

In steady-state $P_{mec,real} - P_{mec,dis} = 0$ (and $P_{mec,mod} = 0$), the amplitude of vibration is constant, the absorbed active electrical power is constant. In steady-state $P_{el,act} = P_{ss}$ and $P_{mec,real} = P_{mec,dis} = K_{31} \cdot P_{ss}$.

In steady-state, the value of P_{ss} (and the amplitude of the vibration too) depends on the value of the shift of phase α (a negative value) generated by the regulator and the natural modal damping of the cantilever beam. The dependence of P_{ss} on the value of α is

experimentally proved in Figure 3.12. This Figure presents the evolution of the active electrical power absorbed by the actuator starting immediately after the moment the feedback loop with positive derivative gain was closed and lasting until the steady-state is achieved (no external excitation).

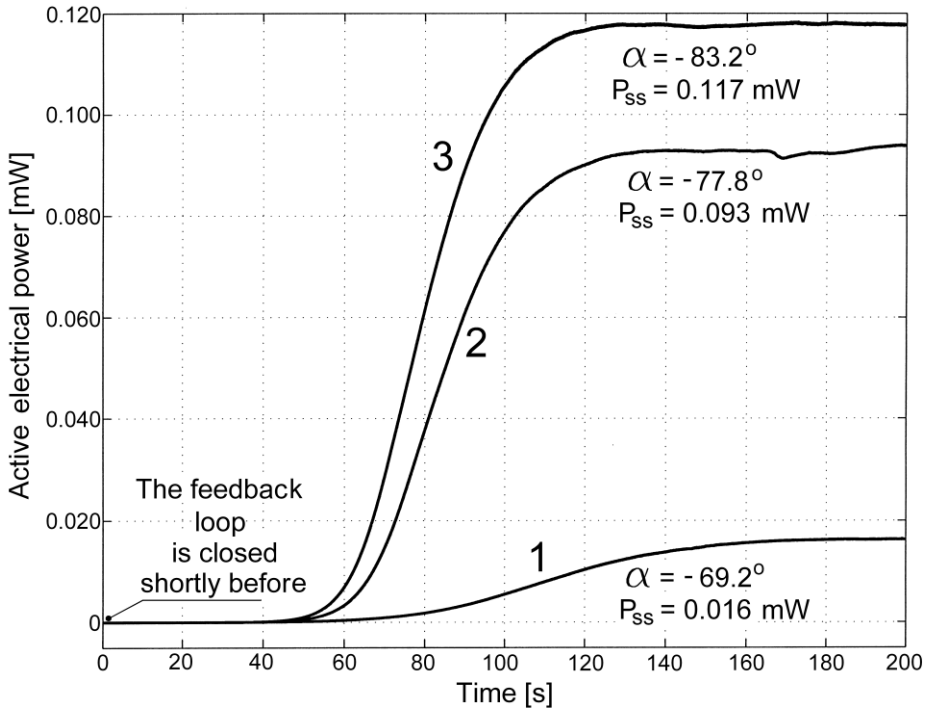

Fig. 3.12: *Time evolution of the active electrical power until steady state for several different value of phase shift α (self excited vibratory regimes with positive derivative feedback).* ***See also the chapter 3.7.***

An unstable behavior with self excited vibrations on first bending mode is produced for each value of shift of phase α (the natural modal damping is constant). Finally, each steady-state is characterized by a different value P_{ss}.

The dependence of P_{ss} on natural modal damping is experimentally proved on Figure 3.13.

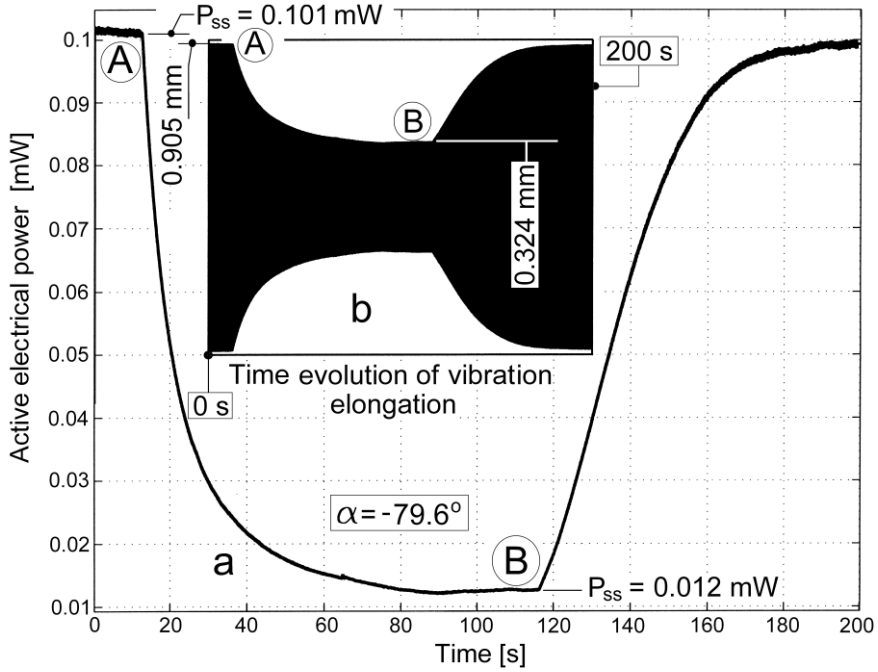

Fig. 3.13: ***(a)*** *The influence of natural damping on steady state value* P_{ss}*;* ***(b)*** *The influence of natural damping on vibration amplitude (positive derivative feedback with instability).* ***See also the chapter 3.7.***

As a result of the same experiment, Figure 3.13 (a) presents the evolution of the active electrical power absorbed by the actuator (positive derivative feedback with instability, $\alpha = -79.6^{o}$) and Figure 3.13 (b) presents the evolution of vibration elongation of the free end of the cantilever beam. Before A the system vibrates in steady-state with $P_{ss}=P_{ss,max}=0.101$ *mW* and 0.905 mm the amplitude of vibration. In A the coil of the voice-coil actuator (marked with 2 on Figure 3.2) is placed in short-circuit. The coil and the permanent magnet placed on

the free end of the cantilever beam generate a viscous damping force, the natural modal damping of the cantilever beam having increased. In consequence, immediately after this moment, the absorbed active electrical power and the amplitude of vibration start to decrease, a new steady-state is installed with $P_{ss}=P_{ss,min}=0.012\ mW$ and 0.324 mm amplitude, before B. The dynamic system loses modal energy, $P_{mec,mod} > 0$. In B the short-circuit is removed (the coil is in open circuit), the damping force disappears. As a result, immediately after this moment, the absorbed active electrical power and the amplitude of vibration start to increase exponentially to the previously steady-state value (before A). The dynamic system receives and stores modal energy, $P_{mec,mod} < 0$.

If the natural modal damping further increases $P_{ss}=0$ and the instability behavior of the dynamic system disappear. As an important remark, this feature ($P_{ss}=0$) can be considered an indicator of stability of a dynamic system.

3.4.3 Some considerations concerning the electrical impedance of the actuator

In vibration engineering the magnitude of electrical impedance is often used [11, 16 and 40] in order to characterize the behavior of a piezoelectric actuator (the electrical impedance can be directly related to the mechanical impedance of the cantilever beam [40]). However, it is shown below that the evolution of the active electrical power provides a better characterization of the dynamic phenomena in which the actuator is involved.

`The current value of the magnitude of electrical impedance of the actuator $Z(t_k)$ is the ratio between the amplitude of the voltage ($U_a(t_k)= \sqrt{2}\cdot U_{a,rms}(t_k)$) and the amplitude of the current ($I(t_k)= \sqrt{2}\cdot I_{rms}(t_k)=U_B(t_k)/R_m$) and can be written as:

$$Z(t_k)=\frac{U_a(t_k)}{I(t_k)}=R_m\cdot\frac{U_a(t_k)}{U_B(t_k)}=\frac{U_{a,rms}(t_k)}{I_{rms}(t_k)} \tag{3.11}$$

here $U_{a,rms}(t_k)=\frac{max|u_a(t_j)|}{\sqrt{2}}$ and $I_{rms}(t_k)=\frac{max|u_B(t_j)|}{\sqrt{2}\cdot R_m}$

In Eq. (3.11) $t_k=k\cdot T/2$, $k = 0, 1, 2...n$, n is the number of samples and $t_k<t_j<t_{k+1}$. The sampling ratio of the electrical impedance is $2/T$.

All previous experiments can also be described by the evolution of the magnitude of electrical impedance of the actuator. The experiment from Figure 3.5 (b) (the evolution of vibration amplitude) described in Figure 3.6 (the evolution of the active electrical power absorbed by the actuator) can be also described in terms of magnitude of impedance evolution, as Figure 3.14 indicates (a numerical low-pass filtered evolution). The correspondence between the Figures 3.5 (b), 3.6 and 3.14 is provided by the three events: in A_1 the supplying circuit of the voice coil actuator is switched-on; in B_1 this circuit is switched off; in C_1 is generated the free viscous damped response of the cantilever beam. It is easy to correlate Figures 3.5 (b) and 3.6, but the evolution of magnitude of impedance given in Figure 3.14 seems to be very difficult

to explain. An overview of this figure shows that a negative active electrical power flow to the actuator is accompanied by the increasing of the magnitude of impedance of the actuator.

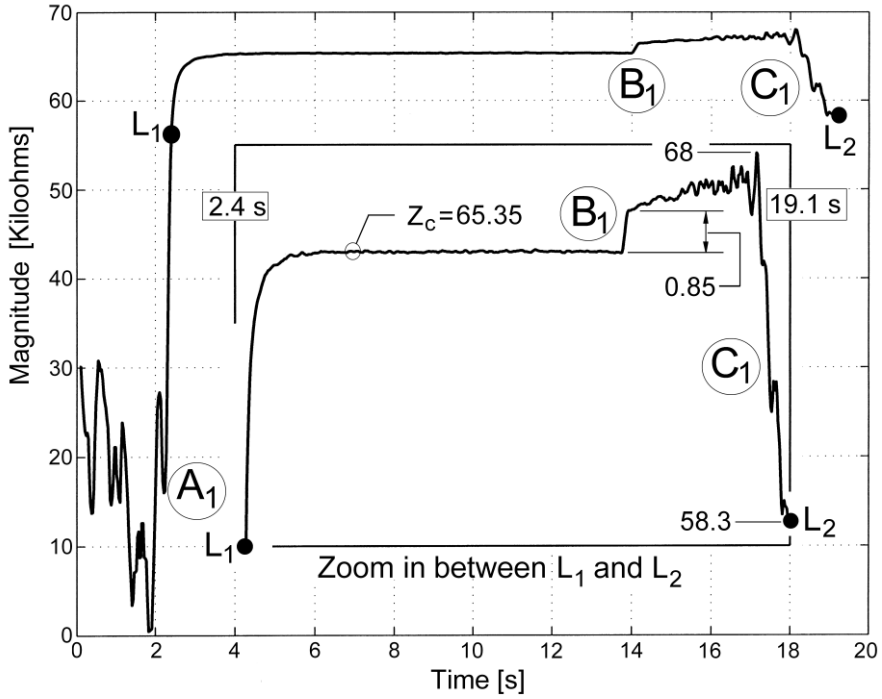

Fig. 3.14: *Time evolution of the magnitude of electrical impedance Z during the experiment from Figures 3.5 (b) and 6.* ***See also the chapter 3.7****.*

The magnitude increases quickly (less than 2 seconds) after the moment A_1, from 16 KΩ to a constant value $Z_c=65.35\ K\Omega$ that keeps until B_1. Before A_1, the vibration amplitude and the active electrical power are zero, it is impossible to correctly describe the evolution of the magnitude of impedance (on Figure 3.14 this evolution is generated by the electrical noise, the signals u_a and u_B should be zero). Nevertheless the actuator has a very interesting behavior mirrored in

the evolution of the magnitude of impedance on Figure 3.14, in the area B_1. The level of the magnitude rapidly increases (with 850 Ω) when the supplying circuit of the voice coil (used to excite the cantilever beam) is switched-off. In B_1 the forced response of the cantilever beam (due the harmonic excitation on 17.58 Hz) disappears and is replaced by a free viscous damped response on 17.60 Hz frequency.

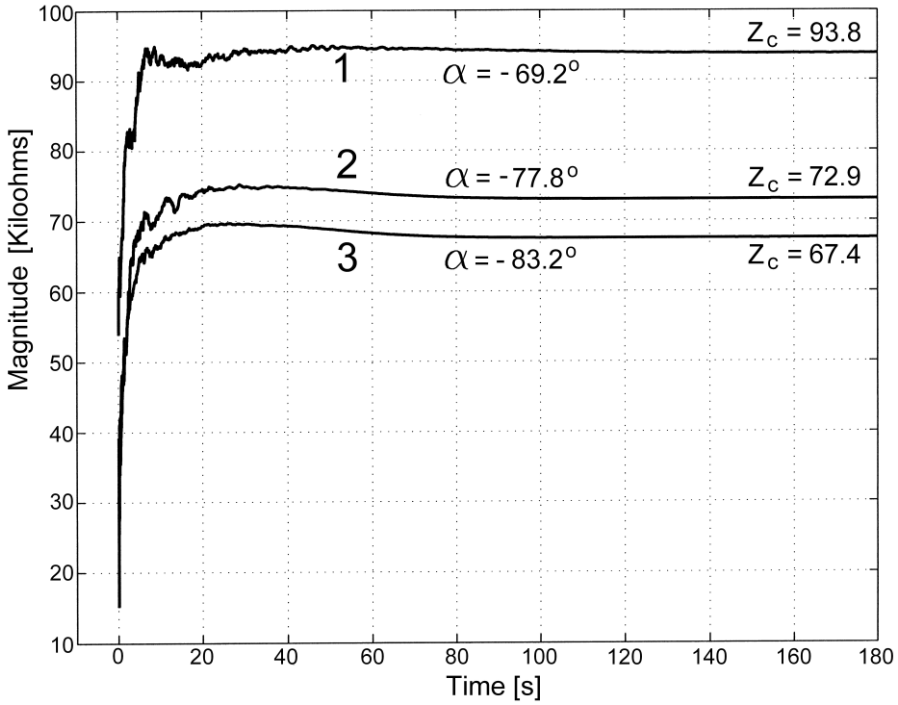

Fig. 3.15: *Time evolution of the magnitude of electrical impedance Z during the experiments described in Figure 3.12 (**see also the chapter 3.7**).*

The experiment from Figure 3.12 (active electrical power evolutions with self excited vibration due to a positive feedback with instability, for different values of shift of phase α) is described in terms of evolution of the magnitude of impedance in Figure 3.15 (see the

curves 1, 2 and 3 on both figures). Here the magnitude also increases quickly to a constant value Z_c which depends on the value of α. It is experimentally revealed that the shift of phase φ between the instantaneous current $i(t)$ and voltage $u_a(t)$ also decreases rapidly to a constant value ($\varphi=13.2^o$ for curve 1, $\varphi=24.5^o$ for curve 2 and $\varphi=28.9^o$ for curve 3).

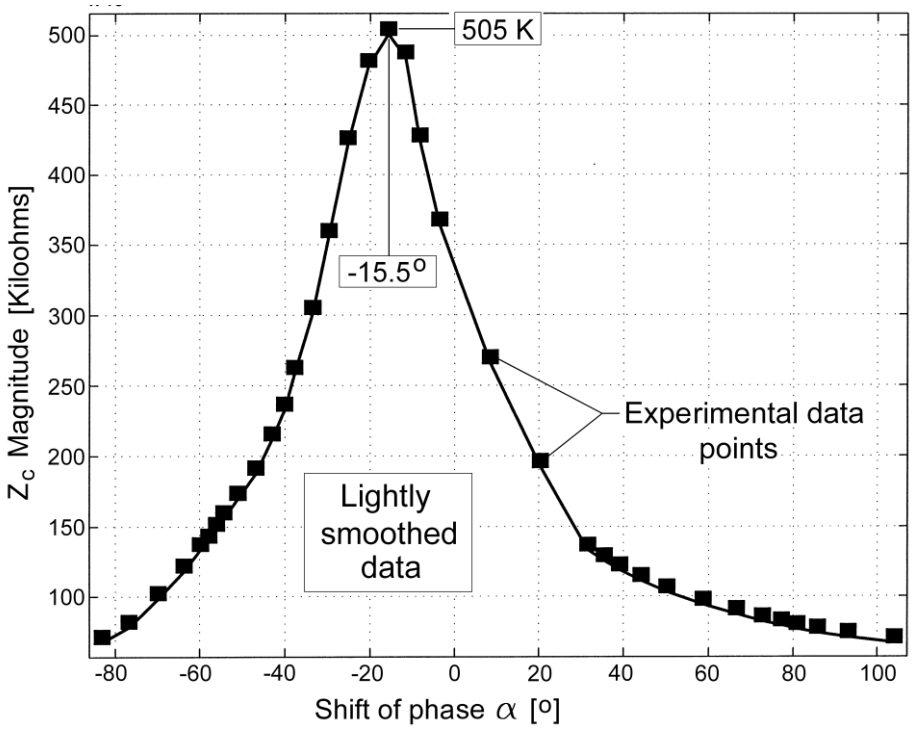

Fig. 3.16: *The evolution of magnitude of electrical impedance Z_c related to the shift of phase α.*

This means that according to Eqs. (3.7) and (3.11), during the experiment described in Figures 3.12 and 3.15 the ratio $U_{a,rms}/I_{rms}$ is constant but the mathematical product $U_{a,rms}\cdot I_{rms}$ is variable for a while (until $P_{el,act}=P_{ss}$, in steady-state).

The same behavior of the magnitude of electrical impedance (it tends to a constant value Z_c) can be observed for all the experiments initiated with a pulse excitation for different values of α.

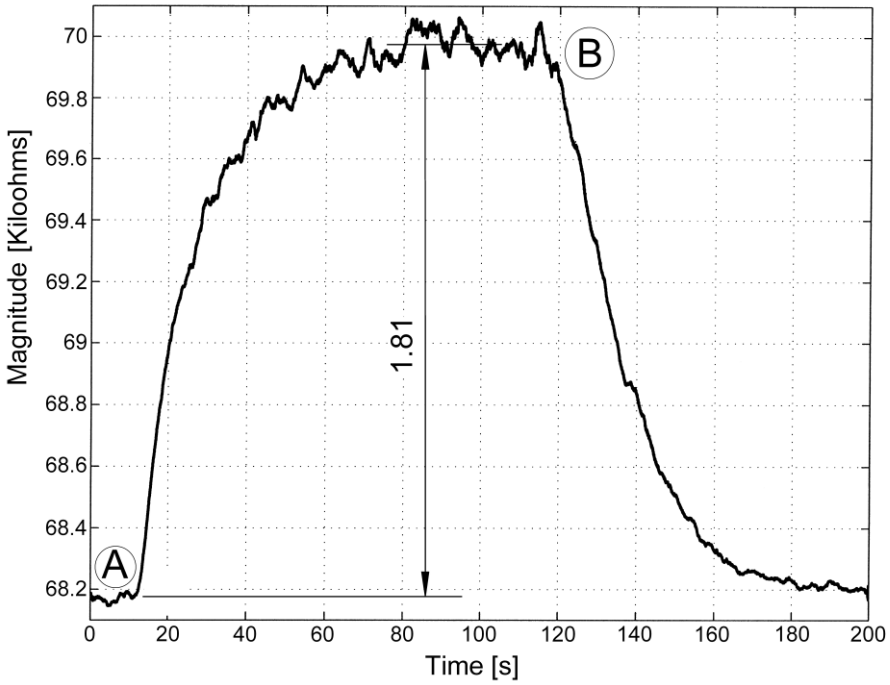

Fig. 3.17: *Time evolution of the magnitude of electrical impedance Z during the experiment described in Figure 3.13 (**see also the chapter 3.7**).*

The dependence $Z_c(\alpha)$ is graphically described in Figure 3.16. The maximum value of the magnitude (Z_c=*505 KΩ*) is generated for a shift of phase α=*-15.5º*. It is expected that the maximum value of the magnitude should be placed at α=*0º*. We haven't found an explanation for this difference of maximum value location yet.

The experiment described in Figures 3.13 (a) and 3.13 (b) can also be described by the evolution of magnitude of electrical impedance

of the actuator, as Figure 3.17 indicates. There is a big difference between the maximum percentage variation of the impedance $100\cdot(Z_{max}-Z_{min})/Z_{max}=2.57\%$ and the electrical active power variation $100\cdot(P_{ss,max}-P_{ss,min})/P_{ss,max}=88.11\%$. This result also confirms that is better to use the evolution of active electrical power than the evolution of the magnitude of impedance, in order to characterize and to understand the dynamic phenomena driven by the actuator in a closed-loop system with derivative feedback.

3.4.4 A study on the dependence between the synthetic modal damping and the derivative gain.

The first bending mode of vibration of the cantilever beam is characterized by the modal damping ratio ζ. The damping ratio has two components: the natural (structural) damping ratio ζ_n and the synthetic damping ratio ζ_{sd}, with $\zeta = \zeta_n + \zeta_{sd}$. The natural damping ratio ζ_n has a constant positive value; it is passively generated by air friction and internal friction inside the material of the cantilever beam. The synthetic damping ratio ζ_{sd} has a positive or negative value; it is actively generated by the derivative feedback inside the closed-loop system. It is presumed that the synthetic damping ratio is directly proportional to the derivative gain $C_d(\alpha)$, so: $\zeta_{sd}=C_{sd}\cdot C_d$, with C_{sd} a positive, constant value. The damping ratio can be written as it follows:

$$\zeta(\alpha)=\zeta_n+\zeta_{sd}=\zeta_n+C_{sd}\cdot C_d(\alpha) \tag{3.12}$$

This relationship can be confirmed as it follows. For several different values of the angle α (chosen in order to keep the stability of the cantilever beam), the cantilever beam is excited with an impulse excitation as already shown.

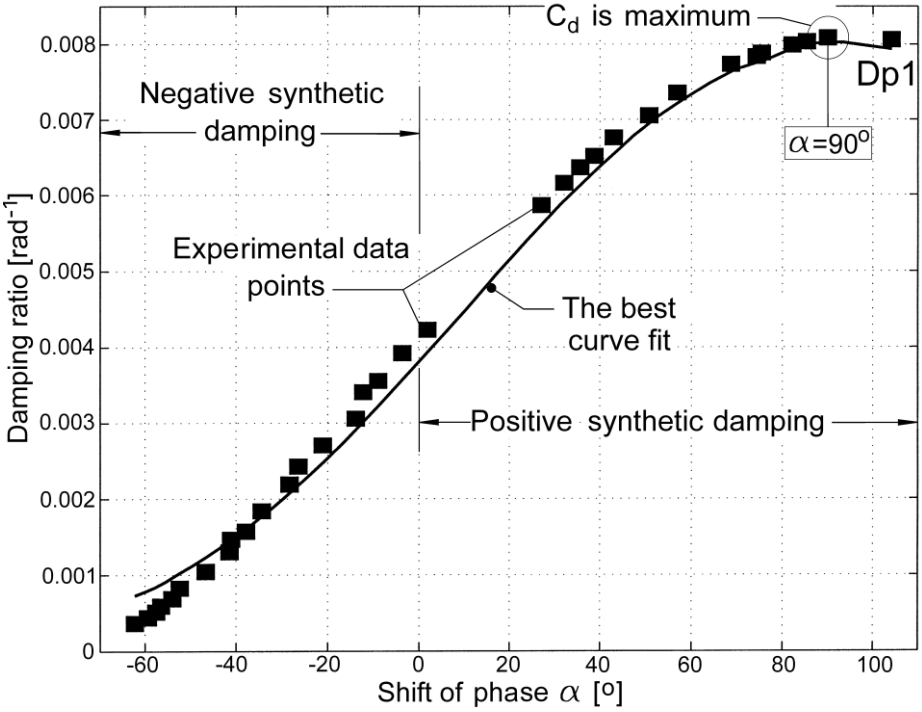

Fig. 3.18: *Experimental and fitted evolution of the damping ratio ζ depending on the shift phase angle α* ***(see also the chapter 3.7).***

In consequence, for each value of α they are experimentally determined by free response data fitting the values of: damping ratio ζ, damped modal natural angular frequency ω_1, undamped modal natural angular frequency ω_0, voltage gain C_v, derivative gain $C_d=C_v \cdot sin(\alpha)/\omega_1$ and the power peak P_{pv}. A graphic representation $\zeta(\alpha)$ with experimental data points of α and ζ coordinates (represented by

blackened squares on Figure 3.18, starting with Dp1 data point) is numerical fitted using the Eq. (3.12) in order to find out the values of ζ_n and C_{sd}. The result (see the best curve fit given in Figure 3.18) is significant: there is a good fit between the curve and the data points. This indicates a good measurement precision. The following values were found by fitting: $\zeta_n = 0.0038\ rad^{-1}$ (or $\zeta_n = 0.38\%$) and $C_{sd} = 0.4388$. The Eq. (3.12) is confirmed with a good approximation.

As it was presumed, the synthetic damping is practically directly proportional to the derivative gain, and $C_{sd} > 0$. There is another confirmation: the value of ζ_n is very close to that already found in Figure 3.5 (a) (0.41%). An experimental hypothesis can be formulated due to the appearance of the curve fit: if $\zeta_n > \zeta_{sd}$ whatever the value of α is (the dynamic system of the cantilever beam is stable) $\zeta(\alpha)$ has an almost harmonic evolution. Figure 3.14 partially confirmed this hypothesis. Large values of positive synthetic damping are often required for technical applications.

Two ways are available to obtain this: the first is to use piezoelectric transducers with large K_{31} values; the second is to increase the derivative gain C_d (according to Eq. (3.12)). In order to follow the second way an increase of the value of the voltage gain C_v (according to Eq. (3.2)) is necessary. In the setup described in Figure 3.1, a high voltage amplifier should be placed between the phase shifter 8 ($\alpha = 90^o$) and the actuator PA 10. We shall consider that the voltage gain C_v in feedback closed-loop is produced by this amplifier. The positive synthetic damping can be maximized if this gain (therefore the

applied voltage to the actuator) is increased up to the limit imposed by the phenomenon of dielectric breakdown in the actuator.

3.4.5 A study on the dependence between the synthetic damping and the active electrical power absorbed by the actuator.

As confirmed before, the synthetic damping is directly proportional with the derivative gain in the feedback closed-loop. Some previous experimental results prove that there is a relationship between the active electrical power absorbed by the actuator and the synthetic damping generated (e. g. Figures 3.7 and 3.10). It is expected that a negative absorbed active power should generate a positive synthetic damping and a positive power should generate a negative synthetic damping. There is an experimental approach which confirms this presumption and describes the character of dependence between the active power and the synthetic damping in graphical terms. Some experimental results already found before (in order to plot the Figure 3.18) are used. Figure 3.19 (b) shows the evolution of power peak P_{pv} depending on the evolution of the angle α (experimental points of coordinates α and P_{pv} joined by line segments, lightly smoothed data). A comparison between Figures 3.18 and 3.19 (b) shows that there is a logical correlation between the damping and the active electrical power. It is easier to see this correlation by following this reasoning: P_{pv} depends on α, (according to Figure 3.19 (b)), ζ_{sd} depends on α (a result

found by curve fitting in Figure 3.18, according to Eq. (3.12)) and so ζ_{sd} depends on P_{pv}. This last dependency is revealed on Figure 3.19 (a) (experimental points of coordinates P_{pv} and ζ_{sd} joined by line segments on curve 1, lightly smoothed data).

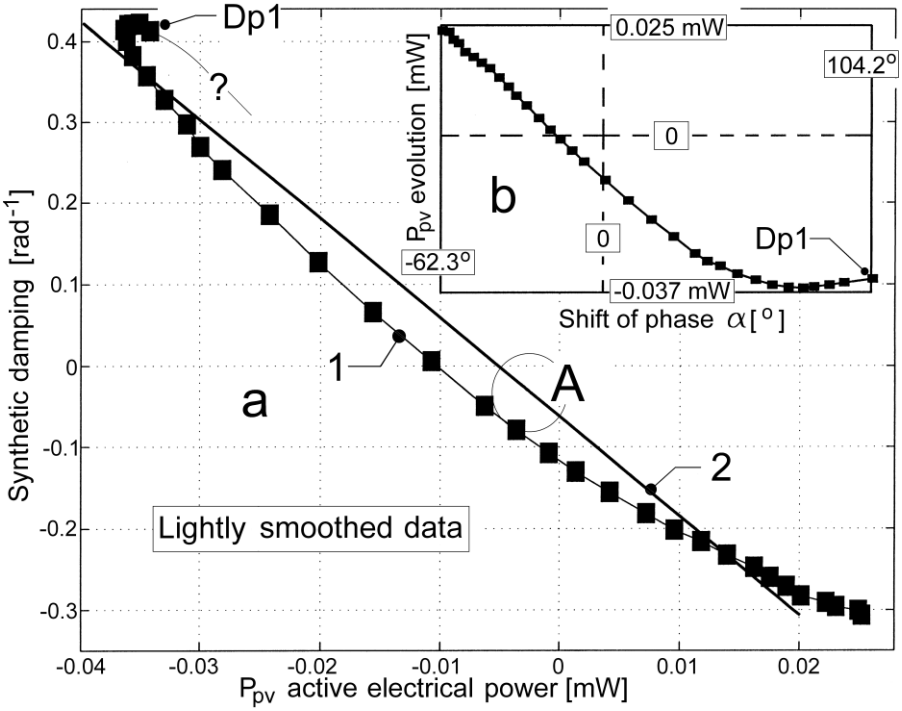

Fig. 3.19: ***(a)*** *Experimental and fitted evolution of the synthetic mechanical damping ratio ζ_{sd} depending on power peak value P_{pv};* ***(b)*** *Experimental dependence of P_{pv} on the shift phase angle α* ***(see also the chapter 3.7).***

The dependence $\zeta_{sd}(P_{pv})$ is close to a linear regression. The result of $\zeta_{sd}(P_{pv})$ data fitting (slope-intercept form, curve 2) is described by:

$$\zeta_{sd} = a \cdot P_{pv} + b = -121.75 \cdot P_{pv} - 6.25 \cdot 10^{-4} \qquad (3.13)$$

The negative slope ($a = -121.75$) proves that -as expected- a positive active electrical power produces a negative synthetic damping; a negative power generates a positive synthetic damping. This way it was once again shown that the actuator and the closed-loop feedback with derivative gain work as an active damper which is able to generate positive or negative damping adjusted by means of the phase angle α and of course by means of the voltage gain C_v.

An observation is in order: in the area marked with A the active electrical power and the synthetic damping are negative (and also the intercept in Eq. (3.13) is negative) because the evolution $P_{pv}(\alpha)$ doesn't pass through zero when $\alpha=0$ (Figure 3.19 (b)). This evolution is shifted 15.5º to the left. The evolution of the impedance $Z_c(\alpha)$ given in Figure 3.16 is also shifted in the same manner. We didn't find an explanation of these phenomena for now and we take it as a challenge to understand and to write about it in a future paper. An experimental hypothesis can be formulated: if $\zeta_n > \zeta_{sd}$ whatever the value of α is (the dynamic system of the cantilever beam is stable) the $P_{pv}(\alpha)$ has an almost harmonic evolution (see Figure 3.19 (b)) and $\zeta_{sd}(P_{pv})$ describes a closed curve (almost an ellipse, see Figure 3.19 (a)).

3.4.6 A study on the dependence between the synthetic modal stiffness and the proportional gain.

A collateral result of the experimental research is useful for a complete understanding of the behavior of a closed-loop dynamic control system with proportional and derivative feedback.

The proportional gain C_p in the feedback closed-loop should generate a mechanical synthetic modal stiffness k_{ss} (positive and negative). A positive value for C_p (with $-\pi/2<\alpha<\pi/2$) generates a negative proportional feedback therefore a positive synthetic modal stiffness k_{ss} because the sensor and the actuator have different poling directions. If $C_p<0$, due to the positive proportional feedback, $k_{ss}<0$. This means that the undamped natural frequency of the first mode $f_0=\omega_0/2\pi$ depends on C_p, therefore f_0 depends on α. It is presumed that $k_{ss}=C_k \cdot C_p$ (k_{ss} is directly proportional with C_p, C_k is a constant value). The frequency f_0 can be written approximately as follows:

$$f_0 = \frac{1}{2\pi} \cdot \sqrt{\frac{k_m + k_{ss}}{m_m}} = \frac{1}{2\pi} \cdot \sqrt{\omega_m^2 + \omega_{ss}^2} = \frac{1}{2\pi} \cdot \sqrt{\omega_m^2 + C_{ss} \cdot C_p} \tag{3.14}$$

Here k_m is the open-loop modal stiffness, m_m is the open-loop modal mass, $\omega_m = \sqrt{k_m / m_m}$ is the open-loop undamped natural modal angular frequency of the first bending mode ($\omega_m=\omega_0$ if $C_p=0$), $\omega_{ss} = \sqrt{k_{ss} / m_m} = \sqrt{C_{ss} \cdot C_p}$ is undamped synthetic angular frequency, and $C_{ss}=C_k/m_m$ is a synthetic stiffness constant.

Figure 3.20 presents the experimental evolution of the frequency f_0 depending on the values of α (unsmoothed data points of α and f_0 coordinates, represented by blackened squares). On the same figure the best curve fit is drawn as result of fitting of data points using the Eq. (3.14). There is a good fit between the curve and the

experimental data points, which means that all assumptions we have made so far are valid. This is also a description of the measurement precision. The fitting provides the values of ω_m and C_{ss} (ω_m = *110.20 rad/s* and C_{ss} = *89.07* rad^2/s^2). The synthetic modal stiffness k_{ss} is zero in the point of coordinates $\alpha = 90^o$ and $f_m = \omega_m/2\pi$ =*17.54 Hz*.

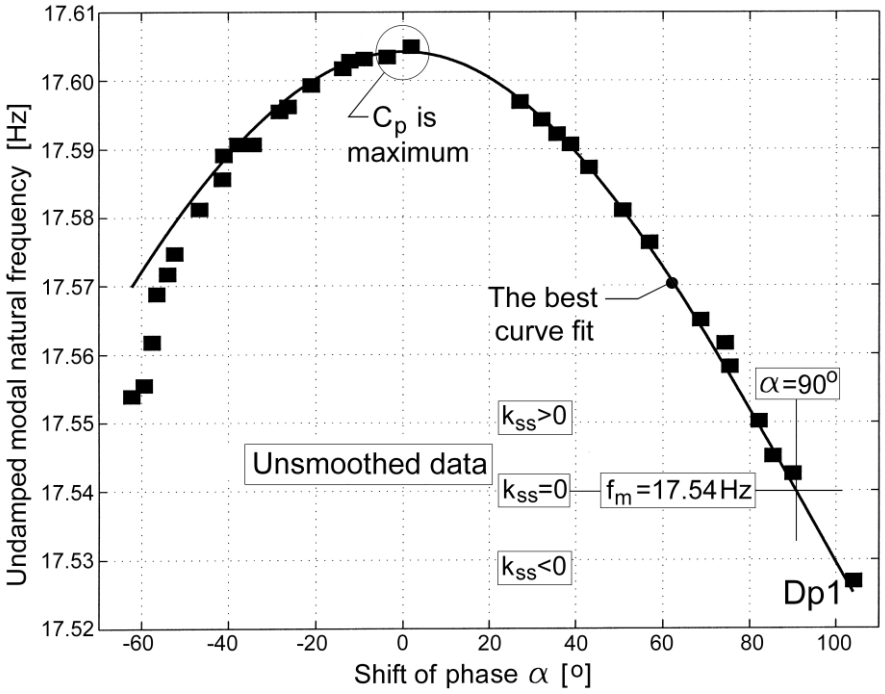

Fig. 3.20: *Experimental and fitted dependence of the undamped natural modal frequency f_0 on the shift phase angle α (**see also the chapter 3.7**).*

It was shown in this manner that the actuator and the closed-loop feedback system with proportional gain work as an active synthetic modal stiffness generator which is able to generate positive or negative stiffness, adjusted by means of the shift of phase angle α and the voltage gain C_v. It is worth noting that, according to Figure 3.20, the

influence of the proportional gain on the undamped natural frequency of the first mode f_0 is extremely small.

A first hypothesis can be formulated: if $\zeta_n > \zeta_{sd}$ no matter the value of α is (the dynamic system of the cantilever beam is stable) $f_0(\alpha)$ has an almost harmonic evolution. This is partially verified in Figure 3.20.

A second hypothesis can be formulated as well: in order to generate synthetic stiffness, the actuator should absorb negative modal reactive electrical power.

3.5 CONCLUSIONS

Many advantages can be drawn from the monitoring of the active electrical power absorbed by a piezoelectric actuator placed in a closed-loop feedback system for dynamic correction (damping) of a mechanical structure. First of all because it uses a very simple computer assisted technique. The active power evolution describes (better than the magnitude of the electrical impedance) the behavior of the actuator related to the derivative gain in feedback loop and related to the dynamics of the mechanical structure (in stable and unstable regimes).

Especially the concept of negative active power flow involved in producing of synthetic positive modal damping (active damping) has been treated theoretically and experimentally. A new theoretical approach of active damping is taking shape: an actuator (transducer) placed on a mechanical structure generates modal damping if it is

electrically powered by a negative active electrical modal power supply. This approach is available for any type of transducer (e.g. a piezoelectric stack transducer [42, 16], a voice-coil transducer [16, 39], a magnetostrictive transducer [41], a DC motor, etc). There is a possibility that this might be practically exploited later.

The relationship between the reactive electrical power flow to the actuator and the synthetic modal stiffness (generated by proportional feedback in this paper) is a possible topic for future research.

3.6 REFERENCES

1. J. Distefano, A. R. Stubberud, I. J. Wiliams, (1995), *Feedback and Control Systems*, Schaum's Outline Series, McGraw-Hill Professional, 1995.
2. J. Doyle, B. Francis, A. Tannenbaum, (1990), *Feedback Control Theory*, Macmillan Publishing Co., 1990.
3. K. J. Aström, R. M. Murray, (2008), *Feedback Systems: An Introduction for Scientists and Engineers*, Princeton University Press, Princeton, 2008.
4. H. F. Olson, (1956), *Electronic control of noise, vibration and reverberation*, J. Acoust. Soc. Am. 28 (5) (1956) 966-972.
5. A. Preumont, (2002), *Vibration Control of Active Structures. An introduction*, 2nd ed., Kluwer Academic Publishers, 2002.
6. C. R. Fuller, S. J. Elliott, P. A. Nelson, (1996), *Active Control of Vibration*, Academic Press, 1996.

7. M. J. Balas, (1979), *Direct velocity feedback control of large space structures,* J. Guid. Control Dynam. 2 (3) (1979) 252-253.
8. L. Benassi, S. J. Elliott, P. Gardonio, (2004), *Active vibration isolation using an inertial actuator with local force feedback control,* J. Sound Vibr. 276 (1-2) (2004) 157-179.
9. Li Jun, Shen Rongying, Hua Hongxing, (2004), *Cubic velocity feedback control of high-amplitude vibration of a nonlinear plant to a primary resonance excitation*, Shock Vib. 14 (1) (2007) 1-14.
10. P. Gardonio, S. J. Elliott, (2005), *Modal response of a beam with a sensor–actuator pair for the implementation of velocity feedback control*, J. Sound Vib. 284 (1-2) (2005) 1-22.
11. A. Preumont, (2006), *Mechatronics: Dynamics of Electromechanical and Piezoelectric Systems,* Springer, 2006, pp. 95-190.
12. M. Horodinca, N. E. Seghedin, E. Carata, M. Boca, C. Filipoaia, D. Chitariu, (2014), *Dynamic characterization of a piezoelectric actuated cantilever beam using energetic parameters,* Mechanics of Advanced Materials and Structures 21 (2) (2014) 154-164.
13. J. J. Dosch, D. J. Inman, E. A. Garcia, (1992), *Self-sensing piezoelectric actuator for collocated control*, J. Intel. Mat. Syst. Str. 3 (1) (1992) 166-185.
14. G. E. Simmers Jr., J. R. Hodgkins, D. D. Mascarenas, Gyuhae Park, Hoon Sohn, (2004), *Improved piezoelectric self-sensing actuation,* J. Intel. Mat. Syst. Str. 15 (12) (2004) 941-953.

15. S. O. R. Moheimani, (2003), *A survey of recent innovations in vibration damping and control using shunted piezoelectric transducers*, IEEE T. Contr. Syst. T. 11 (4) (2003) 482-494.
16. B. de Marneffe, (2007), *Active and passive vibration isolation and damping via shunted transducers*, Ph.D. thesis, Université Libre de Bruxelles, Brussels, Belgium, 2007.
17. N. W. Hagood, A. von Flottow, (1991), *Damping of structural vibrations with piezoelectric materials and passive electrical networks*, J. Sound Vib. 146 (2) (1991) 243-268.
18. K. W. Wang, (2001), *Vibration suppression utilizing piezoelectric networks*, In: The Mechanical Systems Design Handbook Modeling, Measurement, and Control, ed. O. D. I. Nwokah and Y. Hurmuzlu, CRC Press, 2001, chapter 15.
19. G. A. Lesieutre, (1998), *Vibration damping and control using shunted piezoelectric materials*, Shock Vib. Dig. 30 (3) (1998) 187-195.
20. C. H. Park, D. J. Inman, (2003), *Enhanced piezoelectric shunt design*, Shock Vib. 10 (2) (2003) 127-133.
21. F. Dell'Isola, S. Vidoli, (1998), *Damping of bending waves in truss beams by electrical transmission lines with PZT actuators*, Arch. Appl. Mech. 68 (9) (1998) 626-636.
22. F. Dell'Isola, S. Vidoli, (1998), *Continuum modelling of piezoelectromechanical truss beams: an application to vibration damping*, Arch. Appl. Mech. 68 (1) (1998) 1-19.

23. C. Maurini,F. dell'Isola, D. Del Vescovo, (2004), *Comparison of piezoelectronic networks acting as distributed vibration absorbers*, Mech. Syst. Signal Pr. 18 (5) (2004) 1243-1271.
24. A. J. Fleming and S. O. R. Moheimani, (2003), *Adaptive piezoelectric shunt damping*, Smart Mater. Struct. 12 (1) (2003) 36-48.
25. K. Morimoto, I. Kanno, K. Wasa, H. Kotera, (2010), *High-efficiency piezoelectric energy harvesters of c-axis-oriented epitaxial PZT films transferred onto stainless steel cantilevers*, Sensor. Actuat. A-Phys. 163 (2010) 428–432.
26. K. W. Wang, J. S. Lai, W. K. Yu, (1996), *An energy-based parametric control approach for structural vibration suppression via semi-active piezoelectric networks*, J. Vib. Acoust. 118 (3) (1996) 505-510.
27. Y. Sabzehmeidani, M. Hussein, M. Mailah, M. Z. Md Zain, M. R. Abdullah, (2011), *Intelligent hybrid control of piezoelectric actuated micro robot*, International Journal of Systems Applications, Engineering & Development, 5 (3) (2011) 306-313.
28. M. C. Brennan, A. M. Rivas McGowan, (1997), *Piezoelectric power requirements for active vibration control*, Proceedings of SPIE: Smart Structures and Materials, vol. 3039, pp. 660–664, 1997.
29. A. Mukherjee, S. P. Josh, (2001), *Design of actuator profiles for minimum power consumption*, Smart Mater. Struct. 10 (2) (2001) 305–313.

30. C. Niezrecki, H. H. Cudney, (1994), *Improving the power consumption characteristics of piezoelectric actuators*, J. Intell. Mat. Syst. Str. 5 (4) (1994) 522-529.
31. Yu-Hsiang Hsu, Chih-Kung Lee, Wen-Hsin Hsiao, (2003), *Optimizing piezoelectric transformer for maximum power transfer*, Smart Mater. Struct. 12 (3) (2003) 373-383.
32. D. Bondoux, (1996), *Piezodamping: a low-power-consumption technique for semi-active damping of light structures*, Proceedings of SPIE 2779, Smart Structures and Materials, vol. 2779. pp. 694-699, 1996.
33. S. Saadon, O. Sidek, (2011), *A review of vibration-based MEMS piezoelectric energy harvesters*, Energ. Convers. Manage. 52 (1) (2011) 500-504.
34. H. Shen, J. Qiu, M. Balsi, (2011), *Vibration damping as a result of piezoelectric energy harvesting*, Sensor. Actuat. A-Phys. 169 (1) (2011) 178-186.
35. S. Chandrasekaran, D. K. Lindner, (2000), *Power flow through controlled piezoelectric actuators*, J. Intel. Mat. Syst. Str. 11 (6) (2000) 469-481.
36. C. J. Swigert, R. L. Forward, (1981), *Electronic damping of orthogonal bending modes in a cylindrical mast-theory*, J. Spacecraft Rockets 18 (1) (1981) 5-10.
37. R. L. Forward, (1981), *Electronic damping of orthogonal bending modes in a cylindrical mast-experiment*, J. Spacecraft Rockets 18 (1) (1981) 11-17.

38. H. Zhao, H. Y. Hu., (2009), *Active control of vertical tail buffeting by piezoelectric actuators*, J. Aircraft 46 (4) (2009) 1167-1175.
39. M. Horodinca, N. E. Seghedin, E. Carata, C. Filipoaia, M. Boca, D. Chitariu, (2013), *Experimental investigations of the power absorbed at mechanical resonance*, Experimental Techniques, 30 (7) (2013) 31-21.
40. G. Park, D. J. Inman, (2007), *Structural health monitoring using piezoelectric impedance measurements*, Philos. T. Ro. Soc. A., 365 (1851) (2007) 373-392.
41. J. Pratt, A. B. Flatau, (1995), *Development and analysis of a self-sensing magnetostrictive actuator design*, J. Intel. Mat. Syst. Str. 6 (5) (1995) 639-648.
42. Mandar Kulkarni, Gulshan Kumar, Prasanna Mujumdar, Ashok Joshi, (2010), *Active Control of Vibration Modes of a Wing Box by Piezoelectric Stack Actuators*, 51st AIAA /ASME /ASCE/ AHS/ASC Structures, Structural Dynamics, and Materials Conference
 18th AIAA/ASME/AHS Adaptive Structures Conference
 12th, SDM-61: Control and Aeroservoelasticity, 15-15 April 2010.

3.7 A SUMMARY OF SOME EXPERIMENTAL FIGURES

Some experimental figures from this paper can be reproduced by any reader as it is indicated here below. First please download the folder **Data paper 3** (see the download indications from preface).

Figure 3.3

You need the folder **Data Fig. 3.3.** In order to obtain the color version of Figure 3.3 you should run the Matlab program **fig33.m**. Based on the experience gained in the previous two papers the reader is invited to analyze each of three voltages generated during this free response of the cantilever beam in order to find the frequency of vibration and the damping ratio. Normally the values of these two parameters should be the same for all voltages.

Figure 3.4

You need the folder **Data Fig. 3.4.** In order to obtain the main parts of Figure 3.4 you should run the Matlab program **fig34.m**. Please have a look also on task #3 in the chapter 3.8.

Figure 3.5

You need the folder **Data Fig. 3.5.** In order to obtain the main parts of Figure 3.5 you should run the Matlab program **fig35.m.**

Figure 3.7

You need the folder **Data Fig. 3.7.** In order to obtain the main parts of Figure 3.7 you should run the Matlab program **fig37.m.**

Figure 3.8

You need the folder **Data Fig. 3.8.** In order to obtain the main parts of Figure 3.8 you should run the Matlab program **fig38.m.** The reader is invited to perform the same study as it was indicated previously at Figure 3.3.

Figure 3.9

You need the folder **Data Fig. 3.9.** In order to obtain the main parts of Figure 3.9 you should run the Matlab program **fig39.m.** The program needs almost 40 s in order to generate this Figure. The reader is invited to do a comparation between Figure 3.9 (with positive active power) and Figure 3.4 (with negative active power).

Figure 3.10

You need the folder **Data Fig. 3.10.** In order to obtain the main parts of Figure 3.10 you should run the Matlab program **fig310.m.**

Figure 3.11

You need the folder **Data Fig. 3.11.** In order to obtain a coloured version of Figure 3.11 you should run the Matlab program **fig311.m.** Please have a look also on the task #6 in the chapter 3.8.

Figure 3.12

You need the folder **Data Fig. 3.12.** In order to obtain a coloured version of Figure 3.12 you should run the Matlab program **fig312.m.** Please have a look also on the task #6 in the chapter 3.8.

Figure 3.13

You need the folder **Data Fig. 3.13.** In order to obtain Figure 3.13 you should run the Matlab program **fig313.m**. The program needs almost 44 s in order to generate this Figure.

Figure 3.14

You need the folder **Data Fig. 3.14.** In order to obtain the main part of Figure 3.14 you should run the Matlab program **fig314.m**.

Figure 3.15

You need the folder **Data Fig. 3.15.** In order to obtain the main part of Figure 3.15 you should run the Matlab program **fig315.m**. In order to generate this Figure the PC needs almost 152 s.

Figure 3.17

You need the folder **Data Fig. 3.17.** In order to obtain the main part of Figure 3.17 you should run the Matlab program **fig317.m**.

Figure 3.18

You need the folder **Data Fig. 3.18.** In order to obtain the main part of Figure 3.18 you should run the Matlab program **fig318.m**.

Figure 3.19

You need the folder **Data Fig. 3.19.** In order to obtain the main part of Figure 3.19 you should run the Matlab program **fig319.m**.

Figure 3.20

You need the folder **Data Fig. 3.20.** In order to obtain the main part of Figure 3.20 you should run the Matlab program **fig320.m**.

3.8 THEORETICAL AND EXPERIMENTAL WORK TASKS

1. Perform the experimental setup described in Figures 3.1 and 3.2.

2. Try to design a Matlab program that ensures the determination of phase shift (α) generated by the phase shifter based on the experimental evolutions of the voltage u_s and u_B (Figure 1) during the free response of the cantilever beam. You can use the indications given at task #3 in paper 1.

3. Perform the experiment described in Figure 3.4 in order to find out the evolution of the active electrical power (Figure 3.4 c.) for different values of phase shift α. You find the folder **paper3task3** in the folder **Data paper 3**. There you find the Matlab program **figure34** and the data file **proba.txt** used to generate Figure 3.4. Try to adapt yourself this program for these

requirements. Optionally you can use for this purpose the Matlab program **putact**.

For each value of α you should excite the cantilever beam (using the switch K, see Figure 3.1) in order to generate a free response (mirrored in the voltages u_A, u_B or u_s). This free response should be used to find out the exact values of the frequency f of free response and the damping ratio ζ (see the task # 3 in paper 1). This value of frequency should be written in line 8 of the program, in first instruction: (`filtr=(l1/timp(l1))/`**`17.5451`**; replacing the current value marked with bold.

4. Produce a mathematical argument in order to explain that the Equations (10) are correctly.

5. Perform the experimental study which proves the reliability of the second part of Eq. (3.10), $\zeta_1 = 2 \cdot \zeta$ for different values of shift of phase α. Here ζ is the damping ratio of the free response (mirrored in the evolution of the voltages u_A, u_B and u_s, see the previous task), ζ_1 is the damping ratio of the free response mirrored in the evolution of active electrical power $P_{el,act}$, see the first part of Eq. (3.10) $P_{el,act}(t_j) = P_0 \cdot e^{-\zeta_1 \cdot \omega_0 \cdot t_j}$. In order to find out ζ_1 is necessary to interpolate the evolution of the active electrical power (see the task 3 here above). It is possible to do this job by running the program **idenput** (stored also in the folder **paper3task3**). This program is able to find out

by numerical interpolation the values of P_0 and $\zeta_1 \cdot \omega$ for the evolution of the active electrical power from Figure 3.4.c. The graphical result of this interpolation is given here below in Figure 3.21. The numerical result is displayed as *d(1)* = P_0 = *-3.1862e-005 W* and *d(2)* = $\zeta_1 \cdot \omega$= *1.8141*, so $\zeta_1 = d(2)/\omega_0$. Here $\omega_0 \approx 2 \cdot \pi \cdot f$ and *f* is the frequency of the free response mirrored in the evolution of the voltages u_A, u_B or u_s (see task #3).

6. Try to generate a value of shift of phase α in order to produce negative sintetic damping with instability. Perform the experiment which produces the result given in Figure 3.11. It may be useful to run the Matlab program **fig311** from the folder **paper3task6** (ask the teacher for this folder). Here it is an interesting problem. After a long period of time, the values of the active electrical power absorbed by the actuator PA become constant on both curves. The reader is invited to search if these values are the same. And if these values are not the same, the reader is invited to produce some arguments on this item.

7. Please have a look on Figure 3.12. Imediately after the feedback loop between the sensor and actuator is closed the system starts to vibrate and to absorb more and more active electrical power. The reader is invited to investigate how the system starts to vibrate on first flexural bending mode of the free end of the cantilever beam. Remember that there is no external excitation!

8. Using the results from task #3 (frequency f and damping ratio ζ for each value of shift of phase α) try to obtain the graphical results shown in Figure 3.18 and Figure 3.20.